박 사 학 위 논 문

# 모바일 기기에서의 인지 기반 진동 렌더링

류 종 현 (柳 鍾 鉉)

전자컴퓨터공학부 (컴퓨터공학 전공)

포항공과대학교 대학원

**2010**

# 모바일 기기에서의 인지 기반 진동 렌더링

# Perception-based Vibration Rendering
# in Mobile Device

# Perception-based Vibration Rendering
# in Mobile Device

by

Jonghyun Ryu

Division of Electrical and Computer Engineering
(Computer Science and Engineering)
POHANG UNIVERSITY OF SCIENCE AND TECHNOLOGY

A thesis submitted to the faculty of Pohang University of Science and Technology in partial fulfillment of the requirements for the degree of Doctor of Philosophy in the Division of Electrical and Computer Enginneering (Computer Science and Engineering)

Pohang, Korea

December 2, 2009

Approved by

_____

Seungmoon Choi, Major Advisor

# 모바일 기기에서의 인지 기반 진동 렌더링

류 종 현

위 논문은 포항공대 대학원 박사 학위 논문으로 학위 논문 심사
위원회를 통과하였음을 인정합니다.

2009 년 12 월 2 일

학위논문 심사위원회 위원장        최 승 문 (인)

위　원        김 정 현 (인)

위　원        이 근 배 (인)

위　원        이 승 용 (인)

위　원        한 성 호 (인)

## Abstract

Personal mobile devices, such as the cellular phone, PDA (Personal Digital Assistant), and portable gaming device, are one of the recent technical advances that have dramatically impacted our daily life. One of the most interesting advances for user interaction with mobile devices is *vibrotactile rendering* for information delivery through the haptic sensation channel. Despite its popularity, relevant perceptual data have been relatively scarce. In this thesis, we present the perceptual data associated with mobile device vibrations and propose *perception-based vibration rendering* which improves the discriminability of vibrotactile messages.

First, the characteristics of two most frequently used vibration actuators, a vibration motor and a voice-coil actuator, have been investigated. According to our results, the vibration motor should be controlled by applied voltage lower than 3.5 V since its perceived intensity is saturated when applied voltage is higher than 3.5 V. For the voice-coil actuator, the voltage frequency from 220 Hz to 320 Hz and the voltage amplitude from 0.6 V to 1.2 V are recommended to generate desired vibration effects. Second, the perceived intensities of mobile device vibrations were estimated for various frequencies and amplitudes using a shaker system. By fitting a nonlinear function to the measured data based on Stevens' power law, we constructed a psychophysical magnitude function that enables us to predict the perceived intensity of mobile device vibration in a large parameter range. Also, we evaluated the applicability of the model by comparing it to the previously measured perceptual characteristics of the two vibration actuators. The evaluation results showed very

high correlations, indicating that the psychophysical magnitude function can reliably explain the perceived intensity of mobile device vibration. Third, we proposed and evaluated perceptually transparent vibration rendering (PTR) which allows desired haptic effects to be designed in the perceptual dimension and to be played through the haptic interface as they should be. In an experiment that used pure tone vibrations to evaluate the benefits of PTR, using the PTR maintained higher percent correct scores with even large stimulation levels. By using PTR, the maximum number of discriminable vibrations was $5 - 6$, in contrast to just $3 - 4$ without PTR. We also evaluated PTR in an experiment using vibrotactile melodies. The discriminability of melodies rendered using PTR was improved, since users could identify the perceived strength of each melody note in an improved accuracy. Finally, we developed a vibration pattern editor named the posVibEditor which offers quick-and-easy vibration design for even novice users. The posVibEditor also supports perceptually transparent rendering.

The present study contributes to enlarging our understanding of the utility of perception-based vibration rendering in mobile devices.

# Contents

# List of Figures

# List of Tables

# Chapter 1

# Introduction

## 1.1 Motivation

Personal mobile devices, such as the cellular phone, PDA (Personal Digital Assistant), and portable gaming device, are one of the recent technical advances that have dramatically impacted our daily life. Related technology and user interface have been rapidly evolving, including the use of *vibration rendering* for information delivery through the haptic sensory channel. In addition to the traditional usage for an alternative ring tone, vibration rendering are now used for various purposes, e.g., for special effects in mobile gaming, vibratory rhythms accompanied with music [25], touch interactions in full-screen mobile devices, or tactile messages of a predefined meaning (called a haptic icon or tacton) [39]. Despite plenty of applications developed so far, understandings on the perceptual characteristics of vibration rendering in the mobile device are lacking in related research.

Traditionally, desired vibration effects have been empirically designed by changing input voltage applied to vibration actuators without concrete knowledge on the relationship between physical vibrations and its perceptual characteristics. The methodological difference of the perception-based vibration rendering we proposed is an approach for designing and rendering vibrations in the perceptual dimension, such as perceived intensity, not input voltage. Firstly, designers compose vibrotactile messages in terms of the variation of the perceived intensity, expecting the vibrotactile effects to be perceived as desired. Then, the

1

| Design | Rendering | Generation | Perception |
|---|---|---|---|
| Vibration patterns are designed by using a authoring tool | The designed patterns are converted to analog signals that would drive an actuator | The actuator generates physical vibrotactile stimuli | The vibrations are sensed by the user's skin |
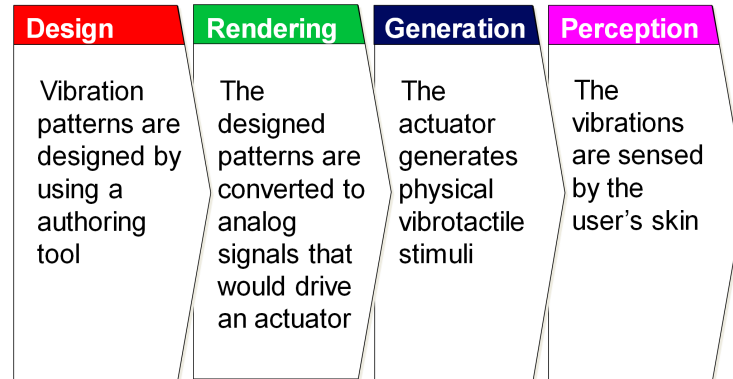
**Fig. 1.1: Flow for transmitting sound and vibration to users.**

perception-based vibration rendering we provide converted automatically desired perceived intensities to the corresponding physical signals applied to a vibration actuator. The major advantage of the perception-based vibration rendering is that designers can predict exactly perceptual vibration effects same to their desire. In our study, we have goals to provide the perceptual data of mobile device vibrations for the perception-based vibration rendering and improve the discriminability of vibrotactile messages by using it.

## 1.2  4 Steps of Vibration Transmission

To design and utilize vibrotactile effects in applications, we usually need to repeat the following four steps:

- Step 1 (Design): Vibrotactile messages appropriate to the goals of an application are designed, preferably using a dedicated authoring tool.

- Step 2 (Rendering): The designed messages are converted to corresponding analog signals that drive a vibration actuator.

- Step 3 (Generation): Vibrotactile stimuli are generated from the actuator, and transmitted to the surface of an enclosure in which the actuator is embedded.

- Step 4 (Perception): The vibrations are sensed through the user's skin in contact with the enclosure, resulting in percepts.

Some advanced techniques will be required in order to make each step to be effective. First, we should know the restriction of vibration actuators in terms of physical and perceptual characteristics. Generally the different kinds of actuators have different hardware restriction, e.g. correlated frequency and amplitude of a vibration motor [32], limited frequency bandwidth of a voice-coil actuator (the available frequency of most voice-coil actuators is fixed to their resonance frequency), and high input voltage required for a piezoelectric material. For effective vibration feedback, we should select suitable vibration actuators considering the restriction of vibration production. Second, perceptual data associated with mobile device vibrations will be provided. Despite the popularity of vibrotactile feedback in the mobile device, psychophysical researches about comprehensive data for perception of mobile device vibrations have been lacked yet. Since the skin and brain of the users are the end point of the vibration transmission procedure, understanding the human perception of mobile device vibrations is important. The perceptual data represented as some relations how physical vibration signals convert to perceived intensities in perception domain are used in our perception-based vibration rendering. Third, vibration rendering methods incorporating the vibration perception model and actuator characteristics are needed, such as perceptually transparent vibration rendering (PTR) [53]. The PTR was proposed for enhancing the perceptual correctness of transmitted vibrations. And it guarantees that the users feel vibration effects equivalent to the designer's desire without any distortions and the number of vibration stimuli which are reliably discriminated and identified could be increased with the PTR. [51]. Lastly, vibration authoring tools, similar to the sound design tools, are required for quick and easy design of vibrations. Music composing and sound mixing tools are very popular and provide easy learnability for even novices.

## 1.3  Contributions

The major contributions of this dissertation are summarized as follows:

- investigation of characteristics of two most used vibration actuator,

- first attempt to identify the perception model of mobile device vibration,

- increasing the feasibility of information transfer through the mobile device vibration with high discriminability by using perceptually transparent rendering,

- improved functionality and usability of the vibration pattern editor.

## 1.4 Organization

In Chapter 2, previous works with respect to vibration rendering in both mobile devices and other applications are presented. Chapter 3 describes analysis of two most used vibration actuators, a vibration motor and a voice-coil actuator, in terms of physical and perceptual characteristics and also provides guidelines to control them. In Chapter 4, the perceived intensities of mobile device vibrations are estimated for various frequencies and amplitudes using a shaker system, and a psychophysical magnitude function is constructed by fitting a nonlinear function to the measured perceived intensities. The psychophysical magnitude function is helpful to predict the perceived intensities of mobile device vibrations. In Chapter 5, we propose perceptually transparent vibration rendering and evaluate its benefits. The perceptually transparent rendering achieves the higher discriminability of pure tone vibrations and vibrotactile melodies. Chapter 7 presents a vibration pattern editor which called "posVibEditor". Additionally, in Chapter 8, we introduce another vibration rendering technique for vehicle application. Finally, we conclude this study in Chapter 9.

# Chapter 2

# Background and Previous Work

## 2.1 Vibration Rendering in Mobile Devices

In the past decade, a multitude of studies have been conducted to make use of vibrotactile rendering for diverse purposes (see [17, 40] for recent reviews). In what follows, those related to mobile devices are briefly reviewed.

### 2.1.1 Touch Interaction

One of the most traditional and practical goals of using vibrotactile rendering has been to improve the UI of mobile device, especially for virtual buttons displayed on a touch screen. It has become more important with the recent advent of full touch-screen mobile phones without physical keypads. For instance, it was shown in [16] that character input speed using soft buttons on a touch screen improves with vibrotactile feedback, especially in noisy environments. Nashel and Razzaque presented diverse vibrotactile effects suitable to different contact events, such as pushing a soft button, crossing button edges, and lingering on a button [45]. Recently, Hoggan et al. demonstrated in a usability study that vibrotactile feedback enhances accuracy and completion time for text entry for a virtual keypad in a mobile device, with a significantly reduced subjective workload [23].

Research for the use of vibrotactile rendering along with other GUIs (Graphical User Interfaces) has also been active. Poupyrev et al. developed a miniature vibrotactile actuator,

named TouchEngine, which used piezoelectric bending motors in multiple layers for large vibration output [48]. They proposed to use vibrotactile feedback as an ambient sensory cue to assist user interaction in a mobile device, and demonstrated that task completion time was reduced by 22% in a 1D text scroll task where the user controlled the scroll speed by tilting the mobile phone with vibrotactile feedback. This work was extended to designing vibrotactile signals appropriate for the different finger movements interacting on a touch screen, such as touching down, holding, dragging, and lifting off [47]. Rekimoto and Schwesig added another input dimension by sensing the pressing force of a finger and used the information for changing the degree of GUI response, e.g., scaling the screen scroll speed with pressure [49]. In addition, Hall et al. suggested the need of GUIs designed solely for mobile devices instead of those adapted from the desktop GUIs [21]. They conceptualized and evaluated one such GUI, T-Bar, which can prevent a user's finger from occluding visual icons on a touch screen and guide the finger movement via vibrotactile feedback for menu selection.

### 2.1.2 Information Transfer

Another topic to which significant research efforts have been devoted is how to deliver abstract information effectively via vibrotactile rendering in mobile devices. For instance, Brown and Kaaresoja designed tactile icons (tactons) for three types of mobile phone alerts and three alert priorities, thus a total of nine tactons, and demonstrated an acceptable recognition rate [6]. Töyssy et al. proposed a coding scheme for time using a simple sequence of vibrotactile pulses [65]. The recognition rate was as high as 80% without training. Recently, Li et al. developed an interesting system, PeopleTones, which notifies the presence of friends in the vicinity via musical and vibrotactile cues played by a mobile phone [37]. A vibrotactile pattern for a song was made by use of amplitude thresholding and bandpass filtering on the wave file of the song. Ghiani et al. installed two vibration motors to deliver directional information to the visually impaired using a PDA [19]. We note that in a more general context not limited to the mobile device, designing effective tactons (or haptic icons) with high discriminability and learnability has received great attention in the haptics

community, and recommend [40] for a review.

### 2.1.3 Multi-Modality

Multimodal rendering using two or more sensory channels also has great potential for improving the UI of a mobile device. Hoggan and Brewster proposed crossmodal icons that combine intuitively similar earcons and tactons in pairs [24]. Each pair shared the same properties, such as rhythm, roughness, intensity, and spatial location. Simultaneous playback of music and tactile vibration also was a topic of interest [11]. From a music file, they made vibrotactile patterns by amplifying the music signals in a low frequency bandwidth or synthesizing one if no such low frequency components were present. The vibrotactile patterns played together with music was reported to enhance the perception of sound quality.

Another multimodality research is dynamic vibrotactile feedback by using sensor fusion data. As each sensor and sensor fusion technology are advanced, various types of data captured from our environments can be used for vibrotactile feedback. Vibrotactile rendering has also been used with gesture recognition. Brown and Williamson developed a multimodal messenger, Shake2Talk, which integrated inertial sensing, gesture recognition, and vibrotactile feedback [5]. In Williamson et al., a ball-bouncing application for mobile phones was presented by combining device motion sensing, vibrotactile feedback, and realistic impact sound [71].

### 2.1.4 Multiple Actuators

Even though most mobile devices have just one vibration actuator due to the compact form factor, research using multiple actuators also has surfaced to enrich vibrotactile sensations. For instance, Sahami et al. developed a prototype phone with six vibration motors [56]. Spatial identification rate of a stimulation site was 75% for the motors in the corners, but 36% for the motors located midway. When the motors were activated in groups, the identification rate was higher in 64 − 76%. Hoggan et al. designed 2D tactons by varying the rhythm and stimulation site for a tactile progress bar [22]. Faster task completion time was observed when three actuators were placed on the sides of a mobile phone. Kim et al. in-

stalled two different vibration actuators for texture rendering [33]. A solenoid actuator that could generate relatively larger amplitude was used for large-scale textures, and a piezo-electric actuator with a faster response time was used for detailed textures.

### 2.1.5 Commercial Product

Perhaps the most important recent commercial product was VibeTonz[TM] system [25]. The system includes the VibeTonz Studio that is a graphical authoring software that enables mobile application designers to create vibration signals as they compose music or by extracting patterns from a MIDI (Musical Instrument Digital Interface) file, thereby greatly facilitating the design process of vibrotactile patterns. This is a significant advance from the previous practice of using vibrotactile signals in fixed levels chosen manually. The VibeTonz[TM] technology has been adopted by many mobile device manufacturers and service providers including Samsung and SK Telecom (the leading service provider in Korea). For special effects in mobile gaming, vibratory rhythms accompanied with music [25], touch interactions in full-screen mobile devices, or tactile messages of a predefined meaning (called a haptic icon or tacton) [39].

## 2.2 Vibration Rendering in Other Applications

In addition to mobile device applications, a number of studies have examined the advantages of vibrotaction for a variety of applications. Vibration feedback are also actively used in console gaming devices, including Sony Playstation [58], Microsoft Xbox [41], and Nintendo Wii [46]. In virtual reality (VR), vibration motors were used for a vibrotactile wear for VR-based motion training [73], whole body vibrotactile feedback for virtual contact [52], and virtual contact simulation in immersive virtual environments [38]. Related applications in human-computer interaction (HCI) include vibrotactile feedback for instant messaging [50].Vibration motors have also been used for an information display in sensory saturated environments, such as in a vibrotactile suit for astronauts and pilots in the cockpit [67, 68] and in a navigation system for detecting and alerting obstacles using a sonar sensor [9].

## 2.3 Human Vibration Perception in Mobile Devices

In spite of the plethora of applications reviewed above, research to provide fundamental knowledge on the perception of mobile device vibration has been rather rare. Very recently, Yao et al. demonstrated that perceived vibration strength increases with an increase in mobile device weight, and with a decrease in vibration frequency when vibration amplitude in acceleration remains constant [74]. Previously, our group published some preliminary data for the case of a vibration motor attached on the thenar eminence on the palm [32] and for the perceived intensity of mobile device vibration in a concise poster format [54]. In this article, we extend our previous papers in a greater extent by reporting the detection thresholds and the perceived intensity for three kinds of vibration actuators.

# Chapter 3

# Characteristics of Vibration Actuators

Chapter 3 shows the physical and perceptual characteristics of two vibration actuators, a vibration motor and a voice-coil actuator. The results of characteristics of two actuators will be used for validating a psychophysical magnitude function in rest of Chapter 4.

## 3.1  Overview of Two Vibration Actuators

One of vibration actuators mostly used in the mobile device is a variant of DC (Direct Current) motors called a *vibration motor*. This motor has many merits compared to other actuators such as small size, very low cost, large vibration amplitude, and relatively small power consumption. A drawback, however, also exists: given a voltage applied to the motor, its vibration is only sinusoidal with correlated amplitude and frequency due to its operation principles [30], significantly limiting the classes of vibration patterns that can be created in the mobile device. Another vibration actuator used also widely is a speaker-like *voice-coil vibration actuator*. The voice-coil actuator has an advantage that the frequency and amplitude of a vibration generated from it can be controlled independently. However, the controllable range of the vibration frequency from the voice-coil actuator should be limited by its operational principle. The voice-coil actuator has a resonance frequency, generally

(a) A vibration motor (LG Innotek; MVMF-A345A;)



(b) A voice-coil actuator (Audiological Engineering Corp.; VBW-32;)
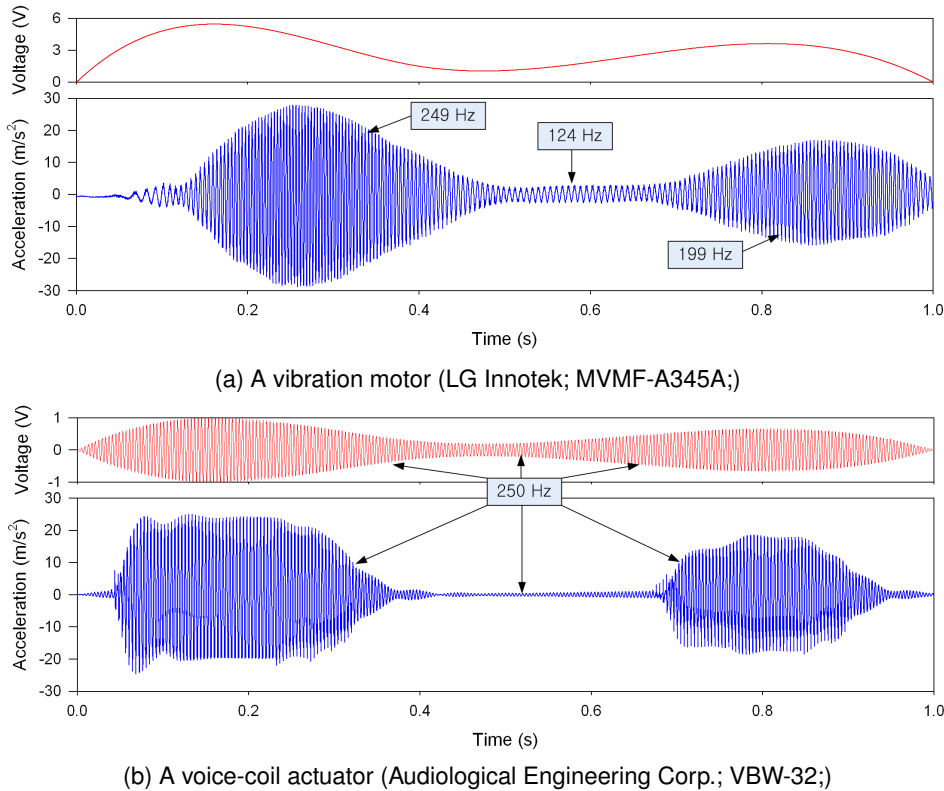
**Fig. 3.1: The measured accelerations of vibrations from the two vibration actuators.**

250 Hz. It could be said that the voice-coil actuator is able to generate a usable vibration with the largest amplitude in only 250 Hz frequency [7].

Fig. 3.1 shows completely the characteristics of sinusoidal vibrations captured from both vibration actuators with smoothly changed magnitudes of applied voltages and a second long. The frequency of applied voltage for the voice-coil was 250 Hz. As shown in this figure, the physical characteristics of two vibration actuators are represented clearly, such as applied voltage type, vibration frequencies and amplitudes changed through applied voltages, and also transient responses. Since the applied voltage type is DC voltage for the vibration motor but AC voltage for the voice-coil actuator, vibration frequencies generated from both actuators had different aspects. The principal frequency of the vibration motor

at a moment was changed through the applied voltage magnitude. The vibration frequency of the vibration motor is determined by the rotation speed of an eccentric mass, and the speed is relative to an applied voltage. Differently, the frequency of the voice-coil actuator was obviously same to that of an applied voltage. Both vibration amplitudes of each actuator were also changed through the applied voltage magnitude, but had different increase rates. The vibration amplitudes of the vibration motor were changed gradually through the smoothly changed voltage magnitudes, but those of the voice-coil were changed sharply at near $v = 0.5$ V. The transient response time of the vibration motor was larger than 100 msec, in contrast very small transient response of the voice-coil. The detailed analysis of vibrations measured from both vibration actuators will be provided in next section.

Even though Fig. 3.1 shows certainly the physical characteristics of the vibration actuators, we could not imagine how a user feels two vibrations with only figures of sinusoids in Fig. 3.1. In order to understand a user's feeling, we should know the perceptual characteristics of the vibration actuators measured by conducting the psychophysical experiment, such as the absolute magnitude estimation [75]. The perceptual characteristics of two vibration actuator will be also explained in the rest of this chapter.

## 3.2   Operation Principle

Before the main experiments, we will present shortly the operational principles and device dynamics of the two vibration actuators in order to understand the theoretical characteristics of them.

### 3.2.1   Vibration Motor

A typical vibration motor is a common DC motor with a rotor of eccentric mass distribution (see Fig. 3.2). The motor is controlled by an applied voltage which is proportional to the angular velocity of the rotor. The rotor, once rotated, results in large centrifugal force due to its unbalanced inertia, which subsequently induces movements of the whole motor package. These movements are transferred through a mobile device containing the motor, and finally
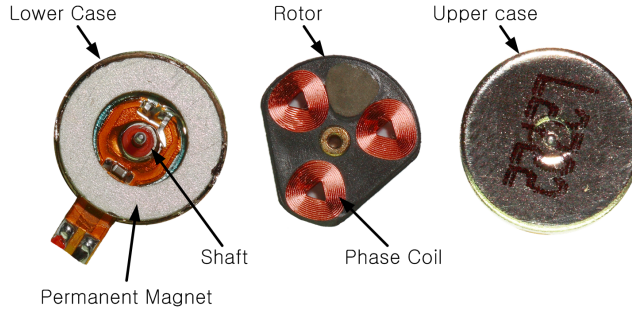
**Fig. 3.2** A coin-type vibration motor (Jahwa Electronics, Korea; model JHV-12C1-L20) and its internal structure.

turned into vibrations that a user feels from the device surface. This is a simple yet effective mechanism to create vibrations with large amplitudes.

As described above, the angular velocity of a rotor in a vibration motor is proportional to applied voltage. The systematic relation between the angular velocity and applied voltage could be theoretically represented as

$$w_m = \frac{kv_f}{R_a b_m + (kv_f)^2} v_a - \frac{T_L R_a}{R_a b_m + (kv_f)^2} \tag{3.1}$$

where $w_m$ is the angular velocity of the rotor, $k$ is the motor constant, $R_a$ is the resistance of the armature winding, $b_m$ is the equivalent mechanical damping constant for the rotor, $T_L$ is the load torque, $v_a$ and $v_f$ are the supplied voltages to the armature and the inductance of the field winding [13].

The $k$ and $b_m$ are constant values determined at the design step of a motor. Since the permanent magnet is used in a vibration motor, $v_f$ is also constant. If the rotor rotates in the steady sate, $R_a$ and $T_L$ become constant. Hence, the relation Eq. 3.1 could be shorten as $w_m = c_1 v_a + c_2$ which represents that the angular velocity of the rotor is linearly proportional to only the supplied voltage to the armature $v_a$. The frequency of a vibration generated from a vibration motor is dependent to the angular velocity which is proportional to the supplied voltage. That means the vibration frequency of a vibration motor is also determined by the supplied voltage.

The amount of mobile device movements actuated by a vibration motor can be derived as follows. As defined in Fig. 3.3, let $\mathbf{c}_r$ be the position of the center of mass of a rotor in a vibration motor, $\mathbf{c}_o$ be that of the other parts of a mobile device except the rotor, and $\mathbf{c}_m$ be that of the mobile device. Their masses are denoted by $m_r$, $m_o$, and $m_m(= m_r + m_o)$, respectively. Also, the center of rotation of the rotor is at $\mathbf{p}_r$, and that of the mobile device is at $\mathbf{p}_m$. When voltage is applied to the motor, these two points rotate with radius of $r_r$ and $r_m$, respectively, whereas $\mathbf{c}_o$ remains fixed at $\mathbf{p}_o$. If we denote the unit vectors in the $x$- and $y$-directions by $\mathbf{u}_x$ and $\mathbf{u}_y$, respectively, then

$$\mathbf{c}_r(t) \;=\; \mathbf{p}_r + r_r \left\{ \sin(2\pi Ft)\mathbf{u}_x + \cos(2\pi Ft)\mathbf{u}_y \right\}, \tag{3.2}$$

$$\mathbf{c}_o \;=\; \mathbf{p}_o, \tag{3.3}$$

$$\mathbf{c}_m(t) \;=\; \frac{m_r\mathbf{c}_r(t) + m_o\mathbf{c}_o}{m_m}. \tag{3.4}$$

Substituting (3.4) with (3.2) and (3.3) results in

$$\mathbf{c}_m(t) = \frac{m_r\mathbf{p}_r + m_o\mathbf{p}_o}{m_m} + \frac{m_r}{m_m}r_r \left\{ \sin(2\pi Ft)\mathbf{u}_x + \cos(2\pi Ft)\mathbf{u}_y \right\}. \tag{3.5}$$

Therefore,

$$r_m = \frac{m_r}{m_m}r_r. \tag{3.6}$$

This indicates that in the steady state, vibration amplitude in position remains constant regardless of vibration frequency in the mobile device.

The relatively simple actuation mechanism of a vibration motor allows one control variable (applied voltage), and this incurs an important limitation for a vibration actuator. The applied voltage is proportional to the motor rotation velocity, and faster rotation induces larger vibration amplitude (in acceleration) and higher frequency. As a consequence, the amplitude and frequency of a vibration signal from the vibration motor cannot be controlled independently, imposing a severe constraint on the generation of vibrotactile waveforms (see Sec. 3.3 for empirical data). Thus, in order to achieve desired perceptual effects, a proper understanding of the relation between applied voltage and vibration characteristics has to be preceded, with the explicit consideration of correlated vibration amplitude and frequency.
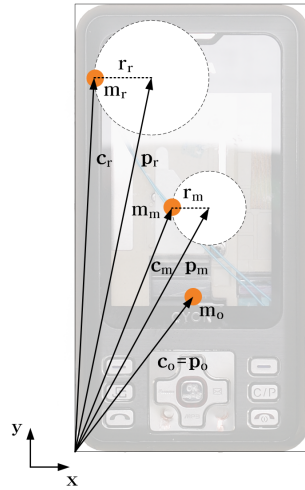
**Fig. 3.3** Coordinate definitions for a mobile device with a vibration motor.

### 3.2.2 Voice-coil actuator

A voice-coil actuator is similar to a typical sound speaker. If a current-carrying coil is placed in a magnetic field produced by a permanent magnet, the *Lorentz force* is being induced. The force is proportional to the applied current and the magnetic flux density. The vibration of the voice-coil actuator is generated by the directional change of the electromagnetic force. When the current direction applied to the tubular coil is changed, the force direction is also changed oppositely. In a voice-coil actuator, a tubular coil is placed into the magnetic field in order to produce the linear movement of the voice-coil. Thus, the sinusoidal AC voltage applied to the voice-coil produces the sinusoidal force of the moving part which might be the coil or the magnet, and then a vibration is generated. Fig. 3.4 shows the internal structure of the voice-coil actuator, VBW-32, used in our research.

To theoretically analyze the characteristics of a voice-coil actuator, we assume that the case of a voice-coil and internal mass are linked by using a spring with the spring stiffness and the user's skin is also modeled with mass, stiffness, and resistance [61]. The dynamic model with the human skin and voice-coil actuator can be represented as
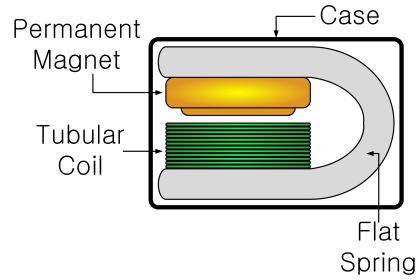
**Fig. 3.4** The internal structure of a voice-coil actuator (Audiological Engineering Corp.; VBW-32).

$$\frac{x}{F} = \frac{A}{B + jC} \tag{3.7}$$
$$A = m_2 w^2$$
$$B = m_1 m_2 w^4 - ((k_1 + k_2)m_2 + k_2 m_1)w^2 + k_1 k_2$$
$$C = -m_2 b w^3 + k_2 b w$$

where $x$ is the displacement of the case, $F$ is the applied force, $m_1$ and $m_2$ are the mass of combined case and skin and internal part, $k_1$ and $k_2$ are the spring constant for the skin and internal mass suspension, $b$ is the damping factor for the skin, and $w$ is the angular velocity [61]. By simulating the model Eq. 3.7, the maximum amplitude is obtained with a peak at the resonance frequency [61]. The peak becomes higher when internal mass $m_2$ is relatively large.

Whereas the vibration motor has a character which is correlated frequency and amplitude of the generated vibration, the voice-coil actuator is able to generate vibrations with the variety of frequencies and amplitudes independently controlled. The resonance frequency of the voice-coil actuator can be designed differently by determining the internal mass $m$ and spring stiffness $k$.

$$f = \frac{w}{2\pi} = \frac{1}{2\pi}\sqrt{\frac{k}{m}} \tag{3.8}$$

That means we can make many special voice-coil actuator for various purpose and environments in which it used.

Obviously, the voice-coil can also generate a vibration with other frequencies different to the resonance frequency. The vibration amplitudes with other frequencies, however, would be much smaller then that with the resonance frequency. As a consequence, the voice-coil actuator has narrow frequency bandwidth in which an enough large vibration is able to be generated.

## 3.3  Experiment I : Physical Characteristics

In our study, we measured the physical characteristics of vibrations emanating from a voice-coil actuator embedded in mobile device held in the hand and the captured data were analyzed in order to find an adequate I/O relation. For comparing with the physical characteristics of a voice-coil actuator, we will also provide the summary of that of a vibration motor referred from [31, 32].

### 3.3.1  Experiment Common Methods

This section describes the details of experiment design.

**Apparatus**

A cellular phone (LG Electronics; model KH-1000) was selected as a representative mobile device. The phone had the size of $51.6 \times 98 \times 22.15$ mm and weighed 101.6 g. Since the original phone had a closed architecture that did not allow direct access to the vibration motor, a phone case available in a repair kit shown in Fig. 3.5a was used in experiments. As shown in the figure, the phone case for repair did not include a few main parts such as a LCD panel.

In this experiment, either a coin-type vibration motor (LG Innotek; model MVMF-A345A; diameter = 10 mm) or a voice-coil actuator (Audiological Engineering Corp.; model Tactaid VBW-32; weight = 10.0 g with an adapter) vibrated the mobile phone used in Experiments I and II. As shown in Fig. 3.6, the vibration motor was included in the phone. The voice-coil actuator was installed on the bottom of the phone using a custom-made adapter since the actuator was thicker than the phone. We preferred the Tactaid voice-coil

actuator to the smaller LRA (Linear Resonant Actuator) currently used in full touch-screen mobile phones since the frequency bandwidth of LRA is very narrow. The Tactaid actuator has also been used frequently in haptics research. A triaxial high-precision miniature accelerometer (Kistler; model 8765A; weight = 6.4 g) was rigidly attached onto the phone using adhesive wax to capture vibration acceleration. Both the voice-coil actuator and accelerometer were not in contact with the participant's hand during the experiment. The total weight of the mobile phone with the vibration motor was 120 g (with the plastic weights inside the phone), and that with the voice-coil actuator was 111.6 g (without the plastic weights to compensate the adapter weight). The actuators and accelerometer were controlled by a PC using a data acquisition board (National Instruments; model PCI-6229).

The coin-type vibration motor was placed horizontally, in parallel to the plane spanned by the width and height directions of the phone (i.e., $xy$ plane in Fig. 3.6). In this case, a rotor with eccentric mass distribution in the motor rotated in the $xy$ plane, and its vibration energy was evenly distributed on the plane (see Appendix B). We thus aligned the $x$- and $y$-axes of the accelerometer to be in the width and height directions, respectively. Vibration in the $z$-direction was substantially weaker (about 1/10). On the other hand, the voice-coil actuator vibrated in one direction ($y$-direction), similarly to the shaker.

**Participants**

Ten university students (five for each actuator) participated in this experiment. Their task was simply to grab the mobile phone comfortably. This was to average the effect of individual differences in skin impedance and gripping force on the measurements of vibration stimuli.

**Procedure**

To drive the vibration motor, ten constant voltages in 1 – 5.5 V with 0.5 V step size were used. The angular velocity of a rotor is proportional to input voltage to a vibration motor. Thus, a DC input produces a sinusoidal vibration in a vibration motor. In a voice-coil actuator, a sinusoidal voltage waveform needs to be applied to obtain a sinusoidal vibration

(a) A mock-up phone

(b) A vibration motor

(c) A voice-coil
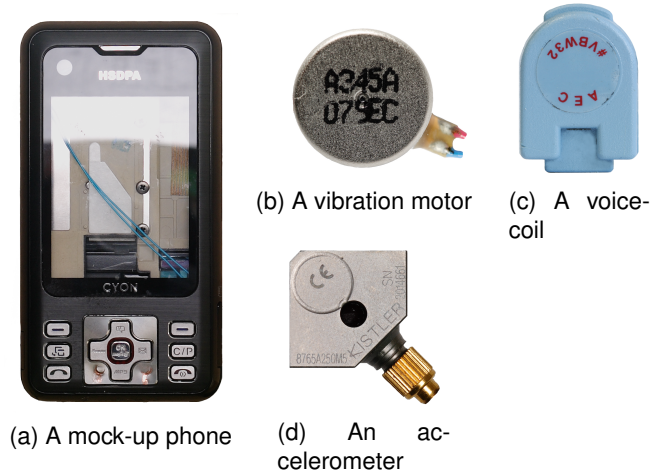
(d) An accelerometer

**Fig. 3.5** A mock-up phone, a vibration motor, a voice-coil actuator and an accelerometer used in experiments.

output. We prepared 168 sinusoidal waveforms by combining 14 frequencies in 50 – 500 Hz (50, 100, 150, 200, 220, 250, 260, 280, 300, 320, 350, 400, 450, and 500 Hz) and 12 amplitudes in 0.1 – 3.0 V (0.1, 0.3, 0.5, 0.55, 0.6, 0.8, 1.0, 1.2, 1.5, 2.0, 2.5, and 3.0 V). The use of finer resolutions in 200 – 350 Hz and 0.5 – 0.8 V was to obtain more detailed data in an input region with better performance found in pilot experiments.

In each trial, a vibration actuator was excited for 1 s, and the resulting vibration acceleration was measured at a sampling rate of 10 kHz. The participants were instructed to comfortably hold the cellular phone in the hand that they usually use to grasp a cellular phone. Average gripping force for an ungrounded mobile device was measured to be 1.75 N with a standard deviation of 1.42 N (see Appendix A). The values were similar to those of the grounded case. The accelerations collected in this way represent the vibrotactile proximal stimuli delivered to the hand skin during the ordinary usage of a mobile device. For the vibration motor, we collected acceleration in the $x$-axis (vibrations in the $x$- and $y$-axes were almost the same). For the voice-coil actuator, acceleration along the $y$-axis was measured. Prior to a next trial, a break was enforced so that the skin impedance was fully restored.
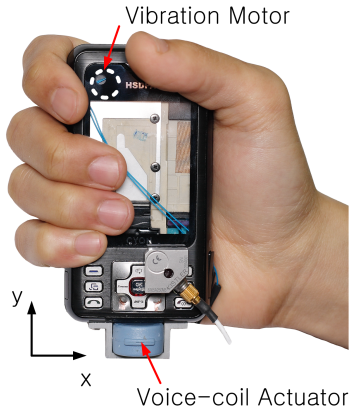
**Fig. 3.6** Experimental setting for Experiment I. The vibration motor was installed inside the phone case. When the vibration motor was used, the voice-coil actuator was not attached.

For analyzing the captured raw data of the vibration accelerations, same procedures – Fast Fourier Transform (FFT) for finding the principle frequency and amplitude conversion from acceleration to displacement – represented in [32] were used.

### 3.3.2    Results: Vibration Motor

The physical characteristics of vibrations generated by the vibration motor are summarized in Fig. 3.7 as a function of applied voltage. The error bars represent standard deviations. Fig. 3.7a presents average principal frequencies taken from the power spectral densities of acceleration measurements. As applied voltage increased from $v = 1.0$ to 5.5 V, the average principal frequency increased from 65 Hz to 284 Hz, but the rate of frequency increase was reduced in high voltages. The principal frequencies were very consistent with very small standard deviations, except for very high applied voltages of 5 and 5.5 V.

Vibration amplitudes in acceleration at the principal frequencies were also found from the power spectral densities, and averaged for each applied voltage. The results are plotted in Fig. 3.7b. The average vibration amplitudes in acceleration increased from 0.14 G at $v = 1.0$ V to 2.61 G at $v = 5.5$ V, with the increase rate diminished after $v \geq 4$ V. The variability of vibration amplitudes was also much larger for $v \geq 4$ V, indicating that vibration motor operation was not very reliable in the high voltage range. Vibration amplitudes
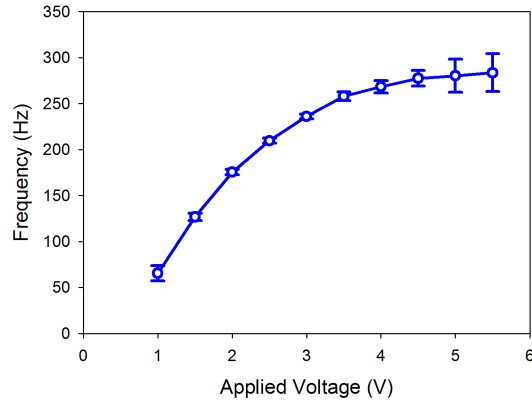
(a)Principal frequency.
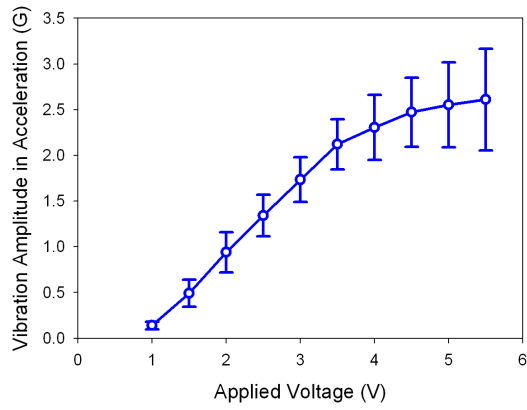


(b)Acceleration amplitude.
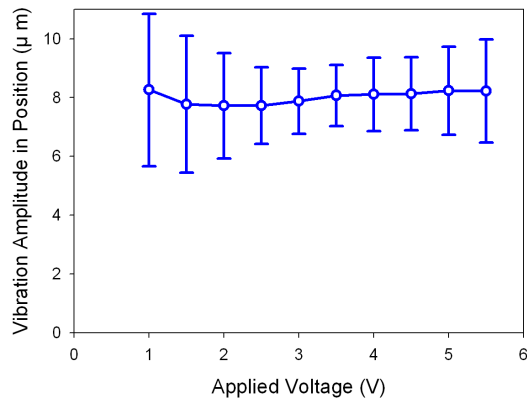


(c)Position amplitude.

**Fig. 3.7** Physical characteristics of vibrations generated by the vibration motor.

in position calculated using the principal frequencies and the amplitudes in acceleration were also averaged, and are shown in Fig. 3.7c. They varied in a range of 7.5 – 8.1 $\mu$m with consistent standard deviations, constituting a nearly flat line. This was to be expected, since the movement of a mobile device driven by a vibration motor is circular and its movement radius should be constant in the steady state (see Sec. 3.2.1).

In general, the rotor angular velocity of a DC motor is linearly proportional to voltage applied to the motor for a constant load [72] (recall that the vibration motor is a DC motor). However, increasing a load exerting on the motor leads to more current flow into the motor for more torque and reduces the motor rotation speed. In the present experiment, the mobile phone was grasped by the participant's hand (mostly in contact with the fingers and palm), which worked as a mechanical load to the vibration motor in addition to the mobile phone case. Thus, the mechanical impedance of the hand needs to be considered for proper understanding of the loading effect. Research in biomechanics demonstrated that the mechanical impedance of the fingers or the palm increases with frequency above 100 Hz [14]. In our measurements in Fig. 3.7a, applied voltages larger than 1.5 V resulted in average principal frequencies higher than 100 Hz. Taken together, the increasing mechanical impedance of the fingers and palm is responsible for the decreasing rate of principal frequency increase observed in the voltage range of 1.5 – 5.5 V. It also needs to be remarked that when loading effect is relatively weak, principal vibration frequency grows almost linearly with applied voltage. Two such cases were previously observed, when a vibration motor itself was attached on the thenar eminence [32] or placed on an impedance head [29].

### 3.3.3  Results: Voice-coil Actuator

Generally, a voice-coil actuator generates unidirectional vibrations in height direction of them, differently to the omnidirectional vibrations of a vibration motor. The waveform of the voice-coil vibration is formed like a sinusoidal waveform, when AC voltage is applied. Fig. 3.8a shows well-formed generated vibration captured from the voice-coil actuator with the applied frequency of 250 Hz. The blue dashed line represents the measured acceleration of the emerging vibration with grey dotted line as a reference of a pure sine wave. However,

(a) 250 Hz.
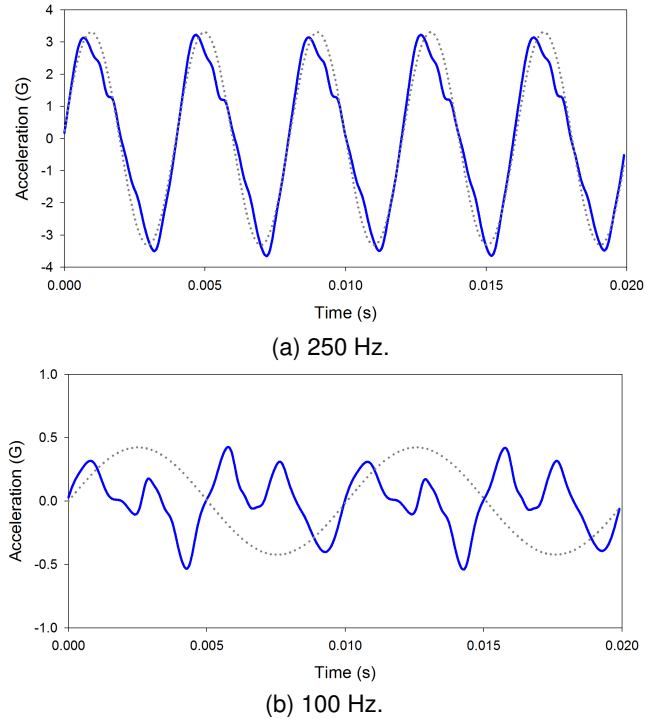


(b) 100 Hz.

**Fig. 3.8** The measured acceleration of the VBW-32 with 250 and 100 Hz frequencies and 1.0 V voltage amplitude.

the hardware limitation makes the output frequencies inconsistent at some range of the input frequencies. For example, whereas the measured acceleration of the VBW-32 for the applied frequency of 250 Hz was formed similar to the pure sine wave of 250 Hz in Fig. 3.8a, for 100 Hz the acceleration had arbitrary fluctuation and was very different to the pure sine wave of 100 Hz in Fig. 3.8b.

Fig. 3.9 presents the physical characteristics of vibrations produced by the Tacaid voice-coil actuator. In Fig. 3.9a, the average principal frequencies of vibration outputs are shown for each input frequency with the error bars indicating standard deviations. It can be seen that only vibrations with input frequencies larger than 200 Hz preserved the input frequencies. The operation of the voice-coil actuator for input signals with lower frequencies were rather erratic with very large variances. This is partly due to the operating principle of a voice-coil actuator. A voice-coil actuator contains mass and spring elements, and makes use

(a)Principal frequency.



(b)Amplitude in Position.
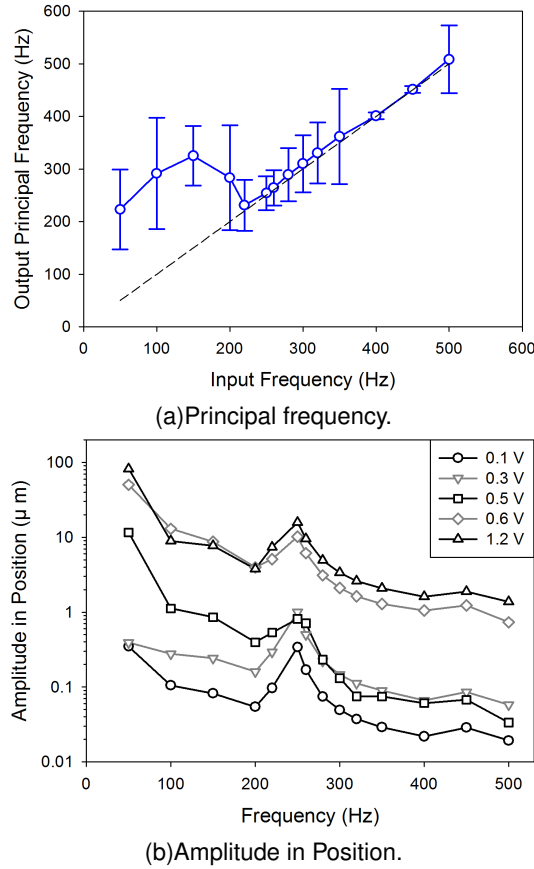
**Fig. 3.9** Physical characteristics of vibrations generated by the voice-coil actuator.

of their mechanical resonance to produce high-amplitude vibration. The nominal resonance frequency of the voice-coil actuator was 250 Hz.

Vibration amplitudes in position induced by the voice-coil actuator are shown in Fig. 3.9b. Out of 12 input amplitudes used in the experiment, the results of only 5 input amplitudes are included for visibility. The data indicate that the magnitude gains of the voice-coil actuator were not linear. The gains were relatively low for input amplitudes in 0.1 – 0.5 V, and increased abruptly in 0.5 – 0.6 V. Further increase of input amplitude did not result in noticeable output increases. Distinct peaks were also observed at 250 Hz, which is the resonance frequency of the actuator.

## 3.4 Experiment II : Perceptual Characteristics

This section reports the subjective perceived intensities of cellular phone vibrations by using a voice-coil actuator with the absolute magnitude estimation [75]. Investigating the perceived intensities would be able to provide a useful design guideline for the driving conditions of mobile device vibration rendering. For comparing with the perceptual characteristics of a voice-coil actuator, we will also provide the summary of that of a vibration motor referred from [31, 32].

### 3.4.1 Experiment Common Methods

Experimental methods common to Experiment I will be not repeated in this section for conciseness.

**Apparatus**

The hardware setup of this experiment was identical to that of Experiment I.

**Participants**

Ten participants (22 – 31 years old with average 25.4) participated in the experiment for the vibration motor, and another ten participants (23 – 31 years old with average 25.2) in the experiment for the voice-coil actuator. All participants were everyday users of a mobile device, and reported no known sensorimotor abnormalities. They were compensated after the experiment.

**Procedure**

In order to estimate the subjective intensities of vibration perception, we used the absolute magnitude estimation paradigm [75] (also see [18] for a review). Each participant finished three sessions. The first session was treated as training, and its results were discarded. In each trial, the participant held the cellular phone in the right hand, felt vibrations driven at the corresponding voltage signal for 1 second, and typed in its absolute subjective intensity

using a keyboard with the left hand in free scales without a standard stimulus. A next trial began in 1 second after the participant response.

After finishing each session, the participants were asked to take a 3-min break. The standard instructions (p. 254 in [18]) for absolute magnitude estimation were translated in Korean and presented to the participants before beginning the experiment. Throughout the experiment, the participants wore headphones that played white noise to prevent any auditory effects from the mobile phone. It took about 15 – 30 minutes to finish the experiment per each participant.

Input signals for the vibration motor were ten DC voltages in 1 – 5.5 V with 0.5 V step size. Those for the voice-coil actuator were 24 sinusoidal waveforms the parameters of which were the combinations of 6 frequencies (220, 250, 260, 280, 300, and 320 Hz) and 4 amplitudes (0.6, 0.8, 1.0, and 1.2 V). 250 Hz was included instead of 240 Hz since 250 Hz was the nominal resonance frequency. The selected parameter range included the well-responding range of the voice-coil actuator observed in Experiment I. The order of input signals to be presented was randomized per each session and each participant.

**Data Analysis**

The results of each participant were normalized following [44]. We first computed the geometric mean ($M_p$) of the all responses from the last two sessions for each participant, and the grand geometric mean ($M_g$) of the responses of all conditions and all participants. Then, a normalization constant for the participant was computed by $M_n = M_g/M_p$. This normalization constant was multiplied to the responses of the participant to obtain normalized perceived intensities.

### 3.4.2 Results: Vibration Motor

The perceived intensities of mobile device vibrations produced by the vibration motor were averaged across all participants, and the results are shown in Fig. 3.10. The error bars represent standard deviations. Overall, the average perceived intensity tended to increase with applied voltage, but its increase rate was slowed down after $v \geq 3.5$ V. Indeed, Tukey's
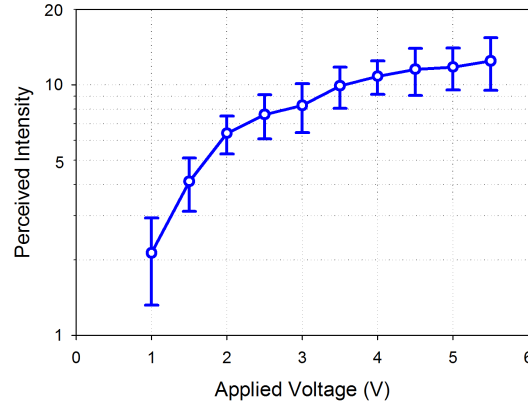
**Fig. 3.10** Mean perceived intensities of the vibration motor measured in [31, 32].

HSD test confirmed that the perceived intensities for $v \geq 3.5$ V were not statistically different ($q(0.95; 9, 190) = 4.53$; minimum significant difference = 2.72). This suggests that for the vibration motor used in the experiment, driving the motor with higher voltages than 3.5 V is not beneficial for perceived vibration strength, while using more electric power.

### 3.4.3 Results: Voice-coil Actuator

Average perceived intensities for the voice-coil actuator are provided in Fig. 3.11 for each input frequency and Fig. 3.13. Overall, given an input amplitude, the perceived intensities exhibited an inverted V-shape as a function of frequency with distinct peaks at 250 Hz. The perceived intensities of 250 Hz vibration were much larger than those of the other frequencies for all input amplitudes. This was because the voice-coil actuator had the largest amplitude gain at 250 Hz (Fig. 3.9b) and the detection threshold was also the smallest around 250 Hz (Fig. 3.12). Except the vibrations of frequencies 250 and 260 Hz, the other vibrations resulted in fairly low perceived intensities smaller than 5. As a result, the voice-coil actuator should be driven with 250 Hz input signals to provide sufficiently large perceived intensity. Other input frequencies around 250 Hz can still be used to make diverse vibration effects, but their discriminability from 250 Hz vibration is in question due to the relatively poor human discriminability of frequency.
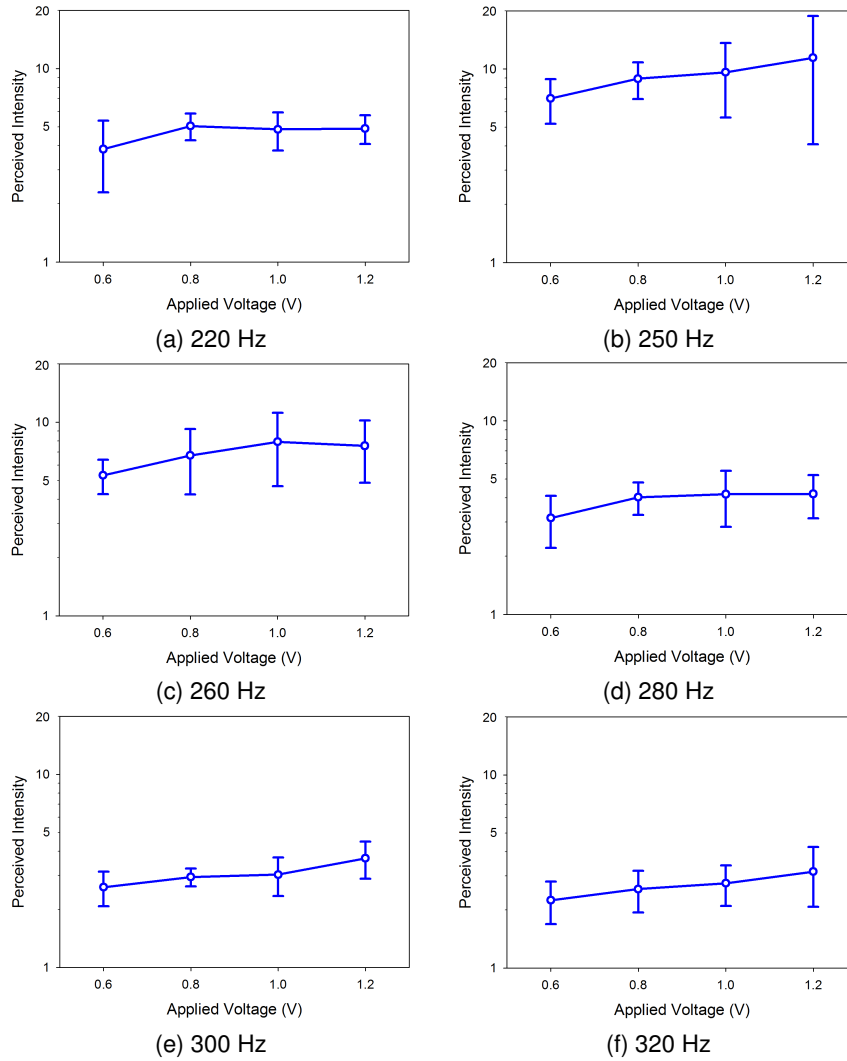
**Fig. 3.11** Mean perceived intensities of the voice-coil actuator (VBW-32) measured in Experiment II.
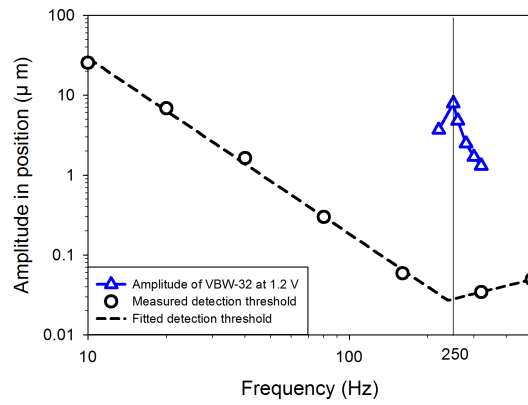
**Fig. 3.12** Amplitude in position at 1.2 V and detection threshold measured in [31].
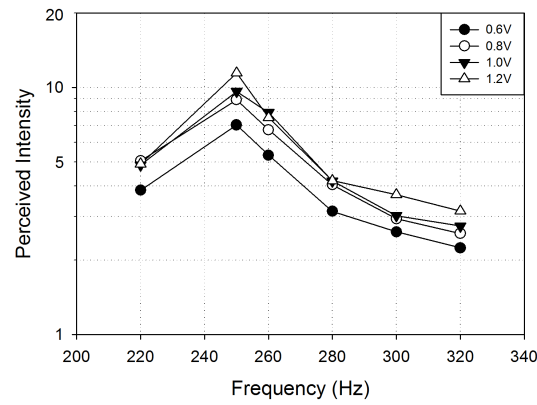


**Fig. 3.13** Perceived intensities of the voice-coil actuator (VBW-32) along with all voltage amplitudes.

# Chapter 4

# Vibration Perception Model

In Chapter 4, we established the vibration perception model for mobile device vibrations by measuring subjective perceived intensities. The measured perceived intensities at the various frequencies and amplitudes in sensation level could be used to understand the perceptual characteristic of vibration actuators in a mobile device.

## 4.1 Experiment III : Psychophysical Magnitude Function

As discussed earlier, perceived intensity is one of the most salient cues for mobile device vibration. In this experiment, we measured the perceived intensities of mobile device vibrations for various frequencies (10 – 500 Hz) and amplitudes (6 – 45 dB SL[1]) using the mini-shaker system. We then regressed a mathematical function to the measured perceived intensities in order to obtain a psychophysical magnitude function. The function can be used to predict the perceived intensity of mobile device vibration from its frequency and amplitude.

### 4.1.1 Methods

This section presents the details of the experiment design.

---

[1]Sensation level in decibel $= 20 \log_{10}(A/AL)$, where $A$ is the signal amplitude and $AL$ is the corresponding absolute limen.
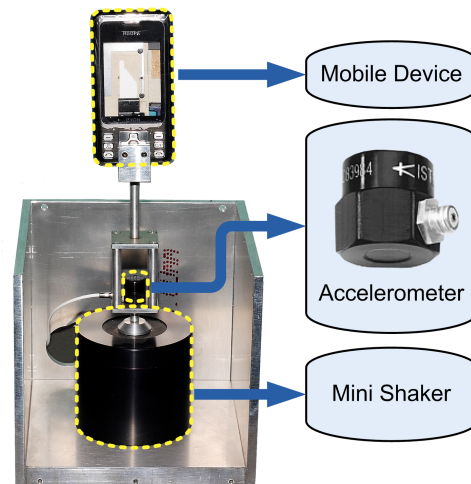
**Fig. 4.1** Mini-shaker system used to measure perceived intensities of vibrations. The front and roof panel is removed for illustration.

### Apparatus

The apparatus used in this experiment is shown in Fig. 4.1. The key component was a commercial mini-shaker (Brüel & Kjær; model 4810) that has high precision and repeatability in a wide bandwidth (18 kHz in the unloaded condition).

The shaker was placed inside a heavy metal enclosure to prevent ambient interferences. A cellular phone (LG Electronics; model KH-1000; size = $51.6 \times 98 \times 22.15$ mm; weight = 120 g) was connected to the shaker through a rigid adapter, and protruded through a hole in the top plate of the enclosure so that it could be grasped by the hand. The phone was taken from a repair kit, and did not have a few parts such as a LCD panel. A high-precision accelerometer (Kistler; model 8630C) was also attached inside the adapter. The total weight of the vibrating assembly including the dynamic mass of the shaker was 183.3 g.

The shaker system was controlled by a computer using a data acquisition board under an open-loop control scheme. An analog signal generated from the board passed through a high-bandwidth linear power amplifier (Brüel & Kjær; model 2718), and the amplifier output excited the shaker vertically (along the length direction of the cellular phone). The accelerometer output was captured by a 16-bit analog-to-digital converter at a sampling rate

of 10 kHz using the data acquisition board.

Since the shaker has frequency-dependent gains, we identified the relationship between input (voltage command in a program) and output (vibration measured by the accelerometer) in the unloaded condition. At each test frequency, the shaker was driven with sinusoidal voltage waveforms of ten amplitudes, and corresponding vibration amplitudes were retrieved from the power spectrum density of measured acceleration. These vibration amplitudes in acceleration, $A_{acc}$, were converted to equivalent amplitudes in position, $A_{pos}$, by $A_{pos} = A_{acc}/(2\pi F)^2$, where $F$ is the signal frequency. This is equivalent to finding the amplitude of a sinusoidal waveform in position by integrating the sinusoidal waveform in acceleration twice, yet more robust to noises. A straight line was then fitted to the data using the least-square estimation, which usually showed very high accuracy ($R^2 = 0.99$). The inverse of the I/O relationship was used to determine a voltage amplitude for a desired vibration amplitude. This procedure was repeated for all frequencies used in the experiment.

The cellular phone on the shaker system vibrated along the length direction, and was mechanically grounded. In contrast, other miniature vibration actuators commonly used in mobile devices, such as a vibration motor or a voice-coil actuator, may have different vibration directions. They also provide ungrounded feedback; the device weight is entirely supported by the hand. However, such actuators were not eligible to Experiment III where highly precise vibrotactile stimuli were required in a wide frequency range. Therefore, our strategy was to use the shaker system, and then carefully consider the differences in comparing and analyzing the data in Sec. 3.3 and Sec. 3.4.

**Participants**

Eleven university students (eight males and three females; $23-27$ years old with an average of 25.1; all right-handed and native Koreans) took part in this experiment. All participants reported that they were everyday users of a mobile device and that they had no known sensorimotor abnormalities. The participants were compensated after the experiment.

**Procedure**

We measured the perceived intensities of sinusoidal vibrations generated by the shaker system in Fig. 4.1. Five frequencies (20, 40, 80, 160, and 320 Hz) and six amplitudes (6, 10, 20, 30, 40, and 45 dB SL) were combined, resulting in a total of 30 experimental conditions. Two frequencies, 10 and 500 Hz, which were included in [31] for absolute threshold measurement were excluded in this experiment. The shaker system were unable to reliably produce vibrations with large amplitudes at the two frequencies. It is noted that vibrotactile signals at such low or high frequencies are rarely used in actual mobile device applications.

In order to estimate the perceived intensity, we used the absolute magnitude estimation paradigm [75]. Each participant finished three sessions each of which presented the 30 vibrations in a random order. The first session was considered as training, and its results were discarded. In each trial, the participant held the cellular phone in the right hand, perceived a vibration for 1 s, and answered its perceived intensity in free scales without a modulus (standard stimulus) using a keyboard with the left hand (see Fig. 4.3). A next trial began in 1 s after the participant's response. After each session, the participant was required to take a break of three minutes. The participant wore a headphone that played white noise to block faint sound emanating from the shaker. Prior to the experiment, the participants were given the standard instructions of absolute magnitude estimation, which were taken from [18, p. 254] and translated to Korean. It took approximately 30 minutes to finish the experiment.

To command vibration amplitude in sensation level, we computed input voltage amplitude to the shaker using the calibrated I/O relation described in Sec. 4.1.1 and the absolute thresholds measured in [31] (see Fig. 4.2). We also recorded acceleration readings during the experiment, and computed errors between the desired and measured displacements to assess the loading effect of the participant's hand.

**Data Analysis**

The results were normalized following [44]. From the data of each participant, we first computed the geometric mean of the 60 responses from the last two sessions, $M_p$. The
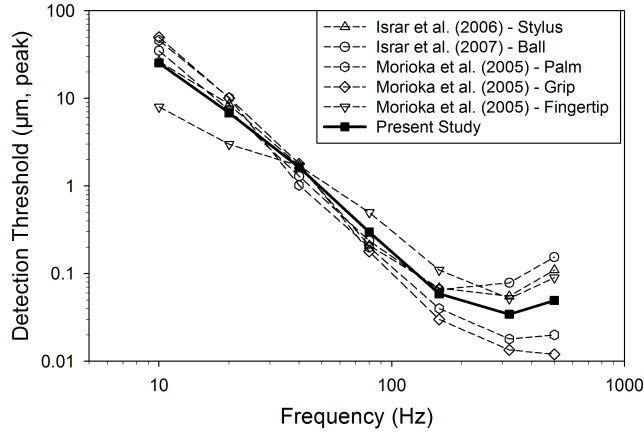
**Fig. 4.2** Detection thresholds of sinusoidal vibrations transmitted to the hand through the cellular phone (reprint from [31]).



**Fig. 4.3** A subject performing Experiment III for measuring the perceived intensities (reprint from [31]).

grand geometric mean of the responses of all conditions and all participants, $M_g$, was also calculated. Then, a normalization constant for the participant was computed by $M_n = M_g/M_p$. This normalization constant was multiplied to the responses of the participant to obtain normalized perceived intensities.

### 4.1.2   Results

We first computed absolute errors between the commanded and captured vibration amplitudes caused by the loading effect of the participant's hand. The absolute errors were very small (0.98 dB on average), and did not exhibit noticeable patterns, except that they were relatively larger at low frequencies (20 and 40 Hz). In Experiment III, however, the errors were rather insignificant compared to the stimulation levels, thus were not compensated in the subsequent analysis.

**Psychophysical Magnitude Function**

Fig. 4.4a – Fig. 4.4e show the average perceived intensities as a function of vibration amplitude for each frequency. In each plot, the circles represent the perceived intensities with the error bars indicating standard deviations. At each frequency, the measured perceived intensities linearly increased with the logarithm of vibration amplitude (note that the amplitude is in dB SL). In Fig. 4.4f, the same data are redrawn as a function of frequency for each amplitude.

In all the plots, the triangles represent points taken from a best-fitting surface shown in Fig. 4.5, which was obtained using the following non-linear regression model:

$$\log_{10} I = A \sum_{i=0}^{4} \alpha_i (\log_{10} F)^i + \sum_{i=0}^{4} \beta_i (\log_{10} F)^i, \tag{4.1}$$

where $I$ is perceived intensity, and $A$ and $F$ are vibration amplitude in dB SL and frequency in Hz, respectively. Given frequency $F$, this regression model is linear to $A$ following Steven's power law ($A$ is already logarithmic in sensation level)[2]. Modeling the exponent and scaling constant of the power function to depend on frequency and interpolating them using the fourth order polynomials of $\log_{10} F$ yielded the best fit. The best-fittings values of $\alpha_i$ and $\beta_i$ are given in Table 4.1. $R^2$ was 0.7622, but a few large standard deviations in Fig. 4.4b and Fig. 4.4c did not allow us to improve $R^2$ further. However, $R^2$ of the model regressed with averaged perceived intensities was 0.9666, it is larger than that regressed

---

[2]In Stevens' power law [60], $\psi = k\phi^a$, where $\psi$ is a sensation magnitude and $\phi$ is a stimulus intensity. Equation 4.1 is in its logarithmic form.
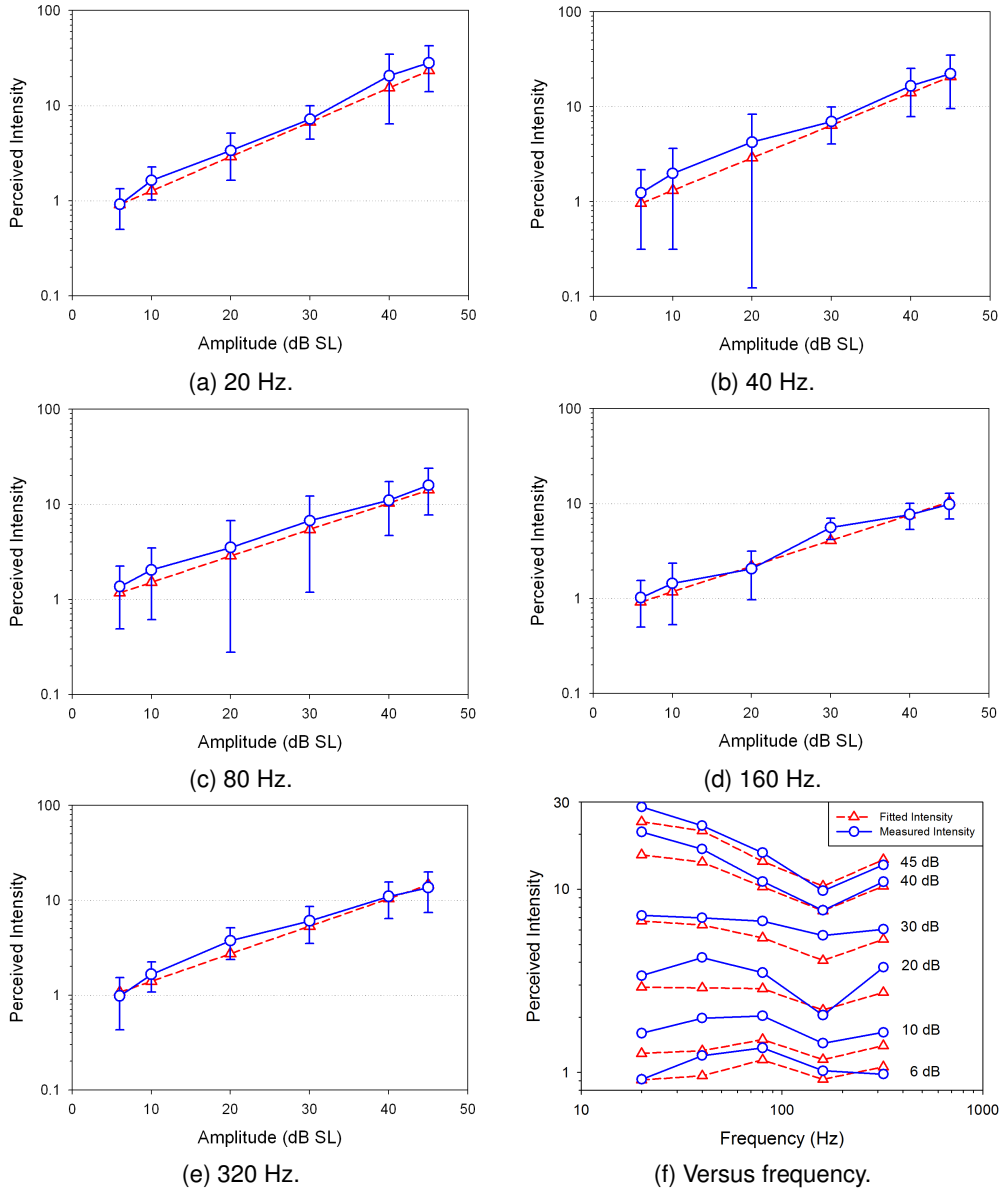
Fig. 4.4: Vibration amplitude versus perceived intensity (a – e), and frequency versus perceived intensity (f). The circles represent the measured values, and the triangles represent those from the fitted model in Fig. 4.5.
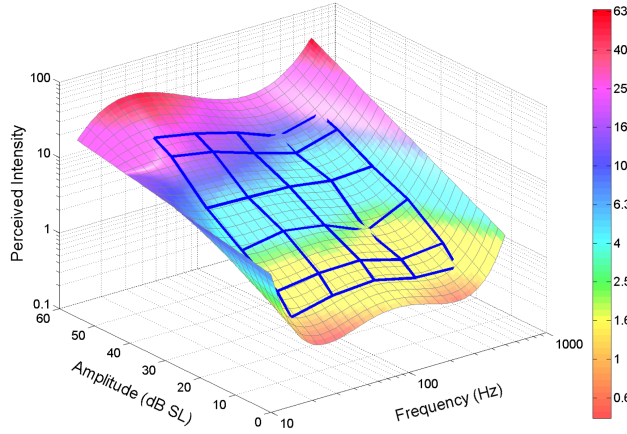
**Fig. 4.5** 3D representation of the perceived intensities (solid lines). Also shown with a color map is a best fitting surface.

**Table 4.1** Coefficients of the psychophysical magnitude function.

| Coefficient index ($i$) | 0 | 1 | 2 | 3 | 4 |
|---|---|---|---|---|---|
| $\alpha_i$ | -0.8592 | 1.9688 | -1.5739 | 0.5419 | -0.0682 |
| $\beta_i$ | 39.6979 | -90.4316 | 75.0109 | -27.0254 | 3.5759 |

with individual perceived intensities with large deviations. It can also be confirmed visually in the figure that the fitted surface well accounts for the measured perceived intensities. Therefore, the model in (4.1) with the coefficients in Table 4.1 can be considered as a psychophysical magnitude function of mobile device vibration.

Fig. 4.4f shows that for low vibration amplitudes (6, 10, and 20 dB SL) the perceived intensity initially increased with frequency, then decreased and reached a minimum at 160 Hz, and then increased again until 320 Hz. For an amplitude of 30 dB SL, the perceived intensities were almost constant regardless of frequency. For high amplitudes (40 and 50 dB SL), the perceived intensities formed a V-shaped curve with a minimum at 160 Hz. In addition, the range of the perceived intensities of the same amplitudes differed by frequency. For example, the range was 0.91 – 1.36 at an amplitude of 6 dB SL, and 9.81 – 28.15 at
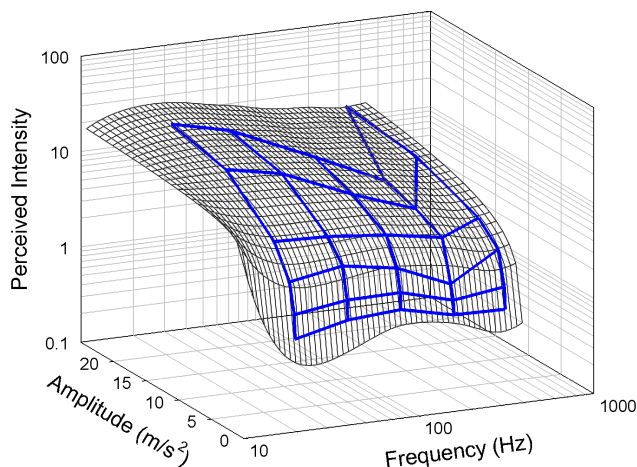
**Fig. 4.6** Another 3D representation of the perceived intensities (solid lines). Vibration amplitudes are specified in acceleration.

45 dB SL. This indicates that the rate of growth of perceived intensity is contingent upon vibration frequency.

The perceived intensities in Fig. 4.5 are redrawn in Fig. 4.6 where vibration amplitudes are specified in acceleration. Given frequency, the perceived intensity increased monotonically with amplitude. Given amplitude, the perceived intensity tended to decrease with frequency, which is consistent with a finding in [74].

### Growth Rate of Perceived Intensity

Whether the rate of growth of perceived intensity with vibration amplitude depends on frequency was a controversial issue [28], with the rate of growth represented by the exponent in Steven's power law. For instance, Verrillo and Capraro showed when the thenar eminence was stimulated by a contactor of 0.28 cm$^2$ area without a surround, the exponents of two different frequencies (60 and 250 Hz) were very similar [69]. In contrast, a recent study by [42] demonstrated clear frequency dependence when a cylindrical handle with 30 mm diameter was grasped in the hand with a much larger contact area. Both studies used the magnitude estimation to measure perceived intensity.
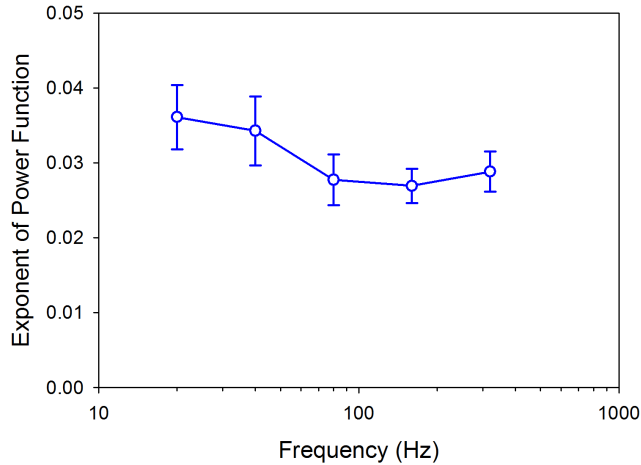
**Fig. 4.7** Exponents of Steven's power law estimated in Experiment III.

Motivated by this, we ran linear regression to find the average slopes of perceived intensity increases for the five frequencies tested in Experiment II, which correspond to the exponents of the power function. The results are provided in Fig. 4.7 with standard errors. With increasing frequency, the exponents initially decreased from 0.036 at 20 Hz to 0.027 at 160 Hz, and then increased to 0.029 at 320 Hz, in a U-shape. ANOVA verified that frequency was statistically significant for the exponent ($F(4, 40) = 3.67$, $p = 0.0122$). Therefore, our data also indicate that vibration frequency affects the rate of sensation growth.

In order to compare our results in Fig. 4.7 with the previous results in [42] and [69], we converted the exponents in Fig. 4.7 in sensation level ($a_{sl}$) to those in acceleration ($a_{acc}$) by $a_{acc} = 20a_{sl}$ (can be easily derived from the power law and the definition of sensation level). The results are summarized in Table 4.2, where values not measured in the studies are interpolated from the neighbor exponents. Compared to [42] and [69], the exponents measured in Experiment III were apt to be larger at the same frequencies, ranging in 0.55 – 0.72. As the experimental methods used in the three studies were not identical, finding direct causes for the larger exponents is not straightforward. However, the most pronounced difference seems to be the contact area; the mobile phone used in the present study stimulated a much larger area on the fingers and the palm. Thus, the exponent differences may

**Table 4.2** Exponents of Stevens' power law representing the rate of sensation growth. Vibration intensities are in acceleration ($\mu$m/s$^2$).

| Frequency (Hz) | 20 | 40 | 60 | 80 | 160 | 250 | 320 |
|:---:|:---:|:---:|:---:|:---:|:---:|:---:|:---:|
| [69] | . | . | 0.40 | . | . | 0.35 | . |
| [42]* | 0.81 | 0.52 | 0.44$^\top$ | 0.46 | 0.41 | 0.44 | 0.32$^\top$ |
| Experiment III | 0.72 | 0.68 | 0.61$^\top$ | 0.55 | 0.54 | 0.55$^\top$ | 0.58 |

*: for the lateral direction ($y$-direction in Fig. 3.3.1). $^\top$: interpolated values.

be related to the spatial summation of the PC channel.

## 4.2   Comparisons of Perceived Intensity

The psychophysical magnitude function for mobile device vibrations in Fig. 4.5 was measured using the shaker in the grounded condition. To evaluate its applicability, the function was compared with the perceived intensities of the two miniature actuators in Fig. 3.10 and Fig. 3.13. For comparison, we first obtained equal sensation contours from the shaker data, as shown in Fig. 4.8. The equal sensation contours represent vibration frequencies and amplitudes that resulted in the same perceived intensity. Perceived intensities are specified on the corresponding contours. The perceived intensities of the miniature actuators were then mapped into the contours, and the results appeared in the upper right side of the figure. It is evident that the parameter range covered by the shaker was incomparably broader than those of the two miniature actuators.

For direct comparison, we interpolated the perceived intensities obtained with the shaker so that they match the vibration frequencies and amplitudes used for the two miniature actuators. The results are presented in Fig. 4.9. In Fig. 4.9a, the predicted perceived intensities from the shaker data are shown in a dashed line, and the perceived intensities measured using the vibration motor are in a solid line. The increasing trends of perceived intensity were remarkably similar between the two actuators. The predicted and actual perceived intensities were highly correlated, with a pearson correlation coefficient $p$ of 0.99. The same
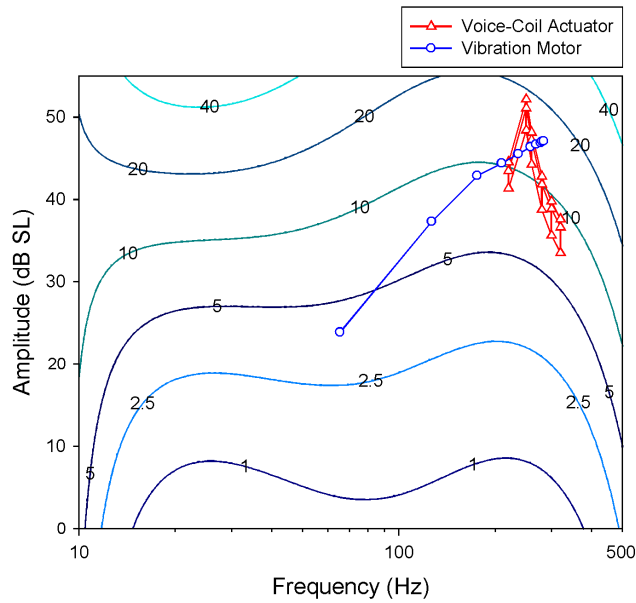
**Fig. 4.8** Equal sensation contours.

can be observed in Fig. 4.9b for the voice-coil actuator. The correlation was also very high, with a coefficient $p$ of 0.97.

However, the perceived intensities obtained using the shaker were consistently larger than those of the miniature actuators by a large amount. In general, the perceived intensity of vibrotactile stimulus is affected by many factors, such as vibration direction [42], grip force [43], and weight [74]. The factors for the present study are summarized in Table 4.3. The table suggests that a main reason was device weight difference; the total weights for the shaker, vibration motor, and voice-coil actuators were 183.3, 120.0, and 111.6 g. It was recently shown in [74] that mobile device weight is an important factor that increases the perceived intensity.

The average ratio between the perceived intensities of the shaker and the vibration motor was 138%, and that of the shaker and the voice-coil actuator was 240%, even though the total weight difference between the vibration motor and the voice-coil actuator was very small (8.4 g). Vibrations produced by the vibration motor was two-dimensional in the $xy$
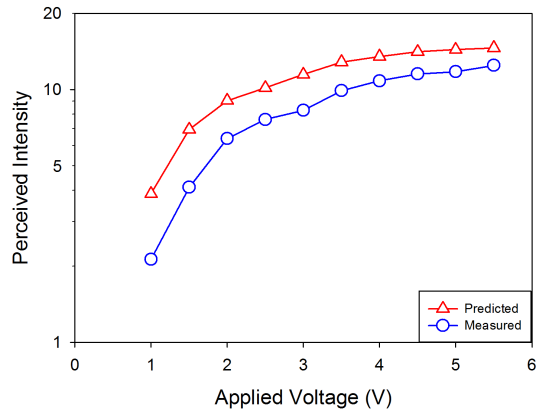
(a)Vibration motor and shaker.
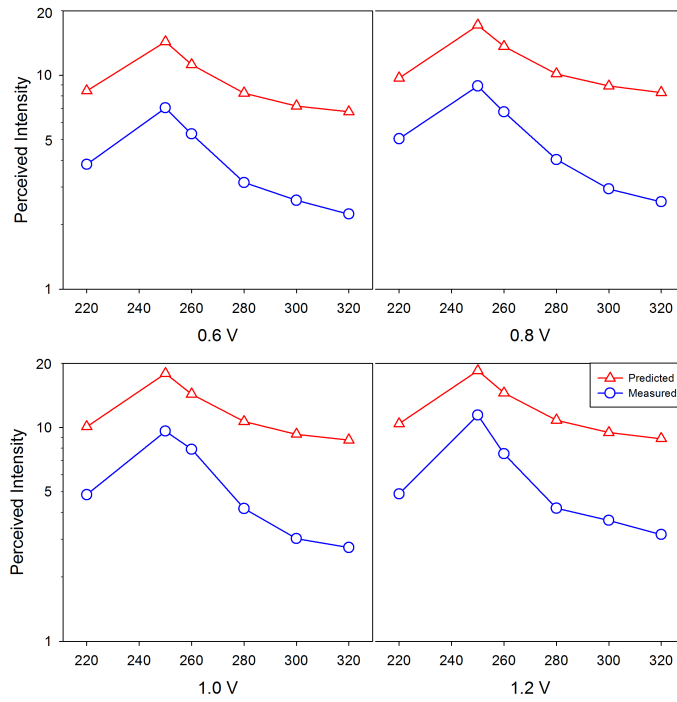


(b)Voice-coil actuator and shaker.

**Fig. 4.9** Comparisons of perceived intensities induced by different actuators.

**Table 4.3** Comparison of experimental setups between the three vibration actuators.

| Actuator | Shaker | Vibration motor | Voice-coil Actuator |
|---|---|---|---|
| Vibration direction | $y$ axis | $x$ & $y$ axes | $y$ axis |
| Phone holding | Grounded | Ungrounded | Ungrounded |
| Grip force | 1.79 N | 1.75 N | 1.75 N |
| Total weight | 183.3 g | 120.0 g | 111.6 g |

plane, stimulating the hand in both the fore-aft and lateral directions (corresponding to the $x$- and $y$-axes in our notation), whereas those by the voice-coil actuator stimulated the hand only along the lateral direction. This may have contributed to the larger perceived intensity of the vibration motor for the same frequency and amplitude.

In addition, the current data do not clearly suggest the effects of phone-supporting condition (grounded/ungrounded). The grip forces were even similar (Appendix A).

The above comparisons allow us to make two conclusions. First, the psychophysical magnitude function measured in Experiment III can be reliable at predicting the changing trends of the perceived intensities of mobile device vibrations produced by miniature vibration actuators. Second, the actual values of the psychophysical magnitude function needs to be scaled up or down depending on the weight of a mobile device. Exact formulas for the scaling is yet unknown.

# Chapter 5

# Perceptually Transparent Vibration Rendering (PTR)

In Chapter 5, we proposed the perceptually transparent vibration rendering in a mobile device and evaluated its benefits in term of pair-wise relative discriminability and absolute identification.

## 5.1 Perceptually Transparent Rendering Framework

Consider a system that has an input $x$ and an output $y$ with a system function $y = f(x)$. If the system function is known and invertible, one can constitute an identity system by cascading $f(x)$ with its inverse $f^{-1}(x)$. This allows to obtain desired system output $y$ by simply setting (identity system input = desired output $y$), without any interferences from the system dynamics. Needless to say, this completely "transparent" system has been pursued in many scientific disciplines such as inverse dynamics control.

In the context of haptics, the transparency of a haptic interface has been extensively studied in order to minimize the effect of interface dynamics upon the proximal stimulus that the user feels from the device [35]. This concept can be extended to *Perceptually Transparent Rendering (PTR)* by also taking into account the corresponding perception process. Cascading the haptic interface dynamics with the perception function may allow to form an I/O
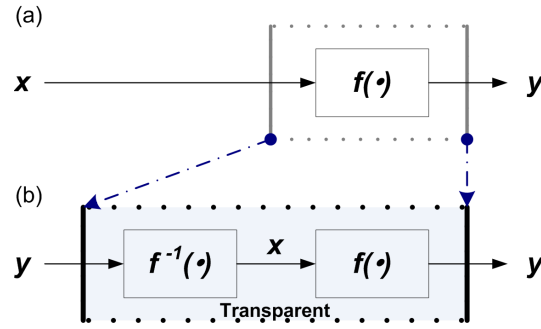
**Fig. 5.1** Block diagrams of (a) a general system and (b) the corresponding identity system.

relation from device command to resulting percept. Using the inverse of I/O relation would enable PTR, but it is often infeasible to empirically find such a system function due to the associated complexity. The I/O relation, physical signal as input and perceived intensity as output, would be defined by conducting the psychophysical experiment of each actuator, such as Sec. 3.4, but the relation could be defined easily by using perception model obtained in Experiment III and device dynamics model obtained in Experiment I. Using two perception and device dynamics model for obtaining I/O relation is explained in Sec. 4.2.

In our previous study [53], however, we claimed that PTR can be applied to vibration rendering in mobile devices where a vibration motor is used. It is because an I/O function from voltage applied to the vibration motor to the perceived intensity of resulting mobile device vibration can be modeled using a simple monotonic function [32]. As a follow-up study, the present study experimentally demonstrates the benefits of PTR for mobile device vibration rendering. In a psychophysical experiment, the discriminability of two vibrations stimulated at different levels was measured, increasing the number of vibration stimuli from 4 to 7. For each case, one set was designed such that stimuli were evenly spaced in terms of applied voltage, and the other set in terms of perceived intensity, that is, PTR was applied to this stimulus set. The results indicated that the stimulus sets that followed the principle of PTR led to much more reliable discrimination.

The common practice prior to PTR was that vibration patterns are designed for a physical variable (e.g., applied voltage) that will be sent to a vibration display (e.g., a mobile
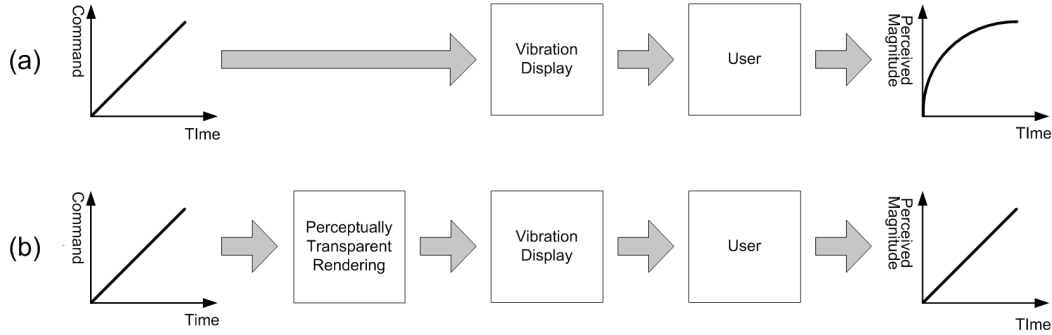
**Fig. 5.2** Conceptual comparison of vibration rendering (a) without and (b) with perceptually
transparent rendering.

phone with a vibration motor), as shown in Fig. 5.2(a). The exerted vibration by the dis-
play is then processed by the human central nervous system. However, the dynamics of the
vibration display and the complex human perception may seriously distort the perceived
vibration effect from the original design intention. For example, when a vibration pattern
that increases linearly with time is transmitted without PTR as is in Fig. 5.2(a), a target
perceptual attribute, the intensity of vibration perceived by the user, may grow nonlinearly
(see [53] for concrete data). This makes it difficult for the designer to predict what percep-
tual effects will be obtained by the vibration patterns s/he is designing. In PTR, the forward
relation with vibration command as input and target percept as output is modeled, and its
inverse relation is used for vibration rendering, as shown in Fig. 5.2(b). Thus, the user can
design a vibration effect with regards to the target percept, and the vibration command that
will induce the intended percept is autonomously computed in a rendering program.

## 5.2 Experiment IV: Pair-wise Discrimination of Simple Sinusoid Vibra-tions

Experiment IV was aimed at evaluating the benefits of the perceptually transparent render-
ing of mobile device vibration in terms of the pairwise discriminability of two vibrations
driven with different voltages.

(a) Experimental environment.      (b) Cellular phone.

**Fig. 5.3** Experimental environment and apparatus.

### 5.2.1 Methods

This section describes the details of experiment design.

#### Apparatus

A mock-up cellular phone (LG Electronics; KH-1000; size = $51.6 \times 98 \times 22.15$ mm; weight = 101.6 g) that includes a vibration motor (LG Innotek; MVMF-A345A; 10 mm diameter) was used to generate vibration in this experiment. The vibration motor was controlled by a PC through a data acquisition board (National Instruments; PGI-6229). The same phone was used in our previous studies that investigated some perceptual characteristics of mobile device vibration, such as perceived intensities in Chapter 4.

#### Participants

Ten students ($20 - 26$ years old with average 22) participated in this experiment. They were experienced users of a mobile device, and reported no known sensorimotor abnormalities.

#### Stimuli

The stimuli used in this experiment were defined using two independent variables: design method (without/with PTR) and the number of voltage levels ($n$). The traditional stimulus design for $n$-level vibration stimulation has been simply using $n$ applied voltages that are evenly spaced between 0 V and the maximum allowed voltage. For example, we can obtain
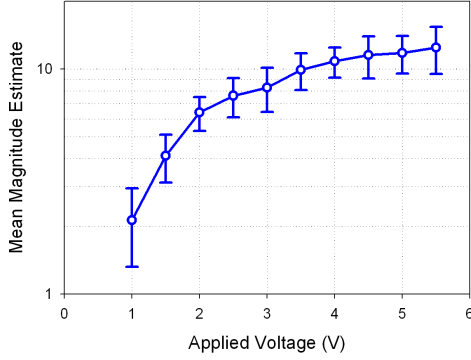
**Fig. 5.4** A psychophysical magnitude
function for mobile device vibration.
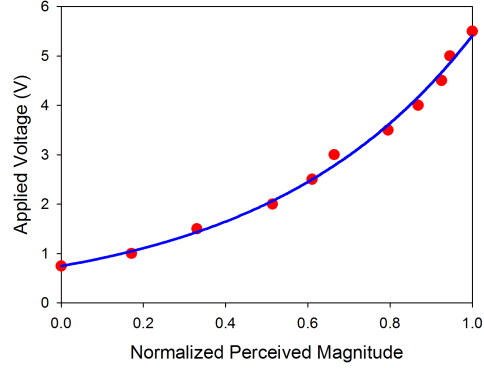


**Fig. 5.5** Inverse of the psychophysical
magnitude function shown in Fig. 5.4.

the applied voltage of level $i$ using Eq. 5.1a, where the maximum voltage to our vibration
motor is 5.5 V. When the other design method, PTR is used, applied voltages are deter-
mined so that the perceived intensities of resulting vibrations are evenly arranged. In this
experiment, we used Eq. 5.1b taken from [53]. This is the inverse relation of a mapping
from applied voltage to perceived intensity obtained using the same cellular phone via the
absolute magnitude estimation in our previous study [32] (see Fig. 5.4 and Fig. 5.5).

$$V_i = \begin{cases} 5.5 \cdot (i/n) \ , & \text{without PTR} \\ 0.7436 \ e^{1.984 \, (i/n)} \ , & \text{with PTR} \end{cases}$$

(5.1a)

(5.1b)

### Procedures

Each participant completed eight sessions defined by four numbers of stimuli ($n = 4, 5, 6,$
and 7) and two stimulus design methods (without/with PTR). The 3-level design was not
tested for its very high discriminability measured in previous work [51]. On each trial, two
stimuli, $V_i$ and $V_j$ ($i \neq j$), were randomly chosen from the $n$-level design of the applied
voltage. 3-IFC (3-Interval Forced Choice) method was applied to present two stimuli se-
quentially. For example, $V_i$ was presented in one of three interval and $V_j$ was presented
twice in other two interval, and vice versa. Vibrations driven with $V_i$ and $V_j$ were presented

(a) When all data are included.

(b) When only data between adjacent levels are included.
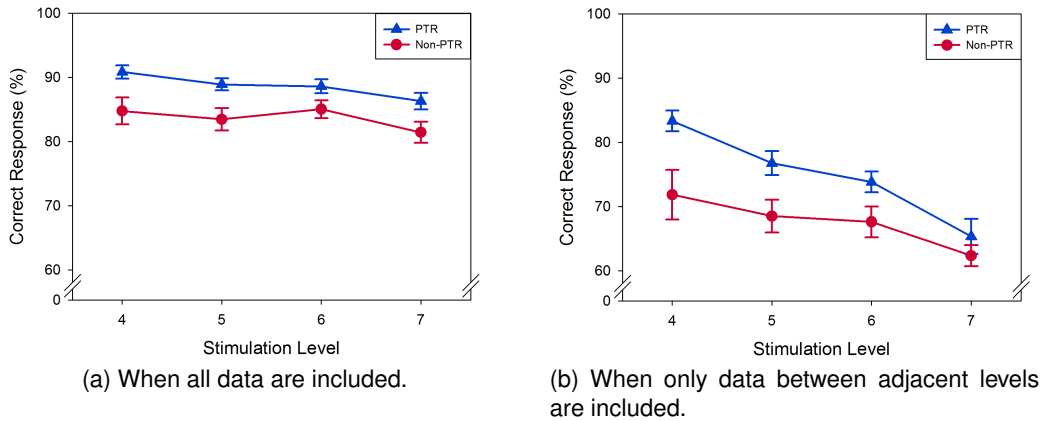
**Fig. 5.6** Average percent correct scores.

to the participant for 1 sec through the cellular phone, with 500 msec inter-stimulus inter-val. The participant was asked to answer the location of a differently perceived vibration in 3 intervals by pressing a corresponding key on a keyboard. Each stimulus sequence was repeated for 10 times in each session. The order of session presentation was randomized per each subject.

During the experiment, the participant was asked to hold the phone comfortably with the right hand while resting the right elbow on a cushion, as shown in Fig. 5.3a. The participant typed in responses with the left hand using the keyboard. The participant wore a headphone to block any auditory cues.

### 5.2.2 Results

The results of this experiment are summarized in Table 5.1 in terms of confusion matrices. A percent correct score in each cell indicates the average rate at which the corresponding vibration presented in one test interval was perceived differently in the experiment. When PTR was not used, the performance began to degrade with increase number of stimulus levels, even reaching the coin toss probability in the data of 4 stimulation levels (see the yellow cells in Table 5.2a). PTR, on the other hand, maintained high percent correct scores for all stimulation levels. And a yellow-marked cell of which score is lower than 50 is

**Table 5.1** Confusion matrices obtained in the Experiment IV

|   | 1 | 2 | 3 | 4 |
|---|---|---|---|---|
| 1 | · | **97** | 100 | 99 |
| 2 | **88** | · | **74** | 93 |
| 3 | 99 | **77** | · | **48** |
| 4 | 97 | 98 | **47** | · |

(a) 4 stimulation levels, Without PTR

|   | 1 | 2 | 3 | 4 |
|---|---|---|---|---|
| 1 | · | **92** | 99 | 100 |
| 2 | **85** | · | **87** | 98 |
| 3 | 96 | **85** | · | **78** |
| 4 | 100 | 97 | **73** | · |

(b) 4 stimulation levels, With PTR

|   | 1 | 2 | 3 | 4 | 5 |
|---|---|---|---|---|---|
| 1 | · | **99** | 99 | 99 | 99 |
| 2 | **94** | · | **81** | 91 | 98 |
| 3 | 99 | **74** | · | **48** | 74 |
| 4 | 100 | 90 | **59** | · | **49** |
| 5 | 97 | 96 | 79 | **44** | · |

(c) 5 stimulation levels, Without PTR

|   | 1 | 2 | 3 | 4 | 5 |
|---|---|---|---|---|---|
| 1 | · | **93** | 99 | 99 | 100 |
| 2 | **92** | · | **79** | 96 | 98 |
| 3 | 99 | **68** | · | **83** | 91 |
| 4 | 99 | 97 | **76** | · | **55** |
| 5 | 99 | 96 | 91 | **68** | · |

(d) 5 stimulation levels, With PTR

|   | 1 | 2 | 3 | 4 | 5 | 6 |
|---|---|---|---|---|---|---|
| 1 | · | **99** | 100 | 100 | 100 | 100 |
| 2 | **96** | · | **83** | 96 | 99 | 98 |
| 3 | 94 | **62** | · | **76** | 91 | 95 |
| 4 | 99 | 91 | **71** | · | **55** | 66 |
| 5 | 97 | 96 | 87 | **49** | · | **38** |
| 6 | 100 | 99 | 93 | 74 | **47** | · |

(e) 6 stimulation levels, Without PTR

|   | 1 | 2 | 3 | 4 | 5 | 6 |
|---|---|---|---|---|---|---|
| 1 | · | **88** | 97 | 98 | 99 | 100 |
| 2 | **90** | · | **72** | 92 | 99 | 98 |
| 3 | 97 | **79** | · | **77** | 94 | 97 |
| 4 | 97 | 93 | **71** | · | **76** | 86 |
| 5 | 98 | 96 | 94 | **70** | · | **56** |
| 6 | 96 | 99 | 94 | 96 | **59** | · |

(f) 6 stimulation levels, With PTR

|   | 1 | 2 | 3 | 4 | 5 | 6 | 7 |
|---|---|---|---|---|---|---|---|
| 1 | · | **97** | 99 | 97 | 99 | 100 | 100 |
| 2 | **91** | · | **78** | 95 | 97 | 97 | 99 |
| 3 | 98 | **70** | · | **75** | 89 | 96 | 95 |
| 4 | 98 | 90 | **55** | · | **56** | 72 | 79 |
| 5 | 98 | 97 | 80 | **48** | · | **38** | 56 |
| 6 | 97 | 95 | 89 | 60 | **50** | · | **41** |
| 7 | 99 | 92 | 87 | 73 | 49 | **49** | · |

(g) 7 stimulation levels, Without PTR

|   | 1 | 2 | 3 | 4 | 5 | 6 | 7 |
|---|---|---|---|---|---|---|---|
| 1 | · | **78** | 95 | 98 | 98 | 99 | 98 |
| 2 | **71** | · | **80** | 90 | 98 | 100 | 98 |
| 3 | 92 | **73** | · | **68** | 95 | 96 | 99 |
| 4 | 100 | 83 | **66** | · | **64** | 93 | 93 |
| 5 | 98 | 96 | 88 | **68** | · | **56** | 79 |
| 6 | 99 | 98 | 97 | 91 | **59** | · | **50** |
| 7 | 98 | 100 | 93 | 93 | 85 | **51** | · |

(h) 7 stimulation levels, With PTR

**Table 5.2** Summary of the statistical analysis of the correct responses in each stimulation
level.

| | All data | | Adjacent data only | |
|---|---|---|---|---|
| | $F(1,9)$ | $p$ | $F(1,9)$ | $p$ |
| 4 | 14.53 | 0.0041 | 13.35 | 0.0053 |
| 5 | 16.84 | 0.0027 | 10.53 | 0.0101 |
| 6 | 27.99 | 0.0005 | 21.15 | 0.0013 |
| 7 | 12.87 | 0.0059 | 2.33 | 0.1612 |

shown at only 7 stimulation level.

The data in the confusion matrices were pooled to attain the average percent correct
scores of conditions without/with PTR. The results are shown in Fig. 5.6 along with the
error bars representing their standard errors. Fig. 5.6a shows the average scores including
all comparison pairs in the confusion matrices, and Fig. 5.6b those of comparison pairs be-
tween adjacent levels only. It is evident in the figures that PTR showed better performance,
particularly when only adjacent stimulation levels were considered. This observation is
supported by the results of two-way ANOVA where in both data sets the number of stim-
ulation levels (all data: $F(3,27) = 6.43$, $p = 0.0020$, adjacent only: $F(3,27) = 20.67$,
$p < 0.0001$) and the stimulus design method (all data: $F(1,9) = 30.54$, $p = 0.0004$,
adjacent only: $F(1,9) = 20.36$, $p = 0.0015$) were shown to be statistically significant,
but their interaction was not. Enhancing percent correct scores with PTR in most stimu-
lation level was statistically confirmed by Table 5.2 which represented statistical analysis
of correct scores without/with PTR in each stimulation level. However, in 7 stimulation
level, difference between without/with PTR was shown to be statistically significant when
considering adjacent data only.

## 5.3 Experiment V: Absolute Identification of Simple Sinusoid Vibrations

Experiment V was also aimed at evaluating the benefits of perceptually transparent rendering of mobile device vibration in terms of the absolute identification of each vibration driven with different voltages.
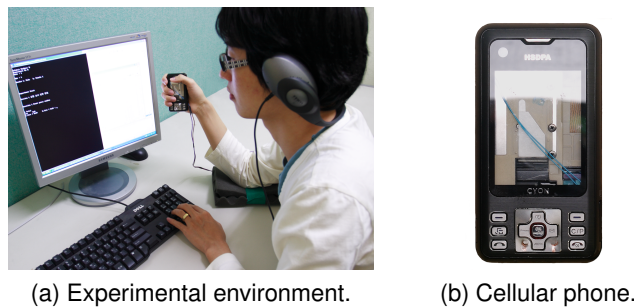
### 5.3.1 Methods

This section describes the details of experiment design.

#### Apparatus

We used the same cellular phone used in Experiment IV. The details about the cellular phone was explained in 5.2.1.

#### Participants

Ten students (18 – 25 years old with average 21.9) participated in this experiment. They were experienced users of a mobile device, and reported no known sensorimotor abnormalities.

#### Stimuli

The stimuli design defined by using two variables, design method and the number of voltage levels, was same to that in Experiment IV. The applied voltages were determined by using Eq. 5.1a for Non-PTR, Eq. 5.1b for PTR.

#### Procedures

Each participant completed ten sessions defined by five numbers of stimuli ($n = 3$, 4, 5, 6, and 7) and two stimulus design methods (without/with PTR). Before each session, the learning of all $n$-level vibrations were repeated at three times. After then, a stimulus, $V_i$, was randomly chosen from the $n$-level design of the applied voltage on each trial. A vibration driven with $V_i$ was presented once to the participant for 1 sec through the cellular
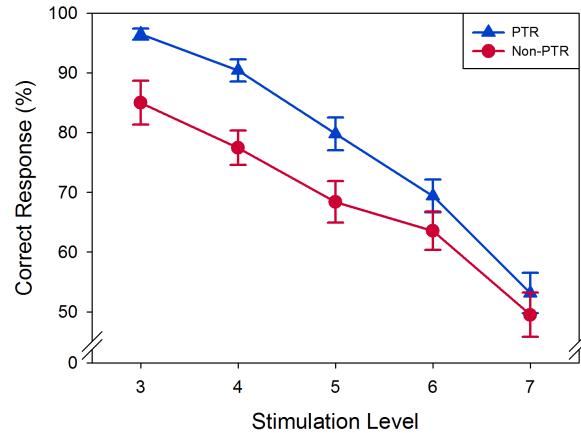
**Fig. 5.7** Average percent correct scores.

phone. The participant was asked to answer which vibration among previously learned
$n$-level vibrations is same to the presented stimulus by pressing a corresponding key on
a keyboard. Each stimulus test trial was repeated for $20 \times n$ times in each session. For
example, there are 60 trials in a session for 3 stimuli level. The order of session presentation
by stimulus design methods was balanced per each subject, but that by the number of stimuli
was randomized in each stimulus design method.

During the experiment, the participant was asked to hold the phone comfortably with the
right hand while resting the right elbow on a cushion, as shown in Fig. 5.3a, and then the
participant typed in responses with the left hand using the keyboard. The participant wore
a headphone with white noise to block any auditory cues.

### 5.3.2 Results

The results of this experiment are summarized in Table 5.3 in terms of confusion matrices.
A percent correct score in each cell indicates the average rate at which the vibration was
absolutely identified in the experiment. Overall performance of the percent correct score,
similar to the result of Experiment IV, was higher when PTR was used. When PTR was
not used, the performance began to degrade with increase number of stimulus levels, even
reaching the coin toss probability in the data of 6 stimulation levels (see the yellow cells

**Table 5.3** Confusion matrices obtained in the Experiment V

|   | 1 | 2 | 3 |
|---|---|---|---|
| 1 | **93** | 7 | 0 |
| 2 | 2 | **74** | 24 |
| 3 | 0 | 12 | **88** |

(a) 3 stimulation levels, Without PTR

|   | 1 | 2 | 3 |
|---|---|---|---|
| 1 | **99** | 1 | 0 |
| 2 | 0 | **97** | 3 |
| 3 | 0 | 6 | **94** |

(b) 3 stimulation levels, With PTR

|   | 1 | 2 | 3 | 4 |
|---|---|---|---|---|
| 1 | **96** | 4 | 0 | 0 |
| 2 | 0 | **78** | 22 | 0 |
| 3 | 0 | 9 | **66** | 25 |
| 4 | 0 | 1 | 29 | **70** |

(c) 4 stimulation levels, Without PTR

|   | 1 | 2 | 3 | 4 |
|---|---|---|---|---|
| 1 | **97** | 3 | 0 | 0 |
| 2 | 0 | **86** | 14 | 0 |
| 3 | 1 | 2 | **93** | 4 |
| 4 | 0 | 0 | 13 | **87** |

(d) 4 stimulation levels, With PTR

|   | 1 | 2 | 3 | 4 | 5 |
|---|---|---|---|---|---|
| 1 | **98** | 2 | 0 | 0 | 0 |
| 2 | 1 | **70** | 26 | 2 | 0 |
| 3 | 3 | 5 | **59** | 30 | 3 |
| 4 | 1 | 1 | 17 | **58** | 23 |
| 5 | 0 | 0 | 4 | 40 | **57** |

(e) 5 stimulation levels, Without PTR

|   | 1 | 2 | 3 | 4 | 5 |
|---|---|---|---|---|---|
| 1 | **97** | 3 | 1 | 0 | 0 |
| 2 | 4 | **83** | 13 | 0 | 0 |
| 3 | 0 | 10 | **77** | 13 | 0 |
| 4 | 0 | 0 | 14 | **67** | 19 |
| 5 | 0 | 0 | 1 | 25 | **74** |

(f) 5 stimulation levels, With PTR

|   | 1 | 2 | 3 | 4 | 5 | 6 |
|---|---|---|---|---|---|---|
| 1 | **94** | 4 | 2 | 0 | 0 | 0 |
| 2 | 0 | **81** | 18 | 1 | 0 | 0 |
| 3 | 0 | 8 | **63** | 26 | 2 | 1 |
| 4 | 0 | 0 | 20 | **49** | 23 | 7 |
| 5 | 0 | 0 | 3 | 24 | **49** | 24 |
| 6 | 0 | 0 | 2 | 13 | 40 | **45** |

(g) 6 stimulation levels, Without PTR

|   | 1 | 2 | 3 | 4 | 5 | 6 |
|---|---|---|---|---|---|---|
| 1 | **91** | 9 | 0 | 0 | 0 | 0 |
| 2 | 20 | **69** | 9 | 2 | 0 | 0 |
| 3 | 1 | 7 | **79** | 13 | 1 | 0 |
| 4 | 1 | 0 | 27 | **57** | 15 | 0 |
| 5 | 0 | 0 | 3 | 27 | **54** | 16 |
| 6 | 0 | 0 | 0 | 6 | 27 | **67** |

(h) 6 stimulation levels, With PTR

|   | 1 | 2 | 3 | 4 | 5 | 6 | 7 |
|---|---|---|---|---|---|---|---|
| 1 | **89** | 11 | 0 | 0 | 0 | 0 | 0 |
| 2 | 14 | **74** | 11 | 1 | 0 | 0 | 0 |
| 3 | 1 | 10 | **53** | 27 | 7 | 1 | 1 |
| 4 | 0 | 4 | 20 | **29** | 31 | 14 | 1 |
| 5 | 0 | 0 | 5 | 26 | **34** | 28 | 7 |
| 6 | 0 | 0 | 3 | 14 | 32 | **33** | 18 |
| 7 | 0 | 0 | 0 | 4 | 19 | 43 | **33** |

(i) 7 stimulation levels, Without PTR

|   | 1 | 2 | 3 | 4 | 5 | 6 | 7 |
|---|---|---|---|---|---|---|---|
| 1 | **76** | 23 | 1 | 0 | 0 | 0 | 0 |
| 2 | 34 | **61** | 4 | 0 | 0 | 0 | 0 |
| 3 | 2 | 20 | **74** | 4 | 0 | 0 | 0 |
| 4 | 2 | 2 | 46 | **43** | 6 | 1 | 0 |
| 5 | 0 | 0 | 7 | 48 | **28** | 16 | 1 |
| 6 | 0 | 0 | 1 | 11 | 33 | **38** | 16 |
| 7 | 0 | 0 | 0 | 1 | 7 | 40 | **51** |

(j) 7 stimulation levels, With PTR

**Table 5.4** Summary of the statistical analysis of the correct responses in each stimulation level.

|   | Diagonal data | |
|---|---|---|
|   | $F(1,9)$ | $p$ |
| 3 | 9.10 | 0.0146 |
| 4 | 20.87 | 0.0013 |
| 5 | 9.44 | 0.0133 |
| 6 | 5.97 | 0.0371 |
| 7 | 0.79 | 0.3970 |

in Table 5.4g). PTR, on the other hand, maintained high percent correct scores for all stimulation levels. When the stimulation level becomes higher, there is little difference of average scores without/with PTR.

With the diagonal data in the confusion matrices, the average percent correct scores of conditions without/with PTR were attained. The results are shown in Fig. 5.7 along with the error bars representing their standard errors. It is evident in the figures that PTR showed better performance similar to the result of Experiment IV. This observation is supported by the results of two-way ANOVA where the number of stimulation levels ($F(4,36) = 55.42$, $p < 0.0001$) and the stimulus design method ($F(1,9) = 18.54$, $p = 0.0020$) were shown to be statistically significant, but their interaction was not. Except 7 stimulation level, average percent correct scores are enhanced in most stimulation level and it is shown to be statistically significant (see Table 5.4 which represented statistical analysis of correct scores without/with PTR in each stimulation level).

## 5.4   General Discussion

The results of this experiment shed some insights on how to design vibratory patterns in mobile devices, for example, for tactons. The tactons are structured tactile messages that are studied mostly for mobile devices by Brewster and Brown [3]. They have conducted a number of studies to test which parameters are good candidates to encode information in,

e.g., frequency [7, 11], amplitude [6, 8], duration[4], rhythm [7, 22], and body site [22]. In particular, it was asserted that magnitude was not an effective parameter with which different meanings can be delivered [7]. We presume that such results might have been due to the fact that the perceptual characteristics of mobile device vibration were not adequately considered in the design of magnitude levels. The present study showed the possibility that more than five vibratory stimuli can be reliably discriminated from each other in a mobile device.

In our pilot study, the difference limens of mobile device vibration perception with respect to voltage applied to the device were measured. It is generally known that if $V_i + DL_i$ is larger than $V_{i+1}$, then vibrations driven with $V_i$ and $V_{i+1}$ would not be reliably discriminated. For example, in 4 stimulation level design without PTR, the applied voltage of $V_3$ is 4.13 V, and the DL for $v = 4.13V$ is 2.02 V. Since the applied voltage 5.5 V of $V_4$ is lower than summation of applied voltage of $V_3$ and DL, we could expect that two vibrations of $V_3$ and $V_4$ would be not discriminated. The results of applied voltages for other stimulation level designs are similar to results of Experiment IV.

# Chapter 6

# Benefits of PTR for Vibrotactile Melody

In previous Chapter 5, we presented the perceptually transparent vibration rendering (PTR) and its evaluation by using a simple sinusoidal vibration. The reduced perceptual distortion of vibrations by using PTR can make users to perceive each vibration exactly. Since using the simple sinusoidal vibrations was suitable to explain the benefits of PTR, but it is still lacking for the feasibility of advanced vibrotactile feedback in mobile devices. Therefore, it is necessary that the benefits of PTR is going to be discussed by using vibrotactile melodies like Tacton and Hapticon which are practical usage in present mobile devices. In this chapter, we will describe the vibrotactile melody and its advantage, and evaluate the discriminability of two kinds of vibrotactile melodies which have constant strength and time-varying strength.

## 6.1    Vibrotactile Melody

A vibrotactile melody consists of rhythm, frequency, and amplitude which are being varied with time. In previous research, they investigated the perceptual characteristics of pure simple sinusoids and researches about Tacton and Hapticon which is combined with rhythm have been progressing [3, 15, 32, 53]. Most researches have resulted commonly

that rhythm is most influencing factor for discriminating vibrotactile messages [63, 66]. Recently, Ternes et al. has resulted that rhythm is main factor on the perceptual distances between vibrations in MDS plot, but frequency and amplitude of vibrations are also influencing secondarily to the perceptual distance [64]. However, Hapticons that Ternes made have various rhythm, but fixed frequency and amplitude to each rhythm [63]. In order to make more rich Tacton or Hapticon, we suggest that not only rhythm, but also frequency and amplitude can be varied with time.

In our study, we build vibrotactile melodies by combinations of rhythm and perceived intensity. Since the frequency and amplitude of a vibration motor is correlated as shown in Sec. 3 and the frequency discriminability of vibrotactile perception is relatively inferior, the strength coding is applied to make vibrotactile melodies, not coding with frequencies and amplitudes independently. It means that we consider the perceived intensity of vibrations as a dimension to design vibrotactile melodies.

### 6.1.1 Classification of Vibrotactile Melody

The vibrotactile melody can be classified into five configuration form as below.

- Binary Vibration

  The binary vibration with on/off fashion has been used generally in most mobile device. There are two states which are vibration emanation and no vibration.

- Multiple Strength Vibration

  In contrast to the binary vibration, the multiple strength vibration has many number of perceived strength, but still without rhythm. The maximum number of designable $N$-level strength vibrations is $N + 1$ including 0 to $N$ level strength. The zero strength means that there is no vibration.

- Vibration with Rhythm

  Most Tacton and Hapticon has a rhythm which is combination of 'Note' and 'Rest'. The Tactons and Hapticons have various form of rhythm by how to arrange the notes

and rests.  However, in this case, they have fixed vibration strength of every notes, generally maximum strength that a vibration actuator can generate.  We represent a time unit as a 'Beat', and a beat has two conditions of note and rest.  So, the rhythm with $k$ beats can be represented as $k$-bit binary code, 0 represents a rest and 1 represents a note. The maximum number of designable vibrations with rhythm is $2^k$, when the rhythm has $k$ beats.

- Constant Strength Vibrotactile Melody

  The constant strength vibrotactile melody (CS melody) is based on the vibration with rhythm and multiple strength vibration. The CS melody has a rhythm and all notes of CS melody equally have one of the $N$-level vibration strength. The number of the CS melodies could be simply determined by $N \cdot (2^k)$ represented by combinations of the $2^k$ rhythms with $k$ beats and $N$-level strength. However, there are $N$ duplicated state of no vibration, so we have to discard $(N-1)$ duplications. Therefore, the maximum number of designable CS melodies is $N \cdot (2^k) - (N-1) = N \cdot (2^k - 1) + 1$, when $N$ is the number of vibration strength and $k$ is the number of beats.

- Time-Varying Strength Vibrotactile Melody

  The time-varying strength vibrotactile melody (TVS melody) is the extension of the CS melody. The difference between them is whether each beat of melodies can have an individual strength.  For example, when there are two beats for a melody, two beats for CS melody have equal strength and the number of melodies is $3N + 1$. But, two beats for TVS melody can have different strength which are combination of both $N + 1$ strength of one beat and $N + 1$ strength of another beat including zero strength.  In this case, the maximum number of designable melodies with two beats is $(N + 1)^2$. Therefore, the maximum number of designable TVS melodies is $(N + 1)^k$, when $N$ is the number of vibration strength and $k$ is the number of beats.

The maximum number of designable melodies with $k$ rhythm beats is represented in Fig. 6.5.  As shown in the figure, it is obvious that many melodies can be made by TVS types
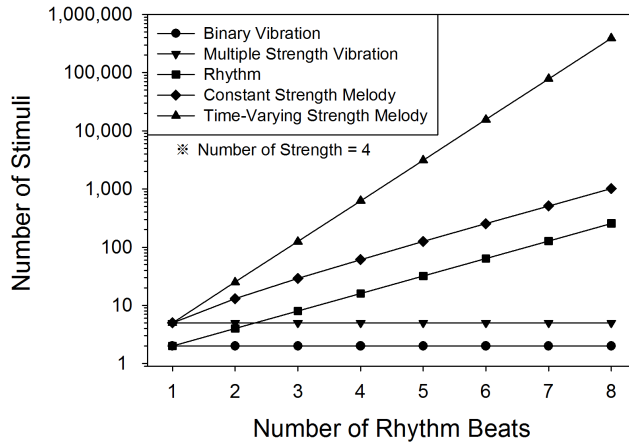
**Fig. 6.1** The number of designable melodies for each kind of the vibrotactile melody (the number of vibration strength ($N$) is fixed to 4).

than any other types of melodies. The vibration with rhythm, CS melody, and TVS melody have the exponentially increased number of designable vibrations. However, the increase rate of the TVS melody is very larger than others.

## 6.2 Experiment VI: Discrimination between Constant Strength Melody and Time-Varying Strength Melody

In this experiment, we design CS and TVS melodies and evaluated whether the discriminability of two melodies become higher when using PTR.

### 6.2.1 Methods

This section describes the details of experiment design.

**Apparatus**

We used a mock-up cellular phone (LG Electronics; model KH-1000) with a vibration motor (LG Innotek; MVMF-A345A; 10 mm diameter) that was used in Experiment IV and V. The details about the cellular phone was explained in 5.2.1.

### Participants

Eleven students (19 – 26 years old with average 22.7; 9 males and 2 females) participated in this experiment. They were every day experienced users of a mobile device, and reported no known sensorimotor abnormalities.

### vibrotactile Melodies

We designed 8 vibrotactile melodies with the combination of four vibration rhythm and two vibration strength type, CS and TVS. Each rhythm represents in Fig. 6.2, dotted and dashed lines represent CS and TVS melodies, respectively. For determining four vibration rhythm, we used dissimilarity data in Ternes' research [64]. The rhythms with the highest dissimilarity rate were chosen and were slightly modified for using them in our research. Basically, they have high dissimilarity between each other.

Vibration strength for melodies divided into the level of 4. We designed adjacent notes in TVS melodies to have different level of vibration strength, in contrast, all notes of CS melodies with equal 4 level strength. Especially, the 1 level vibration strength has been discarded due to unperceptable intensity when note duration is short. The unperceptable intensity was caused by the hardware limitation of a vibration motor, large transient response time until generating vibrations with stable intensity.

### Procedures

In order to estimate the discriminability of vibrotactile melodies, we used the 3 IFC (3 Interval Forced-Choice) Oddity method. The standard melody is delivered in two intervals, and the test melody in other interval. The location of test melody in three intervals was determined randomly. The participants were asked to find the location of differently perceived melody in 3 interval. The standard and test melodies provided in each trial had same rhythm, but different strength variation type, CS or TVS. The experimental conditions were 16 (2X2X4) which were two cases of CS melody as standard/test melody, two rendering methods (without/with PTR), and four rhythms. Since all conditions were repeated 10 times, each participant was presented with 160 trials and it took about 40 minute. We asked
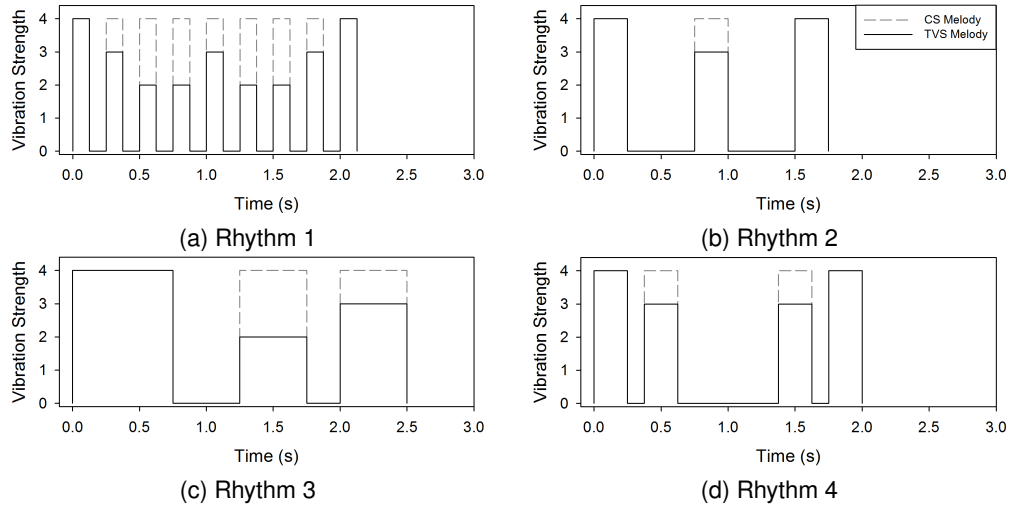
**Fig. 6.2** CS and TVS melodies with 4 different rhythms.

the participants to take a break for a long time they want in every 32 trials. The order of trials was randomized per participant.

After discriminability experiment, automatically next experiment for subjective rating of vibrotactile melodies was conducted. The participants were asked to choose one of two CS and TVS melodies with same rhythm by a metric of enjoyment, easiness to identify, preference for alternating the ring-tone and alarm of cellular phone. 8 experimental conditions that were combination of four rhythm and two rendering method (without/with PTR) were presented randomly.

Prior to the experiments, every vibrotactile melodies were presented to participants at one time for training. During the experiment, the participant was asked to hold the phone comfortably with the right hand while resting the right elbow on a cushion, as shown in Fig. 5.3a. The participant typed in responses with the left hand using the keyboard. The participants were a headphone in order to block any auditory interference.

### 6.2.2 Results

With PTR, the discriminability of CS and TVS melodies was improved. The correct response rates of discriminability between the CS melody and TVS melody were 60.45 %

without PTR, 73.3 % with PTR. The participants could discriminate CS and TVS melodies
with the average correct response rate of two third. Since the CS and TVS melodies have
high discriminability, we can use both CS and TVS melodies in order to deliver different
message. In this case, using the PTR can improve the worth of TVS melodies.

In order to discriminate CS melody and TVS melody, the participants should identify the
relative variation of perceived strength at a moment of strength change. If a TVS melody has
just two adjacent notes with large variation of perceived strength, it is enough to discrimi-
nate CS melody which has no change of perceived strength between adjacent notes. That is,
the higher pairwise discriminability of pure sinusoid could affect the identification of TVS
melody and make the discriminability between CS and TVS melodies to be higher. For
example, there are two adjacent notes with 3 and 4 level strength at 4 stimulation level. In
our previous experiment in Sec. 5.2, the pairwise discriminabilities of pure sinusoids with
3 and 4 level strength at 4-level stimulation level are 75.5 % with PTR and 47.5 % without
PTR. Without PTR, the two adjacent notes can not be discriminated in half of trials, so the
participants feel there are no changes of perceived strength. Since the two adjacent notes are
perceived as equal strength, a TVS melody with the notes would be misidentified as a CS
melody. Due to the misidentification, the correct response rate of discrimination between
CS and TVS melodies could be decreased. Therefore, the improvement of pure sinusoid
discriminability with PTR can improve the discriminabilty of CS and TVS melodies.

Fig. 6.3 shows that the discriminability of vibrotactile melody can be varied via rhythm.
The rhythm 1 and 3 have high discriminability of average 81 %, but the rhythm 2 and 4 have
discriminability of average 54 %. However, the different discriminability among rhythms
would be caused by the relative strength difference of adjacent notes in each rhythm. The
strength level of the rhythm 1 and 3 has been changed as 4-3-2-3-4, 4-2-3, respectively.
As shown results of experiment in Sec. 5.2, the discriminabilities of 2 level and 4 level
were 97.5 % with PTR, 95.5 % without PTR, those of 2 level and 3 level were 86 % with
PTR, 75.5 % without PTR. Those discriminabilities were higher then that of 3 level and
4 level which were composed in rhythm 2 and 4. Since the average discriminabilities of
adjacent notes in rhythm 1 and 3 were higher than that in rhythm 2 and 4, the participants
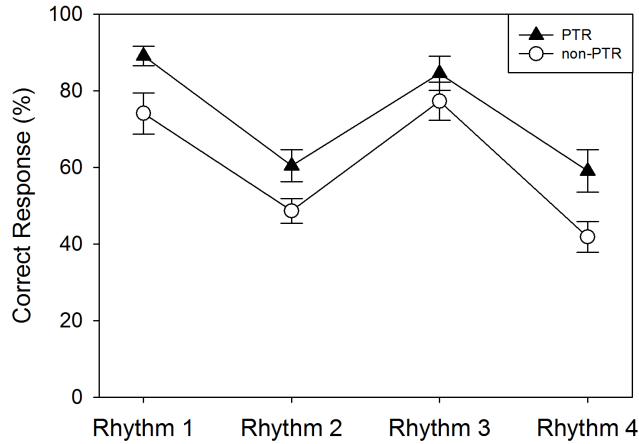
**Fig. 6.3** The correct response rate of the discriminability between CS and TVS melodies.

could identify well TVS melodies with rhythm 1 and 3. Therefore, to design a TVS melody which can be discriminate to a CS melody, it is required that the melody has notes which have high pairwise discriminability between them.

With ANOVA analysis, rendering method (without/with PTR) ($F(1, 10) = 43.28, p < 0.0001$) and rhythm ($F(3, 30) = 40.51, p < 0.0001$) has a significant effect on the discriminability between CS and TVS melodies. There is no significant interaction of two factors.

By subjective rating, 59 % of all participants rated that TVS melody feels to enjoy it, but only 27 % of them rated that TVS melody is easy to identify. The participants said that no change of vibration strength among melody notes can be felt to be clearly identified, but time-varying strength is felt fresh and fun. Also, only 33 % of them preferred TVS melody to be alternative to the ring-tone and alarm of a cellular phone. They said that the ring-tone and alarm must be perceived definitely due to their importance, so the CS melody they can clearly identify is better to replace the ring-tone and alarm. However, in other applications for fun, emotion, and user interaction, users would prefer TVS melody.

## 6.3 Experiment VII: Pairwise Discrimination of Time-Varying-Strength Melodies

In this experiment, we design nine TVS melodies and evaluated whether the discriminability of melodies become higher when using PTR.

### 6.3.1 Methods

This section describes the details of experiment design.

#### Apparatus

We used the same cellular phone used in Experiment VI. The details about the cellular phone was explained in 5.2.1.

#### Participants

Ten students (18 – 32 years old with average 23.7) participated in this experiment. They were every day experienced users of a mobile device, and reported no known sensorimotor abnormalities.

#### vibrotactile Melodies

We designed nine TVS melodies which were combination of three different rhythms and three strength variations for each rhythm. The rhythms were three of 4 rhythms in Fig. 6.2, they had different number of notes. In pilot tests, we designed four strength variations, such as gradually increase, gradually decrease, the shape of 'V', and the shape of inverse 'V'. By the results of pilot tests for each rhythm, the three strength variations among them were determined to have high pairwise discriminability.

#### Procedures

In order to estimate the pairwise discriminability of vibrotactile melodies, we used the 3 IFC (3 Interval Forced-Choice) Oddity method. The number of trials were 720 (9X8X2X5) by pairs between nine TVS melodies (9X8), two rendering methods (without/with PTR),

(a) TVS Melody 1

(b) TVS Melody 2

(c) TVS Melody 3

(d) TVS Melody 4

(e) TVS Melody 5

(f) TVS Melody 6

(g) TVS Melody 7

(h) TVS Melody 8
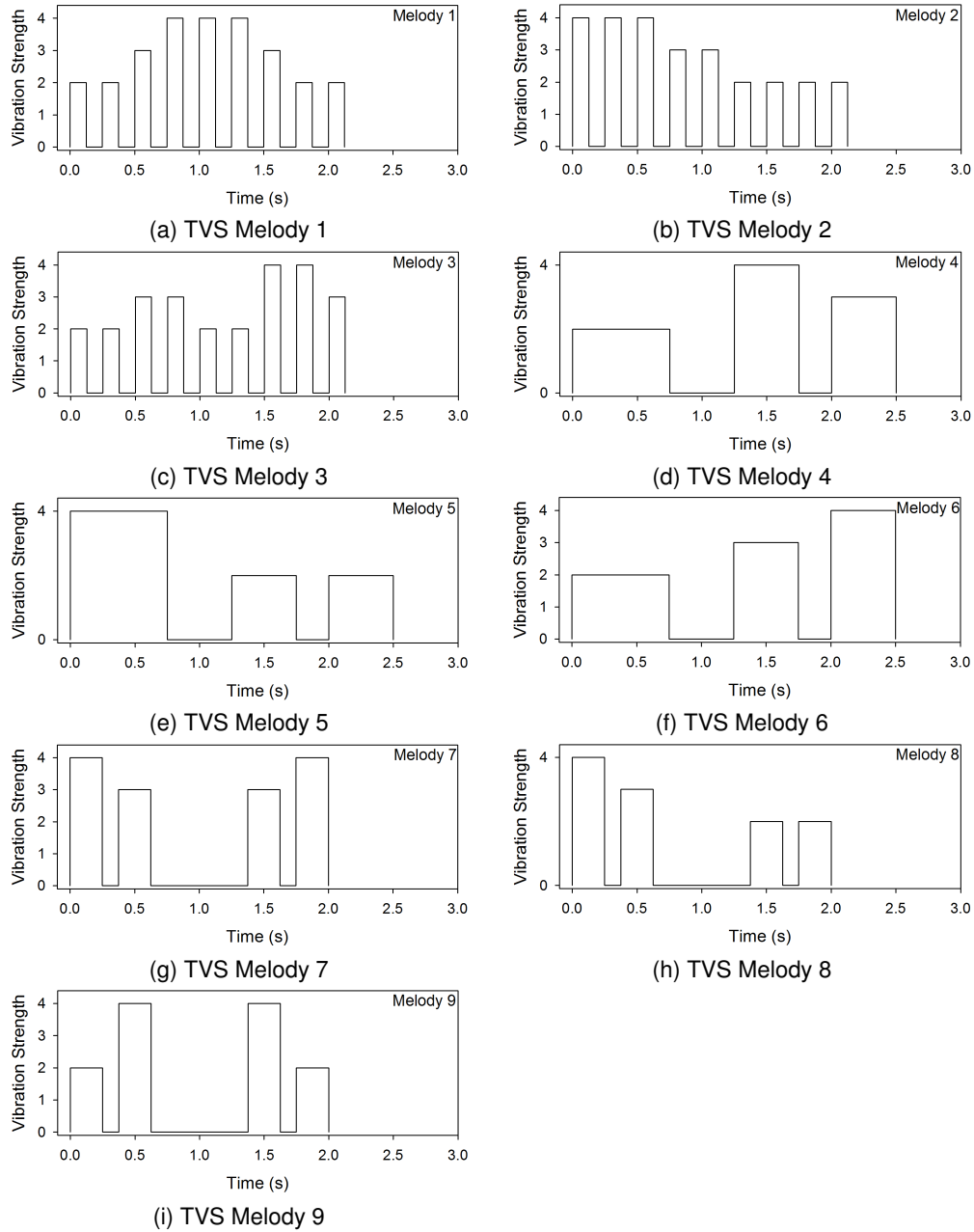
(i) TVS Melody 9

**Fig. 6.4** Nine TVS melodies.

and 5 repetitions. It took about 3 hours, the participants participated this experiment in two days, one and half hour per a day. We asked the participants to take a break for a long time they want in every 36 trials. The detailed procedures were same in Sec. 6.2.1.

### 6.3.2  Results

The correct response rates of the pairwise discriminability of TVS melodies with same rhythm were 84.6 % with PTR and 73.4 % without PTR. There was about 11 % improvement of discriminability when using PTR. However, the correct response rates of the pairwise discriminability of TVS melodies with different rhythm were 96 % with PTR and 98 % without PTR, so there was no difference of discriminability by PTR. In this case, in ANOVA analysis, the PTR has a significant effect on the pairwise discriminability of TVS melodies with same rhythm ($F(1,9) = 22.96$, $p = 0.0010$), but no significant effect for TVS melodies with different rhythm ($F(1,9) = 1.77$, $p = 0.2157$).

The improvement of discriminability with PTR would be caused by the high discriminability of adjacent two notes in TVS melody. As discussed in Sec 6.2.2, the higher correctness of relative strength variation at a moment by using PTR could improve the identification of TVS melodies. For example, The discriminabilities of TVS melodies of number 7 and 8 were 84 % with PTR, 60 % without PTR. There is 24 % improvement of discriminability. The difference between the two melodies of number 7 and 8 was the different strength of third and fourth notes. The strength flow of third and fourth notes was 3-to-4 of TVS melody 7, 2-to-2 of TVS melody 8. If participants can recognize the slight increase of 3 to 4 strength of melody 7, they can discriminate no change of two notes with equal 2 strength of melody 8. Therefore, much more improvement of discriminability of 7 and 8 TVS melodies than other pairs by PTR showed that the correctness of discriminability between TVS melodies also would be affected by whether users can recognize the relative strength variation of adjacent notes.

There was also much more improvement of discriminability of TVS melodies of number 2 and 3 by PTR. The discriminabilities of the two melodies were 88 % with PTR, 66 % without PTR. However, there was no different strength of adjacent two notes like TVS

melodies of number 7 and 8. The strength flows of two melodies were quite different, gradual decrease form of melody 2, arbitrary increase form of melody 3. Also, the durations of every notes of two melodies were 0.125 seconds, it was very short for participants to perceive the strength of each note exactly. We suspect that the 22 % improvement of discriminability by PTR would be caused by the clear absolute identification of each note, even if they have short duration. Based on previous experiment of absolute identification of pure sinusoids in Sec. 5.3, average absolute identification rates were 90 % with PTR, but 77 % without PTR when stimulation level was 4. Also, participants said that, by PTR, they could clearly identify the strength of each notes and easily imagine the strength flow via notes. The reduced ambiguity of perceived strength among melody notes by PTR improves that users can imagine easily the flow of the strength variation via notes. Therefore, since they can identify absolutely each TVS melody, the overall discriminability with PTR was improved.

The rhythm is most important factor for identifying vibrotactile melodies [63, 66]. That showed identically in our results. The average discriminability of melodies with different rhythm was 97 %. In contrast, the discriminability of melodies with same rhythm was 84.6 % even if using PTR. It showed that the correctness of rhythm identification is higher than that of strength variation. However, if we design a vibrotactile melody carefully, the discriminability of melodies with same rhythm could be improved. The 5 and 6 TVS melodies have same rhythm and different strength variation, but the discriminability of them was 100 %. Also, 4 and 5 TVS melodies have the discriminability of 94 %. Generally the rhythm is most influencing factor for vibration identification, however the TVS melodies with careful design could become more effective .

## 6.4   General Discussion

As shown in Sec. 6.1, the TVS melody has wide variety of the number of designable melodies by combination of $N$-strength level for $k$-beat. Its wide variety can make tacton/hapticon to be colorful, and they can use effectively in commercial cellular phones. However, the designer's creativity should be required to select a vibrotactile melody in very

**Table 6.1** Confusion matrices obtained in the Experiment VII. (The melodies in shaded cells have same rhythm.)

|   | 1 | 2 | 3 | 4 | 5 | 6 | 7 | 8 | 9 |
|---|---|---|---|---|---|---|---|---|---|
| 1 | · | **60** | **66** | 100 | 100 | 100 | 100 | 100 | 98 |
| 2 | **66** | · | **66** | 98 | 98 | 100 | 100 | 98 | 100 |
| 3 | **70** | **80** | · | 100 | 100 | 100 | 100 | 100 | 100 |
| 4 | 98 | 96 | 96 | · | **80** | **52** | 96 | 96 | 94 |
| 5 | 100 | 100 | 98 | **92** | · | **96** | 96 | 98 | 96 |
| 6 | 98 | 98 | 100 | **62** | **88** | · | 98 | 100 | 98 |
| 7 | 100 | 96 | 98 | 96 | 90 | 92 | · | **60** | **76** |
| 8 | 98 | 98 | 100 | 94 | 100 | 94 | **74** | · | **72** |
| 9 | 98 | 98 | 98 | 98 | 98 | 100 | **80** | **82** | · |

(a) Without PTR

|   | 1 | 2 | 3 | 4 | 5 | 6 | 7 | 8 | 9 |
|---|---|---|---|---|---|---|---|---|---|
| 1 | · | **76** | **82** | 96 | 100 | 98 | 96 | 100 | 98 |
| 2 | **78** | · | **88** | 98 | 98 | 98 | 100 | 100 | 100 |
| 3 | **76** | **84** | · | 98 | 98 | 98 | 96 | 96 | 94 |
| 4 | 94 | 98 | 94 | · | **92** | **68** | 94 | 92 | 96 |
| 5 | 98 | 100 | 100 | **96** | · | **100** | 96 | 94 | 100 |
| 6 | 100 | 98 | 100 | **72** | **100** | · | 98 | 100 | 98 |
| 7 | 100 | 100 | 98 | 94 | 86 | 88 | · | **84** | **86** |
| 8 | 98 | 100 | 98 | 96 | 88 | 98 | **82** | · | **84** |
| 9 | 96 | 100 | 94 | 96 | 98 | 96 | **86** | **88** | · |

(b) With PTR

large designable pool of melodies. Also, the designed melody would be adaptable to the purpose of applications and the meaning of sending messages. The enjoyment is one of the advantages of TVS melody. In previous subjective rating, many users responded that TVS melodies were felt funny, so that the funny TVS melodies may enhance a user's emotional feeling. If it is possible that the TVS melody would be designed to resemble the music, the designer's emotion can be sent to listeners.

The correctness of melody identification was improved when using PTR. Most users could perceived a strength sequence varying with time in some degree, but, using PTR can make the correctness of perceiving the strength to be higher. We suspected that the im-
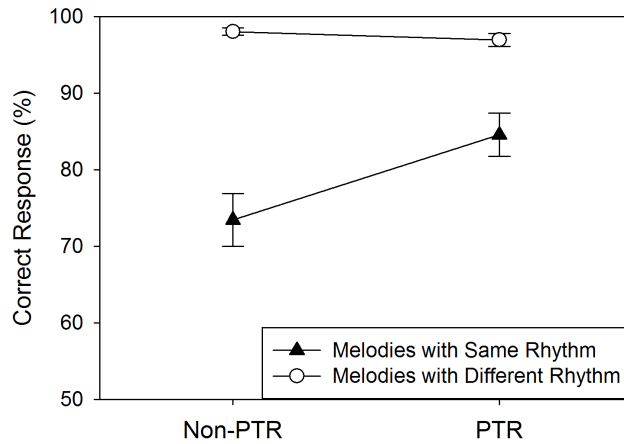
**Fig. 6.5** The pairwise discriminability of TVS melodies.

provement is caused by enhancement of perceiving the strength of each notes in melodies by PTR. That reason was convinced by the results of the pairwise discrimination and absolute identification of pure sinusoid vibrations in Sec. 5.2 and 5.3. The improvement of melody identification by PTR will advance the usefulness of TVS melodies with wide variety and enjoyment property.

Chapter **7**

# PTR-Embedded Graphical Vibration Pattern Editor

In this Chapter 7, we present a graphical authoring tool of vibratory patterns for multiple vibration motors, named "posVibEditor". The posVibEditor supports

- Graphical editing of vibration patterns,

- Drag-and-drop design paradigm,

- Systematic management of vibration patterns,

- XML formats in data files for extensibility,

- Multichannel vibration pattern design,

- Quick test of designed patterns by using a internal player, and

- Perceptually transparent rendering [53].

## 7.1  posVibEditor

### 7.1.1  Overview of User Interface and Internal Structure

The posVibEditor consists of three major panels for user interface. They are labeled with (a), (b), and (c) in Fig. 7.1. Panel (a) is named as the vibration pattern manager, and
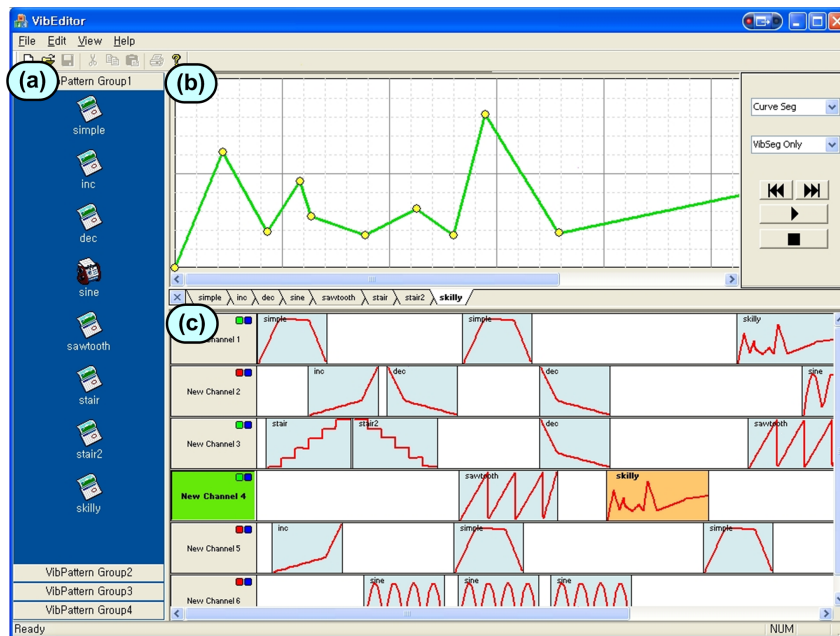
**Fig. 7.1: Screenshot of the posVibEditor.**

is workspace for managing and grouping formerly designed vibration patterns. Multiple
groups of vibration patterns can be administrated using the tabs located in the bottom of the
panel, improving the reusability. Panel (b) is the vibration pattern editor in which a vibration
pattern can be designed via drag-and-drop by moving control points overlaid on the pattern.
Several pre-defined pattern templates are also supported. Panel (c) is the multichannel time-
line interface. A designed pattern can be inserted into this timeline interface for composing
complex multichannel vibration patterns that would be synchronously played via multiple
vibration motors. We note that all of the three panels support drag-and-drop for quick and
easy design of vibration patterns.

The three user interface components interact with five internal functional modules, the
data structure manager module, XML loader, PTR module, player module, and hardware
communication module (Fig. 7.2). Further details on each user interface component and
associated internal modules will be presented in the rest of this chapter.
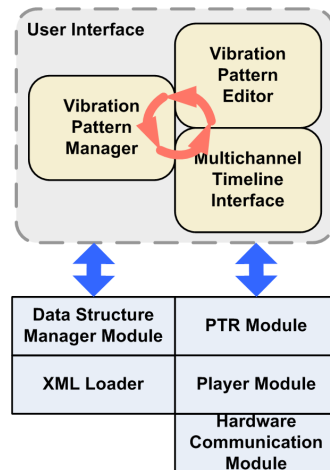
**Fig. 7.2** Internal structure of the posVibEditor.

## 7.1.2 Vibration Pattern Management

All files used in the posVibEditor, e.g., for vibration patterns, database for vibration pattern management, and multichannel configurations, are saved in the XML (eXtensible Markup Language) formats using MSXML (Microsoft Core XML Service) 6.0 . The XML file format has three major characteristics – structurability, extensibility, and interoperability [2, 20]. Since the XML format supports a hierarchical deep nested structure, vibration patterns that have many parameters can be saved in a highly structured form. The XML format can be easily extended to include new parameters by simply adding new corresponding tags defined freely by the developer, without changing the file structure or the program for loading the files. The interoperability of the XML file format also allows designed vibration patterns to be used in all platforms, such as Windows, Linux, Mac, and even embedded system.

The XML schema used to represent vibration patterns is shown in Fig. 7.3. A vibration pattern file should have 'VIBSEG' tag as a root node with 'BASETIME', 'NAME', 'TYPE', and 'CTRPOINT_LIST' tags as child nodes. The 'BASETIME' tag defines the start time of a vibration pattern and can be ignored if the start time is zero. The 'NAME' tag defines the unique name for the vibration pattern. The 'TYPE' tag specifies which of
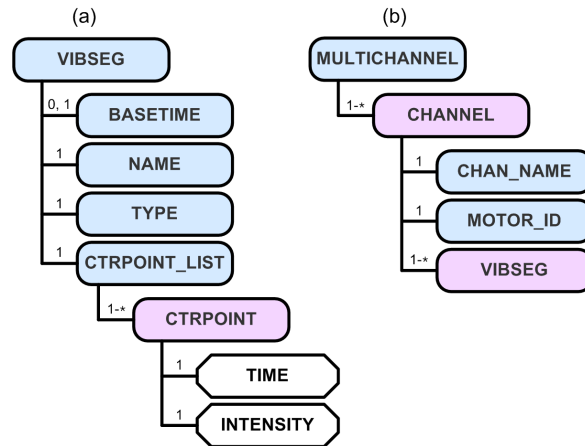
**Fig. 7.3** The XML schema for saving (a) a vibration pattern and (b) a multichannel configuration.

the three types of vibration patterns designable in the vibration editor (see Sec. 7.1.3 for further details) is used for the vibration pattern. For this, the current posVibEditor supports three strings: 'curve', 'line', and 'sine'. The 'CTRPOINT_LIST' tag is to store the list of control points consisting in the vibration pattern and has one more 'CTRPOINT' tags. The 'CTRPOINT' tag has 'TIME' and 'INTENSITY' attributes to describe the start time and vibration magnitude of a control point.

Vibration patterns can be administrated using the vibration pattern manager. Vibration patterns designed using the vibration pattern editor (see Sec. 7.1.3) can be registered in the database of the vibration pattern manager, grouped for efficient management, and reused later. To register a vibration pattern into the manager, the designer can select the corresponding tab on the multi-tab panel in the bottom of the vibration pattern editor, and drag and drop the tab into an adequate location in the vibration pattern manager. The registered vibration pattern is automatically grouped and sorted as an item in the active vibration group. The vibration pattern manager enables the structured storage of vibration patterns and improves the overall reusability of the patterns, in the efficient manner using the fairly standard GUI.

Among the five internal modules shown in Fig. 7.2, two modules, the data structure
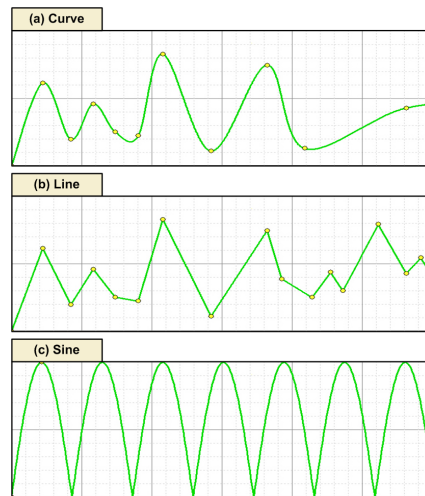
**Fig. 7.4** Three types of vibration pattern supported in the posVibEditor: (a) curve, (b) line, and (c) sine waveform.

manager module and the XML loader are responsible for the vibration pattern manager. As implied in their names, the data structure manager module is in charge of dealing with the data for vibration patterns and multichannel timeline. The XML loader saves and reads data in the XML schema to and from an external storage such as a hard disk.

### 7.1.3 Vibration Pattern Editing and Play

The vibration pattern editor of the posVibEditor (see panel (b) in Fig. 7.1) provides user interface for designing vibration patterns and playing them on the spot. The designer can begin pattern design by choosing one of predefined types of vibration patterns. The current version supports three types: curve, line, and sine waveform (see Fig. 7.4). A segment in the curve pattern consists of two control points, and the control points are interpolated using Catmull-Rom spline [10]. The line waveform also uses two control points for each segment. The sine waveform requires three control points. The time and value of the first control point defines the start time and DC offset, respectively. The amplitude of the sine waveform is determined by the difference between the values of the first and second control points. The last control point determines the finish time.

To edit a vibration pattern, the designer can move control points overlaid on the pattern using a mouse. The left button of the mouse is used for mostly moving a control point to a new position, and the right button for adding and deleting a control point. To add a new control point, the designer presses the right button on a control point near which s/he wants to add a new control point. Then a new control point is created beside the selected control point, and the designer can drag the new control point to a desired position while keeping the right button pressed. A control point can be deleted by pushing the left or right button on it and dragging it outside of the editor panel. Multi-tab interface (see the bottom of the editor) is also provided for simultaneous design of multiple vibration patterns. This intuitive multi-tab interface with the drag-and-drop leads to high accessibility, convenience, and efficiency in vibration pattern design, even for novice users.

A designed vibration pattern can be played and tested using the internal player. The player interface is located in the right of the vibration editor window. When PTR is used, the internal player converts a desired perceived intensity profile into the corresponding voltage sequence using the PTR module, and then transmits the voltage command to the vibration hardware through serial communication. When PTR is not used, a voltage vibration pattern is directly sent to the hardware. Using the internal player, the designer can repeat the design and test of vibration patterns quickly and easily, significantly accelerating the whole design process.

The internal player uses the multimedia timer supported in Microsoft Windows. Since the multimedia timer has 1 ms resolution for timing update, the maximum sampling rate for sending a vibration waveform to the hardware is 1 kHz. At present, we set the sampling rate to 200 Hz considering the computation time for the vibration pattern interpretation, the communication time with the vibration hardware, and the typical actuation delay of vibration motors.

Three internal modules, the PTR, internal player, and hardware communication modules, take care of the user interface for vibration pattern editing and playing. The current communication module uses the serial communication port in a PC, but can be easily extended to support more communication means if necessary.

### 7.1.4   Multichannel Timeline Interface

The multichannel timeline interface (panel (c) in Fig. 7.1) is incorporated in the posVibEditor in order to support the design and test of simultaneously controlled vibration patterns for multiple vibration motors. Using a number of vibration motors for interesting and effective vibration feedback is very common in haptics and VR research (see [12] for a recent example). The multichannel timeline configuration is also saved in the XML format following the schema shown in Fig. 7.3b. The root node 'MULTICHANNEL' has 'CHANNEL' tags. Each of the 'CHANNEL' tag has 'CHAN_NAME' tag, 'MOTOR_ID' tag, and several 'VIBSEG' tags, which define a unique channel name, the ID of a vibration motor corresponding to the channel, and vibration patterns to be played in the channel (as defined in Fig. 7.3a), respectively.

Using the multichannel timeline interface, a designer can create multiple channels each of which corresponds to a specific vibration motor, and arrange desired vibration patterns on the timeline corresponding to the channel. This multichannel timeline design is commonly used in video and audio editing tools. Our multichannel timeline interface for vibration editing is conceptually the same to that of traditional video and audio editors, in that multiple vibration "clips" can be organized along the common timeline and that an individual vibration channel is mapped to a vibration motor similarly to an audio channel mapped to a speaker in the audio system. The drag-and-drop manipulation is also supported in the multichannel interface. To our knowledge, this multichannel feature is unique in the posVibEditor among haptic authoring tools.

For communicating with the vibration hardware, we use serial communication from a PC to our custom controller for multiple vibration motors. Information for driving multiple vibration motors is encoded in a custom-designed protocol using seven bytes for each channel in every frame. One byte is used for a starting flag, and three bytes are for device number, motor number, and vibration level, respectively. The other three bytes duplicate the data bytes for validation. This protocol can be easily extended to take care of other types of vibration hardware if necessary.

### 7.1.5  Perceptually Transparent Rendering

A much more intuitive design mode supported by the posVibEditor is based on the concept of Perceptually Transparent Rendering (PTR) previously proposed in Chapter 5. The common practice prior to PTR was that vibration patterns are designed for a physical variable (e.g., applied voltage) that will be sent to a vibration display (e.g., a mobile phone with a vibration motor), as shown in Fig. 5.2a. The exerted vibration by the display is then processed by the human central nervous system. However, the dynamics of the vibration display and the complex human perception may seriously distort the perceived vibration effect from the original design intention. For example, when a vibration pattern that increases linearly with time is transmitted without PTR as is in Fig. 5.2a, a target perceptual attribute, the intensity of vibration perceived by the user, may grow nonlinearly (see [53] for concrete data). This makes it difficult for the designer to predict what perceptual effects will be obtained by the vibration patterns s/he is designing.

In PTR, the forward relation with vibration command as input and target percept as output is modeled, and its inverse relation is used for vibration rendering, as shown in Fig. 5.2b. Thus, the user can design a vibration effect with regards to the target percept, and the vibration command that will induce the intended percept is autonomously computed in a rendering program. This strategy minimizes the perceptual distortion of vibration rendering, and was shown to improve the pairwise discriminability of vibratory stimuli in a mobile phone [51].

The design mode for PTR implemented in the posVibEditor considers vibration voltage command to a mobile device as input and perceived vibration intensity as output, based on our previous findings on their relations [53, 54]. A vibration pattern can be authored for the perceived intensity of vibration that the user would experience. Then, a module responsible for PTR included in the form of a script in the posVibEditor automatically converts the pattern into voltage values to be sent to a vibration motor in the mobile device. This capability for perceptually transparent rendering is one of the features unique to the posVibEditor.

Table 7.1: Summary of the functionalities of the Haptic icon prototyper, the VibeTonz, and the posVibEditor.

| | Haptic Icon Prototyper [62] | VibeTonz [25] | posVibEditor |
|---|---|---|---|
| Authoring stimulus | Force | Vibration | Vibration |
| Used actuator | Rotary knob | Vibration motor | Vibration motor |
| Designable pattern type | Various | Trapezoidal form only | Various |
| Drag-and-drop | O | O | O |
| Internal player | O | O | O |
| Multichannel timeline | △* | X | O |
| Multiple actuators | X | X | O |
| Perceptually transparent rendering | X | X | O |

* Timeline interface for multiple haptic attributes is included for a single channel haptic knob.

## 7.2 Comparison with Other Editors

Despite the numerous applications of vibrotaction (see [1] for review), effort for developing software tools that enable easy and quick authoring of haptic effects has been somewhat scarce. MacLean et al. presented the "Hapticon Editor" in which haptic icons for a rotary knob can be graphically designed [15]. This editor was subsequently extended to the haptic icon prototyper [62]. In this editor, force profiles with respect to time can be designed using graphical user interface (GUI), and the designed haptic icons can be saved and reused using a palette. A player of the haptic icons is also included. The editor also supports the import capability of force profiles captured from a real knob. This editor can also be used for designing vibration effects, although it is more suited to kinesthetic feedback with a haptic knob.

Another recent notable authoring tool is the VibeTonz system [25] developed by Immersion Corp. This commercial tool provides GUIs for designing vibrotactile effects to be used in mobile devices. Drag-and-drop is also supported. The target vibration actuator is

a vibration motor inside a mobile device, thus vibration patterns are designed in terms of voltage applied to the motor [53]. A unique feature of the VibeTonz system is autonomous generation of vibrotactile patterns from a MIDI file containing music, mostly relying on the rhythm information.

Table 7.1 summarizes the main functionalities of the Hapticon Editor, the VibeTonz, and our posVibEditor. To the best of our knowledge, we are not aware of vibration editing software other than the Hapticon Editor and the VibeTonz.

# Chapter 8

# Vibration Rendering in Other Application

As technology advances, more functions have been, and continue to be added to the vehicle, resulting in increased needs for improved user interfaces. In this article, we investigate the feasibility of using vibrotactile feedback for in-vehicle information delivery. First, we measured the spectral characteristics of ambient vibrations in a vehicle, and designed clearly distinguishable sinusoidal vibrations. We further selected via dissimilarity rating the four sets of sinusoidal vibrations which had three to six vibrations. Second, we evaluated the learnability of the vibration sets when associated with common menu items of a Driver Information System (DIS). We also replaced the two most confused sinusoidal vibrations with vibrotactile melodies, and assessed the degree of learnability improvement.

## 8.1 Stimulus Design

Two vibrotactile stimuli that are close in time or space can mask each other, thereby making one stimulus imperceptible or at least feel significantly weaker [28]. This section describes how we designed vibrotactile signals free from the masking problem associated with ambient in-vehicle vibrotactile noise.

### 8.1.1 Spectral Characteristics of Ambient Vibration

For vibrotactile signal design, we first measured the internal vibration of a relatively old sedan (year = 1996; mileage = 270,000 km) using a three-axis accelerometer (Kistler; model 8630C), at three locations (center fascia, gear lever, and steering wheel) under four driving conditions (stationary/unclutched, stationary/clutched, driving at 60 km/h on a paved city road, and driving at 100 km/h on a highway). The measured time-domain acceleration data were transformed into the frequency domain using the FFT (Fast Fourier Transform), and then the amplitude at each frequency was converted to equivalent displacement. The perceived intensities of the vibrations were assessed as a function of frequency by comparing the displacement amplitudes to the corresponding absolute detection thresholds (Absolute Limens; ALs) of sinusoidal vibrotactile stimuli. The ALs, taken from [27], were for the case in which vibrotactile signals were transmitted through a ball-type tool held in the hand. The ball-type tool, out of all tools the ALs of which are available in the literature, is the most similar to the haptic knob used in our study.

The results clearly demonstrated that the spectral energy of the ambient in-vehicle vibration concentrated below 60 Hz, and that energy above 60 Hz was barely perceptible to the driver. The steering wheel was exposed to more intense vibrations than the other two test locations, due to its direct mechanical connection to the front wheels. The findings suggest that in order to avoid temporal masking, vibrotactile signals for in-vehicle information delivery need to have a principal frequency significantly higher than 60 Hz. Regrettably, in order to conform to a non-disclosure agreement made with an anonymous funding sponsor, we cannot provide more detailed results on the spectrum measurements.

### 8.1.2 Apparatus and Experiment Setup

To produce vibrotactile signals, we used a mini-shaker (Brüel & Kjær; model 4810; see Fig. 8.1) with high precision and repeatability in a wide bandwidth (DC – 18 kHz). A knob controller (Griffin Technology; model PowerMate; radius = 53.8 mm, height = 33.4 mm, weight = 110 g) was mounted on the mini-shaker using a custom-made adapter. A high-precision accelerometer (Kistler; model 8636C10) was installed inside the adapter. See
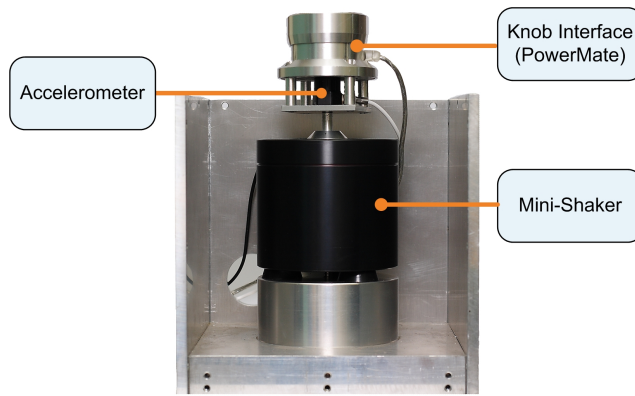
**Fig. 8.1** Mini-shaker system used in all experiments.

[27, 54] for further details about the control and calibration of the apparatus.

During the experiments, participants sat in front of a computer monitor and grasped the haptic knob with the thumb, index finger, and middle finger of the right hand. They were instructed to watch the monitor screen that displayed text information necessary for the progress of experiments. They also wore headphones that played white noise to block auditory noises emanating from the mini-shaker. The apparatus and experimental arrangements were common to all experiments reported in this chapter.

### 8.1.3 Selection of Sinusoidal Vibration Parameters

As presented in Sec. 8.1.1, the frequency range of perceptible in-vehicle vibrotactile noise had the upper bound of 60 Hz. For stimulus design, we determined through experimentation the lowest frequency of a sinusoidal stimulus that could be reliably discriminated from a 60 Hz signal. Five volunteers participated in the experiment. The experiment used the three-interval, forced-choice paradigm, and had 20 trials in total. In ten trials, two randomly selected intervals contained the 60 Hz reference signal while the other interval contained the test signal. In the other ten trials, the test signal was presented in two intervals, and the reference was presented in the other interval. The test stimulus had a frequency higher than 60 Hz. All signals had an amplitude of 30 dB SL (sensation level in decibel; relative to the ALs of the ball-type tool in [27]), and were 1 s long with an inter-stimulus interval (ISI) of

**Table 8.1** Single-tone vibrations used in the experiments.

| ID | 1 | 2 | 3 | 4 | 5 | 6 | 7 | 8 | 9 |
|---|---|---|---|---|---|---|---|---|---|
| Frequency (Hz) | 80 | 80 | 80 | 80 | 80 | 80 | 140 | 140 | 140 |
| Amplitude (dB SL) | 20 | 20 | 20 | 30 | 30 | 30 | 20 | 20 | 20 |
| Duration (s) | 0.5 | 1.0 | 2.0 | 0.5 | 1.0 | 2.0 | 0.5 | 1.0 | 2.0 |

| ID | 10 | 11 | 12 | 13 | 14 | 15 | 16 | 17 | 18 |
|---|---|---|---|---|---|---|---|---|---|
| Frequency (Hz) | 140 | 140 | 140 | 250 | 250 | 250 | 250 | 250 | 250 |
| Amplitude (dB SL) | 30 | 30 | 30 | 20 | 20 | 20 | 30 | 30 | 30 |
| Duration (s) | 0.5 | 1.0 | 2.0 | 0.5 | 1.0 | 2.0 | 0.5 | 1.0 | 2.0 |

500 ms. The order of trials was randomized per participant. In each trial, the participant perceived vibrations in the three intervals, and answered which interval presented a different signal using a keyboard with the left hand.

By increasing the frequency of the test signal and repeating the experiments, we found that vibrations need to have a frequency higher than 80 Hz in order to be distinguishable from the 60 Hz signal with average discriminability higher than 95%. Then, we performed the same experiment with the 80 Hz signal as a reference. The experiment demonstrated that the lowest signal frequency with average discriminability higher than 95% from the 80 Hz vibration was 140 Hz. Another repetition with 140 Hz as a reference frequency yielded 250 Hz. As a result, we selected 80, 140, and 250 Hz for the frequencies of sinusoidal vibrations to be used in the subsequent experiments.

For each signal frequency, two values for amplitude, 20 and 30 dB SL, and three values for duration, 0.5, 1.0, and 2.0 s, were combined. Vibration amplitudes lower than 20 dB SL were excluded to ensure clear perception, and those higher than 30 dB SL could not be properly generated by the mini-shaker system. The difference of 10 dB SL afforded reliable discrimination. Duration is a major contributing factor to vibrotactile discrimination [34, 66], and sinusoidal vibrations with the three durations could be easily distinguished. Durations shorter than 0.5 s were not used since they can be too short to result in stable percepts [70]. Durations longer than 2 s seem excessively long for information delivery. By combining the three frequencies, two amplitudes, and three durations, 18 sinusoidal signals were determined in a full factorial design, as shown in Table 8.1.

By design, the 18 sinusoidal signals were salient against in-vehicle ambient vibration and could be robustly discriminated pair-wise for single parameter changes. Discriminability for multi-dimensional variations (e.g., two signals different in both amplitude and frequency) was considered in Exp. VIII by estimating the perceptual distances between all vibration pairs.

In the stimulus design, we did not consider vibrotactile signals with continuously varying frequency, even though such a pattern could have been easily induced with the shaker system. It was because we considered the Linear Resonant Actuator (LRA) as the most appropriate vibrotactile actuator for implementing a practical system. The LRA is small, has a much shorter response time than a vibration motor, and has been widely used in mobile phones with a full touch screen. The frequency band of LRA, however, is centered at its resonance frequency and thus very narrow. As such, the LRA is not effective for generating signals with continuously varying frequency. Embedding several LRAs with different resonance frequencies into the haptic knob can be the most practical solution for our application.

### 8.1.4   Detection Thresholds for Haptic Knob

To command vibration intensities at a sensation level in the main experiments, we measured the ALs of sinusoidal vibrotactile stimuli perceived via the haptic knob at the frequencies of 80, 140, and 250 Hz. The 79.1% correct ALs were obtained using the three-interval, one-up three-down adaptive staircase method [36]. Three participants, all members of our research team, took part in the experiment. The procedure used in the experiment follows that in [27], except for the tool held in the hand.

The measured ALs are shown in Fig. 8.2, along with the ALs for a spherical tool [27]. The ALs of the haptic knob were much larger than those of the ball-type tool. A primary reason is the difference in contact areas; the contact area of the ball-type tool (= 11 cm$^2$ on average [27]) is much larger than that of the haptic knob grasped by the three fingertips of the thumb, index finger, and middle finger. The AL values were used to command vibration intensities in the following experiments.
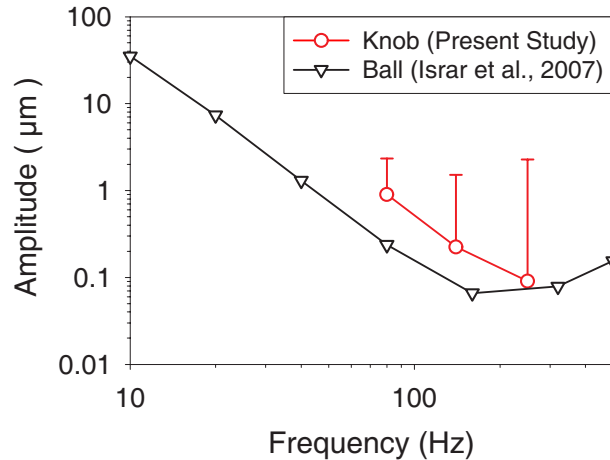
**Fig. 8.2** Absolute thresholds for the haptic knob.

## 8.2   Experiment VIII: Perceptual Distance

In Experiment VIII, we measured the perceptual distances between all pairs of the 18 sinusoidal vibrotactile signals.

### 8.2.1   Methods

Ten paid participants (five males and five females; $20 - 27$ years old with an average age of 24.6) participated in Experiment VIII. The performance of tactile perception (e.g., tactile sensitivity) deteriorates with age [70]. We also tend to become more conservative in accepting new interfaces. Thus, all experiments in this chapter used young participants to control the age band.

In each trial, the participant was presented with a pair of vibrations selected from the 18 sinusoids (Table 8.1) via the haptic knob. The pair was either one of the 153 ($= 18 \times 17/2$) pairs of different sinusoids for measuring perceptual distances, or one of the 18 pairs of same sinusoids for providing the reference of zero perceptual difference. In order to prevent participant fatigue, the experiment was undertaken in two sessions. In the first session, for a vibration pair $i$ and $j$ ($i < j$), vibration $i$ was presented first, and then vibration $j$ with an ISI of 500 ms. The order was reversed in the second session. Each session involved

189 ($= 153 + 18 \times 2$) trials using the 18 pairs of same sinusoids twice. The presentation order of vibration pairs was randomized per participant and session. The results of the two sessions were pooled for data analysis.

The participants rated the perceptual dissimilarity of vibration pairs on a scale of $0 - 100$ using a keyboard. A rating guide was provided to the participants as follows: $0$ = the two vibrations feel identical; $20$ = the vibrations are fairly similar and difficult to discriminate; $40$ = the vibrations are similar but discriminable in some degree; $60$ = the vibrations are discriminable but with some difficulty; $80$ = the vibrations are discernibly different and easy to discriminate; and $100$ = the vibrations are completely different. During training, the participants experienced the pairs of same vibrations to form the perceptual anchor of score $0$.

The measured perceptual distances were averaged across participants, and collectively summarized in a dissimilarity matrix. From the matrix, we determined the sets of vibrations that yielded the highest discriminability as follows. The discriminability of a set was defined as the sum of perceptual distances between all vibration pairs in the set. Specifically, for a set of vibration signals, $\Omega$, the discriminability of $\Omega$ is

$$d(\Omega) = \sum_{i,j \in \Omega, i \neq j} d(i, j) \tag{8.1}$$

where $d(i, j)$ is the perceptual distance between vibrations $i$ and $j$. Then, given the number of vibrations to be used for information delivery, $N$, we found a set with the highest discriminability, $\Omega^*$, such that $d(\Omega^*) \geq d(\Omega)$ for all $\Omega$ with $|\Omega| = N$, by exhaustively computing $d(\Omega)$ for all $\Omega$ and selecting one with the largest $d(\Omega)$. This search utilizes the finite and relatively small search spaces and guarantees a global maximum.

To determine how many vibrations to use, we surveyed the average number of top-level menu items in commercial DISs and noticed that it did not exceed six. Thus, we obtained four best vibration sets with three to six elements ($N = 3 - 6$) via the global search.

**Table 8.2: Dissimilarity matrix measured in Experiment VIII.**

| Vibration ID | 1 | 2 | 3 | 4 | 5 | 6 | 7 | 8 | 9 | 10 | 11 | 12 | 13 | 14 | 15 | 16 | 17 | 18 |
|---|---|---|---|---|---|---|---|---|---|---|---|---|---|---|---|---|---|---|
| 1 | - | 28.8 | 48.8 | 45.85 | 56.6 | 73.5 | 20.85 | 34.6 | 51.55 | 44.8 | 55.85 | 70.8 | 41.05 | 44.5 | 54.9 | 50.1 | 50.45 | 70.85 |
| 2 | 28.8 | - | 33.95 | 52.65 | 48.8 | 61.05 | 36.05 | 21.3 | 34.35 | 49.2 | 51.55 | 43.45 | 49.95 | 43.4 | 50.2 | 52.45 | 45.2 | 59.3 |
| 3 | 48.8 | 33.95 | - | 68.6 | 50 | 48.55 | 55.25 | 38.35 | 21.1 | 61.2 | 40.55 | 45.1 | 54.2 | 53.15 | 47 | 65.7 | 53.1 | 63.1 |
| 4 | 45.85 | 52.65 | 68.6 | - | 27.9 | 53.1 | 52.35 | 58.2 | 68.45 | 33.45 | 53.15 | 69.65 | 64.05 | 64.9 | 77.2 | 49.95 | 67.35 | 75.05 |
| 5 | 56.6 | 48.8 | 50 | 27.9 | - | 35.55 | 59.85 | 52.95 | 62.65 | 44.35 | 38.55 | 45 | 70.2 | 71 | 75.2 | 58.9 | 64.65 | 68.45 |
| 6 | 73.5 | 61.05 | 48.55 | 53.1 | 35.55 | - | 67.45 | 65.8 | 59.05 | 65.05 | 46.75 | 34.2 | 82.7 | 79.05 | 76.65 | 70.45 | 67.2 | 67.6 |
| 7 | 20.85 | 36.05 | 55.25 | 52.35 | 59.85 | 67.45 | - | 33.3 | 52.05 | 36.95 | 52 | 74.1 | 15.8 | 33.15 | 50.4 | 47.7 | 50.45 | 69.45 |
| 8 | 34.6 | 21.3 | 38.35 | 58.2 | 52.95 | 65.8 | 33.3 | - | 27.5 | 44.4 | 45.3 | 56.25 | 33.4 | 23.35 | 32.65 | 47 | 34.45 | 46.5 |
| 9 | 51.55 | 34.35 | 21.1 | 68.45 | 62.65 | 59.05 | 52.05 | 27.5 | - | 66.95 | 51.95 | 49.7 | 49.6 | 36 | 28.15 | 56.1 | 43 | 36.3 |
| 10 | 44.8 | 49.2 | 61.2 | 33.45 | 44.35 | 65.05 | 36.95 | 44.4 | 66.95 | - | 41.1 | 64 | 49.7 | 59.35 | 62.25 | 36.15 | 52.85 | 64.85 |
| 11 | 55.85 | 51.55 | 40.55 | 53.15 | 38.55 | 46.75 | 52 | 45.3 | 51.95 | 41.1 | - | 36 | 59.9 | 54.3 | 62.35 | 42.5 | 36.3 | 51.05 |
| 12 | 70.8 | 43.45 | 45.1 | 69.65 | 45 | 34.2 | 74.1 | 56.25 | 49.7 | 64 | 36 | - | 70.15 | 66.85 | 59.4 | 67.4 | 47.95 | 41 |
| 13 | 41.05 | 49.95 | 54.2 | 64.05 | 70.2 | 82.7 | 15.8 | 33.4 | 49.6 | 49.7 | 59.9 | 70.15 | - | 16.8 | 40.35 | 30.85 | 44.95 | 70.6 |
| 14 | 44.5 | 43.4 | 53.15 | 64.9 | 71 | 79.05 | 33.15 | 23.35 | 36 | 59.35 | 54.3 | 66.85 | 16.8 | - | 26.9 | 45 | 36.65 | 53.4 |
| 15 | 54.9 | 50.2 | 47 | 77.2 | 75.2 | 76.65 | 50.4 | 32.65 | 28.15 | 62.25 | 62.35 | 59.4 | 40.35 | 26.9 | - | 66.9 | 42.6 | 42.7 |
| 16 | 50.1 | 52.45 | 65.7 | 49.95 | 58.9 | 70.45 | 47.7 | 47 | 56.1 | 36.15 | 42.5 | 67.4 | 30.85 | 45 | 66.9 | - | 26.35 | 53.1 |
| 17 | 50.45 | 45.2 | 53.1 | 67.35 | 64.65 | 67.2 | 50.45 | 34.45 | 43 | 52.85 | 36.3 | 47.95 | 44.95 | 36.65 | 42.6 | 26.35 | - | 31.15 |
| 18 | 70.85 | 59.3 | 63.1 | 75.05 | 68.45 | 67.6 | 69.45 | 46.5 | 36.3 | 64.85 | 51.05 | 41 | 70.6 | 53.4 | 42.7 | 53.1 | 31.15 | - |
| Average | 49.63 | 44.80 | 49.86 | 57.76 | 54.74 | 61.98 | 47.48 | 40.9 | 46.73 | 51.56 | 48.19 | 55.35 | 49.66 | 47.51 | 52.69 | 50.98 | 46.74 | 56.73 |

### 8.2.2   Results

The average perceptual distances between vibration pairs are shown in the dissimilarity matrix (Table 8.2). Elements with high scores ($\geq 70$) are marked in boldface with shaded background. From the dissimilarity matrix, we determined the sets of sinusoidal vibrations with the greatest discriminability. For $N = 3, 4, 5, 6$, the sets were $\{6, 13, 18\}$, $\{4, 6, 13, 18\}$, $\{4, 6, 13, 15, 18\}$, and $\{1, 4, 6, 13, 15, 18\}$, respectively. The selected vibrations had a frequency of either 80 or 250 Hz and a duration of either 0.5 or 2 s (Table 8.1); no vibrations with a 140 Hz frequency or a 1 s duration were chosen. Vibrations 6, 13, and 18 were included in all the best sets.

An optimal set found by $d(\Omega)$ in (8.1) may include elements that are too close to each other. Therefore, we further applied MDS on the dissimilarity matrix to map the sinusoids to points in a 2D perceptual space while preserving their perceptual distances. The MDS plot in Fig. 8.3 shows that the mapped points form an approximate circle. The six most discriminative vibrations (1, 4, 6, 13, 15, and 18), which are represented by dark points, were placed on the boundary of the circle without abnormally close pairs. This adds further confidence to the discriminability between the selected vibrations. We used the four best vibration sets in the next experiments.

In comparison to the previous studies, Experiment VIII is unique in that only high-frequency sinusoidal vibrations were considered to avoid masking by ambient in-vehicle vibrotactile noise. We also note that all three parameters were treated in a unified manner.

## 8.3   Experiment IX: Learnability of Single-Tone Vibrations

In Experiment IX, we estimated the learnability of the most discriminative vibration groups determined in Experiment IX when they were mapped to common menus for secondary function control in a vehicle.
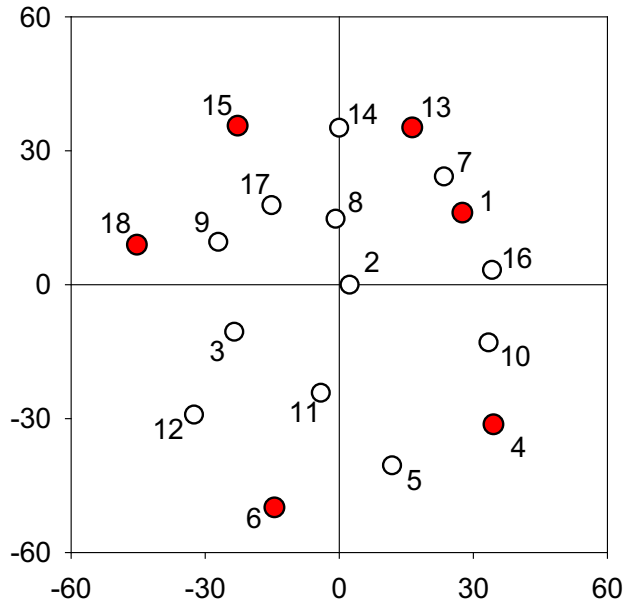
**Fig. 8.3** 2D perceptual space of sinusoidal vibrations estimated in Experiment VIII. The dark points represent the six most discriminative vibrations.

### 8.3.1   Methods

The experiment had four experimental conditions differing in the number of vibration-menu relations used (3 – 6). A total of 80 paid participants (40 males and 40 females; 20 – 32 years old with an average of 24.7) were recruited and randomly assigned to one of four groups in a between-subjects design. Each group had 20 participants (10 males and 10 females) and was devoted to measuring learnability under one experimental condition. All male and 25 female participants were students attending the authors' institution, and the other 15 female participants were not. In particular, all female participants used for five and six vibration-menu relations were the students. This was to balance educational background between genders in the more difficult conditions.

The vibrotactile signals determined in Experiment VIII were associated with the six top-level menu items common in commercial DISs and navigation systems: radio, MP3 & CD, air conditioner, navigation, DMB (Digital Multimedia Broadcasting), and DVD player. A

mapping from the sinusoidal vibrations to the menu items was randomly assigned for each participant and each experimental condition. Each participant experienced the mapping once prior to the experiment.

In each trial, a randomly selected vibration signal was presented to the participant via the shaker system. The participant felt the vibration through the haptic knob, and used a mouse to select a corresponding graphical menu displayed on a monitor screen. A correct-answer feedback was given by showing both the participant's response and the correct answer on the screen. Trials were repeated until it was judged that the participant had completely learned the mapping.

Learning completion was declared if a series of correct answers was encountered. In the series, all mapping relations must be answered correctly at least twice. Any incorrect answer would reset the series of correct answers. If a series of correct answers was found in trials between $n$ and $m$ ($n < m$), learning completion was recorded at trial $n - 1$. This rule counts the number of trials needed for complete memorization. It is adequate to the context of driving applications since complete memorization allows a driver to control secondary functions more quickly.

For performance evaluation, we counted the number of trials necessary to complete learning. This number was normalized by the number of vibration-menu relations of the experimental condition, thereby providing the number of whole relation repetitions required for complete memorization. We also recorded the number of errors made during the learning process.

### 8.3.2 Results and Discussion

The results of Experiment IX are summarized in the two plots of Fig. 8.4. Fig. 8.4a shows the average numbers of repetitions necessary for the complete learning of vibration-menu relations for each experimental condition, and Fig. 8.4b shows the average numbers of errors made during the learning process. Data for the male and female participants were also presented in all plots. The error bars represent standard errors.

The average numbers of repetitions required to learn three and four vibration-menu re-

lations were quite low: 1.1 and 2.2, respectively. However, the performance of five and six relations was considerably worse. Five relations seemed usable for the male participants (average number of repetitions = 4.0), but not for the female (average number of repetitions = 12.5). The average number of repetitions for six relations (= 31.6) was too high to be used in practice, regardless of the gender. The error numbers shown in Fig. 8.4b also exhibited a similar trend. One-way ANOVA confirmed that the number of vibration-menu relations had statistically significant effects on both the number of repetitions ($F(3,72) = 30.66, p < 0.0001$) and the number of errors ($F(3,72) = 29.43, p < 0.0001$).

The female participants tended to require more prolonged training than the male to completely learn five and six vibration-menu relations. The differences were statistically significant in both the number of repetitions ($F(1,72) = 9.42, p = 0.0030$) and the number of errors ($F(1,72) = 8.34, p = 0.0051$). In contrast, Experiment VIII did not exhibit noticeable gender differences in the perceptual distances between vibrations. No statistically significant effects of the gender were found, either in all data of Experiment VIII ($F(1,1528) = 0.78, p = 0.3776$) or in the data of the 15 pairs with high perceptual distances marked in Table 8.2 ($F(1,148) = 0.28, p = 0.5946$). Therefore, the gender difference in learnability implies different performances in associating vibrations and menu items between the male and female participants.

As all menu items were for electronic devices in a vehicle, a subject in which males generally take a greater interest in, we suspected that this might have caused the learnability difference. Thus, we conducted another follow-up experiment using the six items that females are more familiar with: BB (Blemish Balm) cream, lip gloss, eye shadow, leggings, flat shoes, and high heels. Ten participants (five males and five females) who were students of the authors' university participated in this experiment. Prior to the experiment, the participants rated the familiarity of the items in a 5 point Likert scale. The average ratings by the male and female participants were 2.53 and 4.13, respectively. However, the average number of repetitions needed for learning was still smaller in the male participants (14.8) than in the female participants (27.9). The ratios of the numbers between genders were also similar, 2.12 for the DIS menus and 1.88 for the female familiar items. Thus, it is unlikely

(a) Number of repetitions.



(b) Number of errors.
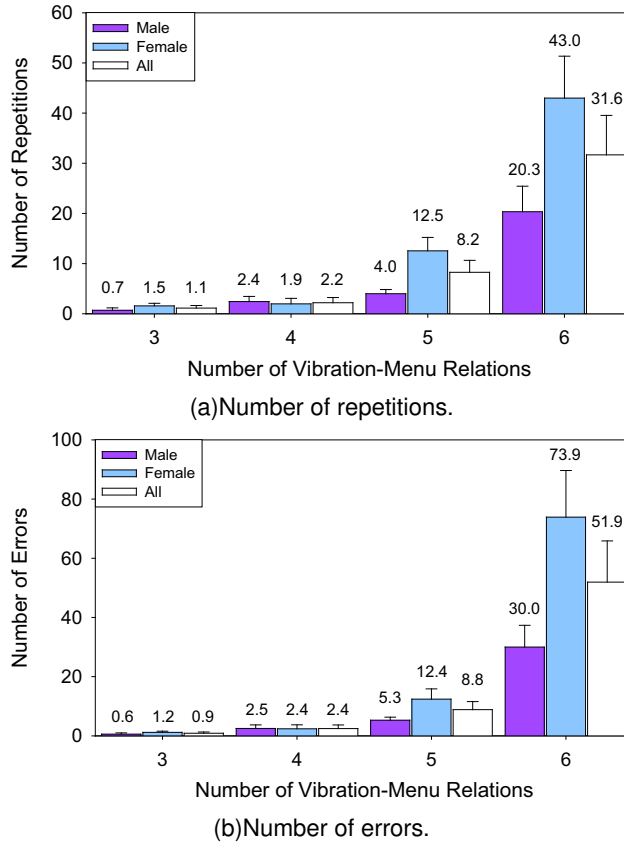
**Fig. 8.4** Results of Experiment IX.

that familiarity to menu items affected the learnability difference in Experiment IX.

In neurophysiology, several related studies demonstrated gender differences, such as the lateralization of brain function of working memory [59] and brain activation by tactile stimuli [55]. It was also reported that males prefer the tactile/kinesthetic resource for learning new information more than females [26, 57]. However, we were unable to find very direct accounts for the learnability difference observed in Experiment IX; the question seems to be an open issue.

Learnability degradation became apparent when vibration 15 was included in the five vibration set, and vibration 1 was included in the six vibration set. According to the experimental record, vibration 15 was confused with vibration 18, and vibration 1 with vibration

4. The confused pairs were different only in amplitude (see Table 8.1). It appears that the 10 dB SL amplitude difference is sufficient for discrimination, but not when meaning association is involved.

This experiment quantified the ability to memorize the meanings of simple sinusoidal signals associated with common secondary function menus in a vehicle. Our results demonstrated relatively low capability, with discernible differences observed between the genders, even though the signals varied in all of the three parameter dimensions with large perceptual distances. The reported data can also be used as a baseline to evaluate the learnability of more complex vibrotactile messages. Such data have been relatively rare in the literature.

## 8.4   Experiment X: Learnability of Vibrotactile Melodies

In Experiment X, we replaced the two sinusoids (vibrations 1 and 15) that significantly degraded learnability in Experiment IX with vibrotactile patterns, and repeated the same experiment.

### 8.4.1   Methods

Two vibrotactile patterns were designed by combining the features of the sinusoidal vibrations. One pattern, denoted by P1, used frequency hopping in a short duration (upper panel in Fig. 8.5). Each bar in the figure represents a time interval during which the corresponding frequency signal is played. Frequency variation in such a wide range can be effective for discrimination, as shown in Experiment VIII. The other pattern, P2, changed rhythm at a fixed frequency (80 Hz) in a longer duration (lower panel in Fig. 8.5). The rhythm is one of the most distinguishable characteristics of effective vibrotactile patterns [63, 66]. The pattern imitated the rhythm of a song used in a popular TV commercial. All pattern components had an amplitude of 30 dB SL.

In this experiment, the vibration set consisted of the four sinusoids (vibrations 4, 6, 13, and 18) and the two patterns. We recruited another 20 paid participants (10 males and 10 females; 20 – 28 years old with an average of 24.8), and measured the learnability of six vibration-menu relations. The other procedures were identical to those of Experiment IX.
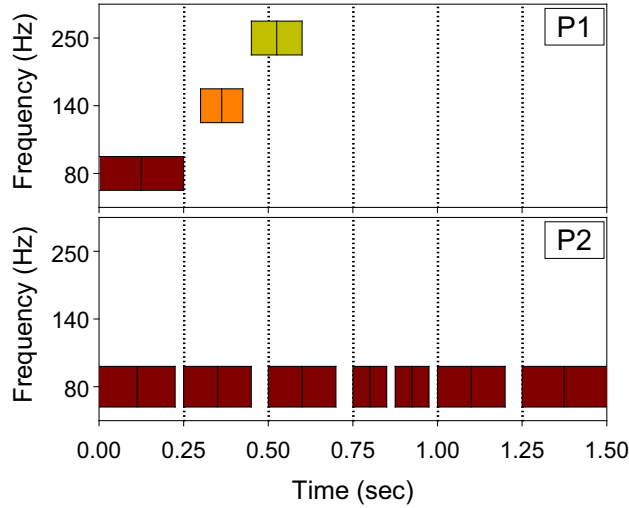
**Fig. 8.5** Two vibrotactile patterns used in Experiment X.

## 8.4.2   Results and Discussion

The results of Experiment X are summarized in Fig. 8.6. The average number of repetitions necessary for learning six vibration-menu relations decreased from 31.6 in Experiment IX to 6.9 in Experiment X, and the average number of errors decreased from 51.9 in Experiment IX to 8.7 in Experiment X. In terms of the number of repetitions, the use of vibrotactile patterns resulted in a performance improvement of 457%. For statistical analysis, we pooled the data of Experiment IX for six vibration-menu relations and the data of Experiment X, and performed two-way ANOVA with experiment number and gender as independent variables. The use of the vibrotactile patterns in Experiment X had statistically significant effects in both the number of required repetitions ($F(1, 36) = 23.73, p < 0.0001$) and the number of errors ($F(1, 36) = 23.92, p < 0.0001$). This proves that the use of vibrotactile patterns demonstrably aids in the memorization of associated meanings. The gender was also a statistically significant factor in both metrics ($F(1, 36) = 6.87, p = 0.0128$ and $F(1, 36) = 8.68, p = 0.0056$, respectively).

To gain further insight, we computed the average rates of correct responses recorded in trials before learning was completed. These results are shown in Fig. 8.7 for each vibration

signal. In Experiment IX where only sinusoidal vibrations were used, the average correct response rates were in 55.3 – 84.5% with a grand mean of 72.8%. In Experiment X, the four sinusoidal vibrations resulted in similar rates (69.4 – 83.3%; grand mean = 74.4%), but the two patterned vibrations resulted in much higher rates (86.7 – 92.2%; grand mean = 89.5%). We also counted the number of participants who did not make any incorrect responses during learning in Experiment X for each vibration signal. The average numbers were 12.5 (out of 20 participants) for the two patterns and 8.25 for the four sinusoids. This comparison clearly indicates that including the patterned signals significantly enhances learnability.

We also suspected that the excellent learnability of the two patterned signals may positively affect the learnability of the other four sinusoidal vibrations, but such interaction was not observed. The average correct response rate of the four sinusoids in Experiment X (= 74.4%) was slightly less than that in Experiment IX (= 77.8%). On the other hand, this implies that further improvements in learnability can be achieved if the four sinusoids are replaced with well-designed vibrotactile patterns.

In Experiment X, the average duration of vibration signals was 1.18 s. Considering the time needed to enter a response, a trial took about 3 s on average. Since 6.9 average repetitions were necessary to learn 6 vibration-menu relations, the average time required to finish the experiment was around 2 minutes (3 s $\times$ 6.9 $\times$ 6 = 124.2 s). Therefore, the learnability of the four sinusoids and two patterns used in Experiment X can be regarded as acceptable. We still expect more improvement if all adequately designed patterns are used as vibrotactile messages.

In summary, the results of Experiment X provide a quantitative comparison, in terms of the learnability under the context of driving applications, between using sinusoids only and including vibrotactile patterns.
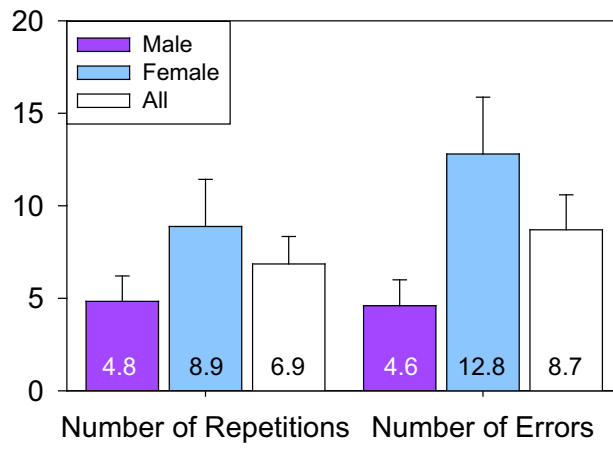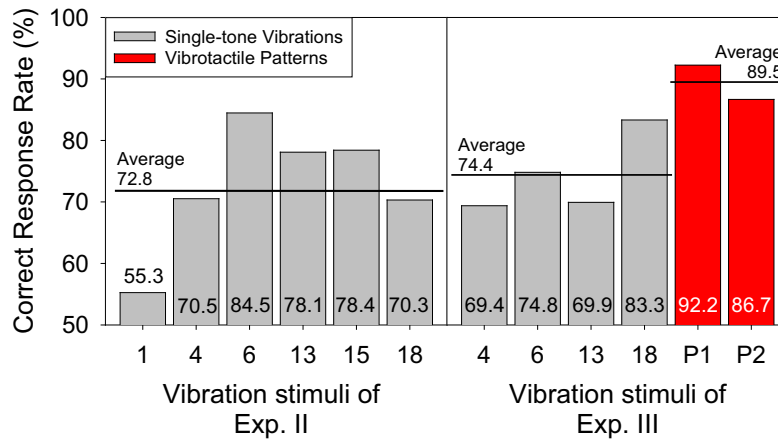
**Fig. 8.6** Results of Experiment X.



**Fig. 8.7** Correct response rates of vibration stimuli recorded prior to learning completion.

# Chapter 9

# Conclusion and Future Work

In this thesis, we first investigated the physical and perceptual characteristics of two minia-
ture vibration actuators and provided guidelines to control them. According to the guide-
line, we recommend that the increasing of the driving voltage above 3.5 V applied to the
vibration motor is not necessary to provide stronger sensations and the voice-coil actuator
should be controlled with narrow bandwidth frequencies around the resonance frequency to
generate desired vibration effects.

Additionally, we measured the perceived intensities at various frequencies and ampli-
tudes for mobile device vibration. The measured perceived intensities of vibrations can be
used to configure the perception model represented with the frequency and amplitude in
sensation level. For the precise prediction of perceived intensities, the computational model
for vibration perception in mobile device has an important role when vibrations have broad-
band frequency. To evaluate its applicability, we compared perceived intensities predicted
by using the model to the perceptual data of two miniature actuators. The high correlation
of comparison results guarantees the feasibility of predicting perceived intensities of mobile
device vibration without any psychophysical experiments.

We also proposed perceptually transparent vibration rendering (PTR) and evaluated the
benefits of it in two experiments using pure tone vibrations and vibrotactile melodies. In
an experiments for pure tone vibrations, pair-wise relative discriminability and absolute

identification of vibration stimuli were tested. The results favored the use of PTR, that is, a larger number of vibratory stimuli were reliably discriminated and identified through the mobile device. With PTR, we can reliably use 5 – 6 upmost vibration levels for information encoding during maintaining higher correct response, but just 3 – 4 levels without PTR. For the practical usage of PTR, we evaluated PTR in an experiment using vibrotactile melodies. The two kinds of vibrotactile melodies, a constant strength (CS) and a time-varying strength (TVS) vibrotactile melody, were used. A TVS melody has high discriminability competed to the CS melodies and other TVS melodies, and the discriminability is increased higher when the melodies were rendered using PTR. The improvement of melody identification using PTR will advance the usefulness of TVS melodies.

Finally, we developed a vibration pattern authoring tool named "posVibEditor" for quick and easy design of multiple vibration patterns. The user interface supports drag-and-drop to maximize the user's convenience and multichannel timeline interface in which synchronized multichannel vibration patterns for multiple vibration motors can be designed. Furthermore, the posVibEditor supports perceptually transparent rendering. Consequently, the novice designer can concentrate on the perceptual effect of a vibration pattern only, which makes the authoring process more intuitive and convenient.

The present study contributes to enlarging our understanding of the utility of perception-based vibration rendering in mobile devices.

In the future, it is required to extend our vibration perception model with considering of user's age, other grip postures, other body locations, and multiple directional vibrations. Also we need to evaluate the usefulness of vibrotactile melody with PTR for information delivery in commercial mobile device and to configure multimodal icons which are combinations of music melodies and vibrotactile melodies. And it is necessary to provide authoring methodology on the levels of not only perceived intensity of vibrations, but also their semantic messages in the vibration editor.

# Appendix

## A. Grip Force Measurement

Eight participants (25 – 30 years old with an average of 27.1) participated in this experiment to measure grip force while holding the mock-up cellular phone. A thin aluminum plate with 10 mm diameter was fastened on the side of the phone which was pressed by the thenar eminence of the hand. A film-type pressure sensor (Tekscan Inc.; model FlexiForce A201) was placed between the phone and aluminum plate. This allowed for reliable grip force sensing despite the small sensing area of the pressure sensor. The attachment position of the aluminum plate was manually determined for each participant due to individual differences in hand posture and size. The pressure sensor was calibrated using standard weights prior to the experiment.

The participants were instructed to hold the phone with a comfortable grip force in two conditions of grounded and ungrounded. In the grounded condition, the phone was attached on the mini-shaker. In the ungrounded condition, the participants held the phone in the air without any mechanical support as they usually do with a mobile device. For each condition, ten trials were repeated, and the grip forces were measured in each trial. The participants were asked to release and grasp the phone again between trials.

On average, the grip forces were 1.79 N for the grounded condition and 1.75 N for the ungrounded condition. Standard deviations were relatively large, 1.13 N and 1.42 N, respectively, due to large individual differences. We confirmed via ANOVA that the phone-

supporting condition was not statistically significant for the grip force ($F(1,6) = 0.03$, $p = 0.8605$).

# Bibliography

[1] M. Benali-Khoudja, M. Hafez, J.-M. Alexandre, and A. Kheddar. Tactile interfaces. a state-of-the-art survey. In *Proceddings of 35th International Symposium on Robotics (ISR'04)*, pages 721–726, 2004.

[2] T. Bray, J. Paoli, and C. M. Sperberg-McQueen. Extensible markup language (xml) 1.0. *World Wide Web Consortium (W3C) Recommendation, http://www.w3.org/XML/*, 1998.

[3] S. A. Brewster and L. M. Brown. Tactons: Structured tactile messages for non-visual information display. In *Proceddings of Australasian User Interface Conference*, pages 15–23, 2004.

[4] S. A. Brewster and A. King. An investigation into the use of tactons to present progress information. In *Proceedings of Interact 2005*, pages 167–176, 2005.

[5] L. Brown and J. Williamson. Shake2talk: Multimodal messaging for interpersonal communication. In *Proceedings of 2nd International Workshop on Haptic and Audio Interaction Design (HAID07)*, pages 44–55, 2007. doi: http://dx.doi. org/10.1007/978-3-540-76702-2\_6. URL `http://dx.doi.org/10.1007/978-3-540-76702-2\_6`.

[6] L. M. Brown and T. Kaaresoja. Feel who's talking: Using tactons for mobile phone

alerts. In *CHI '06 Extended Abstracts on Human Factors in Computing Systems*, pages 604–609, 2006.

[7] L. M. Brown, S. A. Brewster, and H. C. Purchase. A first investigation into the effectiveness of tactons. In *Proceedings of the First Joint Eurohaptics Conference and Symposium on Haptic Interfaces for Virtual Environments and Teleoperator Systems (World Haptics Conference)*, pages 167–176, 2005.

[8] L. M. Brown, S. A. Brewster, and H. C. Purchase. Tactile crescendos and sforzandos: applying musical techniques to tactile icon design. In *Extended Abstracts in CHI 2006*, pages 610–615, 2006.

[9] S. Cardin, D. Thalmann, and F. Vexo. Wearable system for mobility improvement of visually impaired people. *The Visual Computer: International Journal of Computer Graphics*, 23:109–118, 2007.

[10] E. Catmull and R. Rom. A class of local interpolating splines. *Computer Aided Geometric Design*, pages 317–326, 1974.

[11] A. Chang and C. O'Sullivan. Audio-haptic feedback in mobile phones. In *Proceedings of CHI '05 extended abstracts on Human factors in computing systems*, pages 1264–1267, New York, NY, USA, 2005. ACM. ISBN 1-59593-002-7. doi: http://doi.acm.org/10.1145/1056808.1056892.

[12] H.-Y. Chen, J. Santos, M. Graves, K. Kim, and H. Z. Tan. Tactor localization at the wrist. *(EuroHaptics 2008)*, 5024:209–218, 2008.

[13] C. W. de Silva. *Sensors and Actuators: Control System Instrumentation (Chapter 7.2 DC Motor Equations)*. CRC; first edition, 2007.

[14] R. G. Dong, J. Z. Wu, T. W. McDowell, D. E. Welcome, and A. W. Schopper. Distribution of mechanical impedance at the fingers and the palm of the human hand. *Journal of Biomechanics*, 38:1165–1175, 2005.

[15] M. J. Enriquez and K. E. MacLean. The hapticon editor: A tool in support of haptic communication research. In *In Proceedings of the 11th Symposium on Haptic Interfaces for Virtual Environment and Teleoperator Systems*, pages 356–362, 2003.

[16] M. Fukumoto and T. Sugimura. Active click: Tactile feedback for touch panels. In *Proceedings of the Annual CHI Conference on Human Factors in Computing Systems*, pages 121–122, 2001. ISBN 1-58113-340-5. doi: http://doi.acm.org/10.1145/634067. 634141.

[17] A. Gallace, H. Z. Tan, and C. Spence. The body surface as a communication system: The state of the art after 50 years. *Presence*, 16(6):655–676, 2007.

[18] G. A. Gescheider. *Psychophysics: The Fundamentals*. Lawrence Erlbaum Associate, Mahwah, NJ, USA, 3rd edition, 1997.

[19] G. Ghiani, B. Leporini, and F. Paternò. Vibrotactile feedback as an orientation aid for blind users of mobile guides. In *Proceedings of the International Conference on Human Computer Interaction with Mobile Devices and Services (MobileHCI)*, pages 431–434, New York, NY, USA, 2008. ACM. ISBN 978-1-59593-952-4. doi: http: //doi.acm.org/10.1145/1409240.1409306.

[20] C. F. Goldfarb and P. Prescod. *The XML handbook*. Prentice Hall PTR, Upper Saddle River, NJ, USA, 1998.

[21] M. Hall, E. Hoggan, and S. Brewster. T-bars: Towards tactile user interfaces for mobile touchscreens. In *Proceedings of the International Conference on Human Computer Interaction with Mobile Devices and Services (MobileHCI)*, pages 411–414, 2008. ISBN 978-1-59593-952-4. doi: http://doi.acm.org/10.1145/1409240.1409301.

[22] E. Hoggan, S. Anwar, and S. A. Brewster. Mobile multi-actuator tactile displays. *Lecture Notes in Computer Science (2nd International Workshop on Haptic and Audio Interaction Design, HAID2007)*, 4813:22–33, 2007.

[23] E. Hoggan, S. A. Brewster, and J. Johnston. Investigating the effectiveness of tactile feedback for mobile touchscreens. In *Proceeding of the Annual SIGCHI conference on Human Factors in Computing Systems*, pages 1573–1582, 2008. ISBN 978-1-60558-011-1. doi: http://doi.acm.org/10.1145/1357054.1357300.

[24] E. E. Hoggan and S. A. Brewster. Crossmodal icons for information display. In *Proceedings of CHI '06 extended abstracts on Human factors in computing systems*, pages 857–862, New York, NY, USA, 2006. ACM. ISBN 1-59593-298-4. doi: http://doi.acm.org/10.1145/1125451.1125619.

[25] Immersion Corp. Mobility overview, 2007. `http://www.immersion.com/mobility`.

[26] C. A. Isman and N. U. Gundogan. The influence of digit ratio on the gender difference in learning style preferences. *Personality and Individual Differences*, 46(4):424 – 427, 2009. ISSN 0191-8869.

[27] A. Israr, S. Choi, and H. Z. Tan. Mechanical impedance of the hand holding a spherical tool at threshold and suprathreshold stimulation levels. In *Proceedings of the World Haptics Conference*, pages 56–60, 2007.

[28] L. A. Jones and S. J. Lederman. *Human Hand Function*. Oxford University Press, Inc., New York, NY, USA, 2006.

[29] L. A. Jones, M. Nakamura, and B. Lockyer. Development of a tactile vest. In *Proceedings of the International Symposium on Haptic Interfaces for Virtual Environment and Teleoperator Systems*, pages 82–89, 2004.

[30] L. A. Jones, B. Lockyer, and E. Piateski. Tactile display and vibrotactile pattern recognition on the torso. *Advanced Robotics*, 20(12):1359–1374, 2006.

[31] J. Jung. A study on a motion-based remote controller and vibration feedback for mobile device optimal to low power consumption and high perceived intensity. Master's thesis, POSTECH, 2007.

[32] J. Jung and S. Choi. Perceived magnitude and power consumption of vibration feedback in mobile devices. *Lecture Notes on Computer Science (Proceedings of the International Conference on Human-Computer Interaction, Part II, HCII 2007)*, 4551: 354–363, 2007.

[33] S.-C. Kim, T.-H. Yang, B.-K. Han, and D.-S. Kwon. Interaction with a display panel - an evaluation of surface-transmitted haptic feedback. In *Proceedings of International Conference on Control, Automation and Systems (ICCAS 2008)*, pages 278–283, Oct. 2008. doi: 10.1109/ICCAS.2008.4694564.

[34] K. Kosonen and R. Raisamo. Rhythm perception through different modalities. In *Proceedings of Eurohaptics*, pages 365–369, 2006.

[35] D. A. Lawrence. Stability and transparency in bilateral teleoperation. *IEEE Transactions on Robotics and Automation*, 9(5):624–637, 1993.

[36] M. R. Leek. Adaptive procedure in psychophysical research. *Perception & Psychophysics*, 63(8):1279–1292, 2001.

[37] K. A. Li, T. Y. Sohn, S. Huang, and W. G. Griswold. PeopleTones: a system for the detection and notification of buddy proximity on mobile phones. In *Proceeding of the International Conference on Mobile Systems, Applications, and Services (MobiSys)*, pages 160–173, New York, NY, USA, 2008. ACM. ISBN 978-1-60558-139-2. doi: http://doi.acm.org/10.1145/1378600.1378619.

[38] R. W. Lindeman, J. N. Templeman, J. L. Sibert, and J. R. Cutler. Handling of virtual contact in immersive virtual environments: Beyond visuals. *Virtual Reality*, 6(3): 130–139, 2002.

[39] J. Luk, J. Pasquero, S. Little, K. MacLean, V. Levesque, and V. Hayward. A role for haptics in mobile interaction: Initial design using a handheld tactile display prototype. In *Proceedings of the ACM Conference on Human Factors in Computing Systems (CHI)*, pages 171–180. 2006.

[40] K. E. MacLean. Foundations of transparency in tactile information design. *IEEE Transactions on Haptics*, 1(2):84–95, 2008.

[41] Microsoft Corp. Xbox, 2007. `http://www.xbox.com`.

[42] M. Morioka and M. J. Griffin. Magnitude-dependence of equivalent comfort contours for fore-and-aft, lateral and vertical hand-transmitted vibration. *Journal of sound and vibration*, 295(3-5):633–648, 2006.

[43] M. Morioka and M. J. Griffin. Frequency dependence of perceived intensity of steering wheel vibration:effect of grip force. In *Proceedings of World Haptics 2007 (The Second Joint Eurohaptics Conference and Symposium on Haptic Interfaces for Virtual Environment and Teleoperator Systems)*, pages 50–55, 2007.

[44] A. M. Murray, R. L. Klatzky, and P. K. Khosla. Psychophysical characterization and testbed validation of a wearable vibrotactile glove for telemanipulation. *Presence: Teleoperators and Virtual Environments*, 12(2):156–182, 2003.

[45] A. Nashel and S. Razzaque. Tactile virtual buttons for mobile devices. In *Proceedings of the Annual CHI Conference on Human Factors in Computing Systems*, pages 854–855, 2003. ISBN 1-58113-637-4. doi: http://doi.acm.org/10.1145/765891.766032.

[46] Nintendo. Wii, 2007. `http://wii.com`.

[47] I. Poupyrev and S. Maruyama. Tactile interfaces for small touch screens. In *Proceedings of the Annual ACM Symposium on User Interface Software and Technology (UIST)*, pages 217–220, 2003. ISBN 1-58113-636-6. doi: http://doi.acm.org/10.1145/964696.964721.

[48] I. Poupyrev, S. Maruyama, and J. Rekimoto. Ambient touch: Designing tactile interfaces for handheld devices. In *Proceedings of the ACM Symposium on User Interface Software and Technology*, pages 51–60, 2002. ISBN 1-58113-488-6. doi: http://doi.acm.org/10.1145/571985.571993.

[49] J. Rekimoto and C. Schwesig. PreSenseII: bi-directional touch and pressure sensing interactions with tactile feedback. In *Proceedings of the Annual CHI Conference on Human Factors in Computing Systems*, pages 1253–1258, 2006. ISBN 1-59593-298-4. doi: http://doi.acm.org/10.1145/1125451.1125685.

[50] L. Rovers and H. van Essen. Design and evaluation of hapticons for enriched instant messaging. In *Proceedings of Eurohaptics*, pages 498–503. 2004.

[51] J. Ryu and S. Choi. Benefits of perceptually transparent vibration rendering in mobile device. *Lecture Notes on Computer Science (EuroHaptics 2008)*, 5024:706–711, 2008.

[52] J. Ryu and G. J. Kim. Using a vibro-tactile display for enhanced collision perception and presence. In *Proceedings of the ACM International Conference on Virtual Reality Software and Technology*, pages 89–96, 2004.

[53] J. Ryu, J. Jung, S. Kim, and S. Choi. Perceptually transparent vibration rendering using a vibration motor for haptic interaction. In *Proceedings of IEEE Internatiional Symposium on Robot and Human Interactive Communication (RO-MAN)*, pages 310–315, 2007.

[54] J. Ryu, J. Jung, and S. Choi. Perceived magnitudes of vibrations transmitted through mobile device. In *Proceedings of The 16th Symposium on Haptic Interfaces for Virtual Environments and Teleoperator Systems*, pages 139–140, 2008.

[55] N. Sadato, V. Iba轸奏z, M.-P. Deiber, and M. Hallett. Gender difference in premotor activity during active tactile discrimination. *NeuroImage*, 11(5):532 – 540, 2000. ISSN 1053-8119.

[56] A. Sahami, P. Holleis, A. Schmidt, and J. Häkkilä. Rich tactile output on mobile devices. In *Proceedings of the European Conference on Ambient Intelligence (AmI '08)*, pages 210–221, Berlin, Heidelberg, 2008. Springer-Verlag. ISBN 978-3-540-89616-6. doi: http://dx.doi.org/10.1007/978-3-540-89617-3_14.

[57] J. A. Slater, H. L. Lujan, and S. E. DiCarlo. Does gender influence learning style preferences of first-year medical students? *Advances in Physiology Education*, 31: 336–342, 2007.

[58] Sony Computer Entertainment Inc. Playstation, 2007. `http://www.playstation.com`.

[59] O. Speck, T. Ernst, J. Braun, C. Koch, E. Miller, and L. Chang. Gender differences in the functional organization of the brain for working memory. *Neuroreport*, 11(11): 2581–2585, 2000.

[60] S. S. Stevens. on the psychophysical law. *Psychological Review*, 64:153–181, 1957.

[61] I. R. Summers. *Tactile Aids for the Hearing Impaired*. Whurr Publishers Ltd, London, England, 1992.

[62] C. Swindells, E. Maksakov, K. E. Maclean, and V. Chung. The role of prototyping tools for haptic behavior design. In *Proceedings of Symposium on Haptic Interfaces for Virtual Environment and Teleoperator Systems*, pages 161–168, 2006.

[63] D. Ternes and K. E. Maclean. Designing large sets of haptic icons with rhythm. *Lecture Notes on Computer Science (EuroHaptics 2008)*, 5024:199–208, 2008. doi: http://dx.doi.org/10.1007/978-3-540-69057-3_24.

[64] D. R. Ternes. Building large sets of haptic icons: rhythm as a design parameter, and between-subjects mds for evaluation. Master's thesis, The University of British Columbia, 2007.

[65] S. Töyssy, J. Raisamo, and R. Raisamo. Telling time by vibration. In *Proceedings of Eurohaptics*, pages 924–929, Berlin, Heidelberg, 2008. Springer-Verlag. ISBN 978-3-540-69056-6. doi: http://dx.doi.org/10.1007/978-3-540-69057-3_116.

[66] J. B. F. van Erp and M. M. A. Spapé. Distilling the underlying dimensions of tactile melodies. In *Proceedings of EuroHaptics*, pages 111–12, 2003.

[67] J. B. F. van Erp and H. A. H. C. van Veen. A multi-purpose tactile vest for astronauts in the international space station. In *Proceedings of Eurohaptics*, pages 405–408. 2003.

[68] H. A. H. C. van Veen and J. B. F. van Erp. Tactile information presentation in the cockpit. *Lecture Notes on Computer Science (Proceedings of Haptic Human-Computer Interaction)*, 2058:174–181, 2000.

[69] R. Verrillo and A. J. Capraro. Effect of extrinsic noise on vibrotactile information processing channels. *Perception & Psychophysics*, 18:88–94, 1975.

[70] R. T. Verrillo and G. A. Gescheider. Perception via the sense of touch. In I. R. Summers, editor, *Tactile Aids for the Hearing Impaired*, pages 1–36. Whurr Publishers Ltd, 19B Compton Terrace, London N1 2UN, England, 1992.

[71] J. Williamson, R. Murray-Smith, and S. Hughes. Shoogle: excitatory multimodal interaction on mobile devices. In *Proceedings of the SIGCHI conference on Human factors in computing systems*, pages 121–124, New York, NY, USA, 2007. ACM. ISBN 978-1-59593-593-9. doi: http://doi.acm.org/10.1145/1240624.1240642.

[72] S. H. Won and J. Lee. Analysis of flat-type vibration motor for mobile phone. *IEEE Transactions on Magnetics*, 41(10):4018–4020, 2005.

[73] U. Yang, Y. Jang, and G. J. Kim. Designing a vibro-tactile wear for "close range" interaction for VR-based motion training. In *Proceedings of the International Conference on Artificial Reality and Telexistence (ICAT)*, pages 4–9, 2002.

[74] H.-Y. Yao, D. Grant, and M. Cruz. Perceived vibration strength in mobile devices: the effect of weight and frequency. *IEEE Transactions on Haptics*, 2010. Preprint.

[75] J. J. Zwislocki and A. Goodman. Absolute scaling of sensory magnitude: a validation. *Perception and Psychophysics*, 28:28–38, 1980.

# 요 약 문

## 모바일 기기에서의 인지 기반 진동 렌더링

최근 휴대폰, PDA, 휴대용게임기 등과 같은 개인모바일기기의 보급으로 인해 우리의 생활에 많은 변화가 일고 있다. 개인모바일기기는 통신기능의 향상, 다양한 어플리케이션 탑재, 또한 이동성의 극대화와 같은 기술혁신을 통해 끊임없이 우리 생활을 윤택하게 한다. 이러한 모바일기기의 진보된 기술 중 유저인터랙션(UI) 측면에서 최근에 진동렌더링이 각광을 받고 있다. 그러나, 모바일 기기에서의 수많은 진동 응용 기술에 비하면 모바일 기기를 사용하는 인간의 진동 인지능력에 대한 체계적인 연구는 거의 없는 실정이다. 본 연구에서는 진동 인지 능력에 대한 인지심리학적 데이터를 제공함과 동시에 인간의 인지적 특성을 고려한 진동 렌더링 방법을 통해 효과적으로 진동 메세지를 전달하는 데 그 초점이 있다.

이를 위하여 첫 번째로, 모바일기기에서 사용하는 대표적인 진동자(진동모터와 보이스코일)의 진동생성원리 및 물리적/인지적 특성을 조사하고, 물리적 한계 안에서 진동피드백의 효과를 최대화 할 수 있는 진동자 컨트롤 방법을 모색하였다. 두 번째, 넓은 범위의 주파수와 진폭의 조합을 통해 생성된 진동들의 인지적 강도를 정신물리학적 실험을 통해 측정하고, 이를 가지고 Stevens' power law를 기반으로 하는 비선형 함수로 회귀분석하여 모바일기기를 사용할 때의 진동지각모델을 구축하였다. 이러한 진동지각모델은 다른 진동자의 인지적 특성을 정신물리학적 실험 없이도 쉽게 예측하기 위해서 사용 가능하다. 이와같은 진동지각모델을 앞서 구한 두 진동자의 인지적 특성과 비교함으로써 인지 강도 예측을 위한 모델로서의 적용성을 검증하였다. 세 번째, 인간의 진동지각 및 진동자의 물리적 특성을 기반으로 이로 인한 진동 전달

의 왜곡을 최소화하는 인지적으로 명료한 진동 렌더링 방법 "Perceptually transparent vibration rendering (PTR)"을 제안하였고, 이 렌더링 방법의 효과 및 유용성을 실험을 통해 검증하였다. PTR을 사용할 때에는 진동의 강도레벨을 5–6단계로 나누어도 사용자들이 서로 다른 강도를 가지는 진동을 구분할 수 있었지만, PTR을 사용하지 않을 때에는 3–4단계로 나누어도 구분하기 어려워 하였다. 또한, 모바일 기기에서 실사용을 위한 진동 멜로디 간의 구분 정확도가 PTR을 통해 렌더링하였을때 향상됨을 실험을 통해 보였다. 마지막으로, 초보자도 손쉽고 빠르게 진동패턴을 디자인하기 위한 진동 저작 도구를 개발하였다. 개발된 진동 저작 도구는 앞서 제안한 인지모델을 기반으로 하는 진동 렌더링 방법을 기본적으로 적용한다.

모바일 기기에서의 진동을 통한 인터랙션 방법에 대한 관심이 끊임없이 이어지고 있다. 본 연구에서는 인간의 진동 인지 모델을 탐구하고, 이를 기반으로 하는 진동 렌더링 방법을 제안하고 이의 유용성을 검증하며, 초보자도 손쉽게 진동을 디자인할 수 있는 진동 저작 도구를 개발하였다. 따라서, 본 연구는 모바일기기에서의 진동피드백에 대한 관심이 높아져가는 이 시점에 진동 디자인 및 생성, 인지를 위한 효과적인 방법을 제시하는데 그 의의가 있다.

# 감 사 의 글

공학박사의 꿈을 품고 포항에 온지도 8년이 지났습니다. 어색했던 포항 생활도 이제는 한몸이 된듯 익숙하기만 합니다. 오랜 시간동안 쌓아올린 오늘의 결과는 저 혼자만이 아닌 많은 분의 도움으로 이루어졌겠지요.

항상 기도로 지켜주시고 아들의 꿈을 위해 멀리에서도 지원해주셨던 부모님께 특별히 크나큰 감사의 말씀을 드립니다. 인생의 선배로서 조언을 아끼지 않았던 형과 누나도 감사합니다. 포항생활 마지막에 지친 나에게 많은 힘을 주었던 여자친구에게도 감사합니다.

그리고, 대학원 생활의 전반에 걸쳐 지도해 주신 최승문 교수님께 감사의 말씀 드립니다. 또한, 가상현실이란 학문의 길에 한걸음 발을 내딛게 도움주신 박찬모, 김정현 교수님과 바쁘신 가운데도 학위 논문 심사에 선뜻 응해주신 이근배, 이승용, 한성호 교수님께도 감사의 말씀 드립니다.

8여년의 연구실 생활에서 크고 작은 어려움에서도 항상 곁에 있어 주었던 선후배들 덕분에 즐거운 대학원 생활이 가능했습니다. 오랜 인고의 시간을 함께 거쳤던 성길형과 석희에게 감사합니다. 또한, 졸업하신 상윤형, 진석형, 남규형, 재인형, 동식형, 용석형, 태용형, 보현형, 건형, 광훈형, 자연누나, 선형누나, 수영누나, 지혜누나, 형진누나 뿐만 아니라, 선명, 재훈, 재영, 채현에게 감사합니다. 아직 대학원생활이 많이 남아있고 좋은 연구를 수행할 것이라 믿는 성훈, 재봉, 인욱, 인, 갑종, 건혁, 종만에게도 감사합니다.

대학원 생활을 마치는 시점에 이제부터 사회에 나서게 됩니다. 앞으로도 지금까지 그래왔던 것처럼 묵묵히 노력하기를 게을리 하지 않겠습니다.

# Curriculum Vitae

Name              :  Jonghyun Ryu

Date of Birth     :  1980. 2. 18

Present Address   :  대전광역시 서구 괴정동 423-28


# Education

1998–2002         :  B.S. in Computer Engineering, Chungnam National University

2002–2004         :  M.S. in Computer Science and Engineering, POSTECH
                     Thesis Title :
                     가상 환경에서 충돌 느낌 제시와 실재감 향상을 위한 진동 촉감 장비의 사용 방법
                     **(Using Vibro-Tactile Display for Collision Perception and Enhanced Presence)**
                     Advisor: Prof. Chanmo Park

2004–2009         :  Ph.D. in Computer Science and Engineering, POSTECH
                     Thesis Title :
                     모바일 기기에서의 인지 기반 진동 렌더링
                     **(Perception-based Vibration Rendering in Mobile Device)**
                     Advisor: Prof. Seungmoon Choi

# Publications

1. Jonghyun Ryu, Jaemin Chun, Gunhyuk Park, Seungmon Choi, and Sung H. Han "Vibrotactile Feedback for Information Delivery in the Vehicle" *IEEE Trans. Haptics*, (Accepted).

2. Jaebong Lee, Jonghyun Ryu, and Seungmoon Choi "Vbrotactile Score: A Score Metaphor for Designing Vibrotactile Patterns" in *Proceedings of World Haptics Conference*, pp. 302–307, 2009.

3. Jaebong Lee, Jonghyun Ryu, and Seungmoon Choi "Graphical Authoring Tools for Vibrotactile Patterns" in *DVD Proceedings of World Haptics Conference*, pp. 388–389, 2009 (Demonstration).

4. Jonghyun Ryu and Seungmoon Choi "posVibEditor: Graphical Authoring Tool of Vibrotactile Patterns" in *Proceedings of IEEE International Workshop on Haptic Audio Visual Environments and Games (HAVE2008)*, pp. 120–125, 2008.

5. Jonghyun Ryu and Seungmoon Choi "Benefits of Perceptually Transparent Vibration Rendering in Mobile Device" *Lecture Notes on Computer Science (EuroHaptics 2008)*, 5024: 706–711, 2008.

6. Jonghyun Ryu and Seungmoon Choi "Perceived magnitudes of Vibrations Transmitted Through Mobile Device" in *Proceedings of Haptics Symposium 2008*, pp. 139–140, 2008.

7. Jonghyun Ryu, Jaehoon Jung, Seojoon Kim, and Seungmoon Choi "Perceptually Transparent Vibration Rendering Using a Vibration Motor for Haptic Interaction" in *Proceedings of IEEE ROMAN 2007*, pp. 310–315, 2007.

8. Jonghyun Ryu and Gerard Jounghyun Kim "Using a Vibro-tactile Display for Enhanced Collision Perception and Presence" in *Proceedings of VRST 2004*, pp. 89–96, 2004.

9. 천재민, 류종현, 박건혁, 한성호, 최승문 "진동피드백과 운전자 정보 시스템 기능간 매핑의 학습효과 측정" *대한산업공학회 추계학술대회 논문집*, 2008

10. 임동관, 한성호, 류종현, 선미선 "가상 환경에서의 효과적인 네비게이션을 위한 도구 분석" *Journal of the Ergonomics Society of Korea*, 23(1): 23–37, 2004. (대한인간공학회 학술상)

11. 류종현, 최승문 "모바일 기기에서 인지적으로 명료한 진동 렌더링을 통해단진동의 인지 정확도 향상" in *Proc. HCI Korea*, (Accepted), 2010

12. 류종현, 최승문 "posVibEditor: 모바일 기기에서 진동촉감 패턴의 디자인 저작 도구" in *Proc. HCI Korea*, pp. 256–261, 2008

13. 임동관, 한성호, 류종현, 선미선 "가상환경에서 Navigation을 위한 효율적인 도구에 관한 연구" in *Proc. HCI Korea*, 2003